Understanding Hemicellulose and Silica Removal from Bamboo

by

Zhaoyang Yuan

M.Sc., Tianjin University of Science and Technology, 2012

A THESIS SUBMITTED IN PARTIAL FULFILLMENT OF
THE REQUIREMENTS FOR THE DEGREE OF

DOCTOR OF PHILOSOPHY

in

The Faculty of Graduate and Postdoctoral Studies

(Chemical and Biological Engineering)

THE UNIVERSITY OF BRITISH COLUMBIA

(Vancouver)

April 2017

© Zhaoyang Yuan 2017

Abstract

In this work, the hydrothermal pretreatment under both acidic and alkaline conditions were conducted to study hemicellulose and silica removal from bamboo.

In the first part of this work, evolution of proton concentration was examined during both auto- and dilute-acid hydrolysis of hemicellulose from green bamboo. An approximate mathematical model (toy model) to describe the proton concentration based upon conservation of mass and charge during deacetylation and ash neutralization coupled with a number of competing equilibria, was derived. This model was qualitatively compared to experiments where pH was measured as a function of time, temperature, and initial acid level. The toy model predicts the existence of a steady state proton concentration dictated by equilibrium constants, initial acetyl groups, and initial added acid. At room temperature, it was found that pH remains essentially constant both at low initial pH and autohydrolysis conditions. At elevated temperatures, one case of non-monotonic behaviour in which the pH initially increased, and then decreased at longer times, was found.

As silica in bamboo creates processing problems, in the second part of this work, alkaline pretreatment of pure amorphous silica particles, bamboo powder and bamboo chips was carried out to study the underlying mechanism for silica and hemicellulose extraction. Response surface methodology was also used to optimize the treatment

conditions that could completely extract silica and partially extract hemicellulose from bamboo chips prior to processing. Alkaline pretreatment resulted in significant improvement in the delignification of treated bamboo chips during subsequent kraft pulping, offering an option to reduce the effective alkali charge or the H-factor. The pre-extracted silica and hemicellulose in the liquor were recovered through a sequential procedure of CO_2 and ethanol precipitation. Moreover, the feasibility of adopting alkaline pretreatment to the typical kraft pulping process was tested. Results demonstrated that all silica, and up to 50% of hemicellulose in raw feedstocks, could be extracted without degrading cellulose and lignin. Approximately 96% of extracted silica in the APEL could be recovered as a high purity (>99.8%) silica nanoparticles. These results demonstrated that the proposed modification may benefit kraft pulping and fit well into the proposed biorefinery concept.

Preface

In this work, I was responsible for experimental design, experimental procedures and data analysis. Dr. Martinez and Dr. Beatson supervised the research and provided feedback and reviewed the manuscript. The work for the proton evolution during auto- and dilute acid pre-hydrolysis of bamboo chips was co-performed with Dr. Nuwan Sella Kapu, a research associate in our laboratory. A list of journal and conference contributions is given below.

1. Journal Papers

   (a) **Zhaoyang Yuan**, Nuwan S. Kapu, Rodger Beatson, Xue Feng Chang, D. Mark Martinez. Effect of alkaline pre-extraction of hemicellulose and silica on kraft pulping of bamboo (*Neosinocalamus affinis* Keng). Industrial Crops and Products, 2016, 91, 66-75.

   This publication presents a version of Chapters 3 and 4.

   (b) Nuwan S. Kapu, **Zhaoyang Yuan**, Xue Feng Chang, Rodger Beatson, D. Mark Martinez, Heather Trajano. Insight into the evolution of the proton concentration during auto- and dilute acid hydrolysis of hemciellulose. Biotechnology for Biofuels, 2016, 9 (224), 1-10.

   This publication presents a version of Chapter 2.

(c) Lingfeng Zhao, **Zhaoyang Yuan**, Rodger Beatson, Xue Feng Chang, Nuwan S. Kapu, Heather L. Trajano, D. Mark Martinez. Increasing efficiency of enzymatic hemicellulose removal from bamboo for production of high-grade dissolving pulp. Bioresource Technology, 2017, 223, 40-46.

The experiments in the paper were conducted by Lingfeng Zhao and me with advisement from other co-authors.

(d) **Zhaoyang Yuan**, Rodger Beatson, Xue Feng Chang, Nuwan S. Kapu, D. Mark Martinez. An eco-friendly scheme to eliminate silica problems during bamboo biomass fractionation. Nordic Pulp & Paper Research Journal, 2017, 32 (1), 4-13.

This publication presents a version of Chapter 4.

(e) **Zhaoyang Yuan**, Yangbing Wen, Nuwan S. Kapu, Rodger Beatson, D. Mark Martinez. A biorefinery scheme to fractionate bamboo into high grade dissolving pulp and ethanol. Biotechnology for Biofuels, 2017, 10, 38.

The experiments in this paper were conducted by Dr. Wen and me with advisement from other co-authors. This publication presents a version of Chapter 3 and further studies.

(f) **Zhaoyang Yuan**, Yangbing Wen. Evaluation of an integrated process to fully utilize bamboo biomass during the production of bioethanol. Bioresource Technology (Accepted).

This publication presents further investigations according to the experimental results obtained in this work.

(g) **Zhaoyang Yuan**, Nuwan S. Kapu, Rodger Beatson, Xue Feng Chang, Heather L. Trajano, D. Mark Martinez. Insight into the understanding of the mechanism of alkaline pretreatment of bamboo biomass. This paper is in preparation and to be submitted to the peer reviewed journal.

This publication presents the data shown in Chapters 3 and 4.

2. Book Chapter

(a) Jingqian Chen, **Zhaoyang Yuan**, Elisa Zanuso, Heather L. Trajano. Hydrothermal Processing in Biorefineries-Production of Bioethanol and High Added-Value Compounds of Second and Third Generation Biomass. Springer (In press).

In the preparation of this book chapter, I was responsible for writing the part of hydrothermal pretreatment of bamboo and agricultural residues and helped to integrate different parts. Part of this book chapter is presented in Chapters 2 and 3.

3. Conference Presentations

(a) **Zhaoyang Yuan**, Nuwan S. Kapu, Xue Feng Chang, Rodger Beatson, D. Mark Martinez. Effect of alkaline pre-extraction of silica and hemicelluloses on the kraft pulping of bamboo. PACwest Conference – 2016, Jasper, Canada, June, 2016. (Presentation).

(b) **Zhaoyang Yuan**, Nuwan S. Kapu, Xue Feng Chang, Rodger Beatson, D. Mark Martinez. Removal of silica from bamboo for biorefinery applications. 5th International Conference of Biorefinery-Towards Bioenergy,

Vancouver, Canada, August, 2015. (Presentation).

(c) **Zhaoyang Yuan**, Nuwan S. Kapu, Rodger Beatson, D. Mark Martinez. Developing bamboo as an alternative feedstock for biorefinery applications: Solving the silica problem. PaperWeek Canada 2015-Biorefinery Session, Montreal, Canada, February, 2015. (Poster).

(d) Nuwan S. Kapu, **Zhaoyang Yuan**, Xue Feng Chang, Lingfeng Zhao, Colby Song, Joel Kumlin, David Houghton, James Olson, D. Mark Martinez, Rodger Beatson. Developing bamboo as an alternative feedstock for bio-products. Research Day, Department of Chemical & Biological Engineering, UBC, 2013. (Poster).

Table of Contents

List of Tables

List of Figures

Nomenclature

A	Reactant surface area, m^2
Ac	Acetyl group
AcOH	Acetic acid
APEL	Alkaline pre-extraction liquor
aq	Aqueous phase
Ar	Arabinose
BL	Black liquor
C	Cellulose polymer
$Ca(OH_2)$	Calcium hydroxide
CCRD	Central composite rotatable design
CO_2	Carbon dioxide
CSF	Canadian Standard Freeness, mL
CTH	Constant temperature (23 ± 0.5^oC and humidity (50%)
DCOOH	D-gtucopyranosyluronic acid
EA	Effective alkali
ECOOH	Gluconic acid
FTIR	Fourier transform infrared spectra
G	Glucuronic acid

GC	Gas chromatography
H^+	Proton
HCl	Hydrochloric acid
HMF	Hydroxymethylfurfural
H_2O_2	Hydrogen peroxide
HPLC	High performance liquid chromatography
H_2SiO_3	Silicic acid
IFBR	Integrated forest biorefinery
ISO	Brightness unit
KOH	Potassium hydroxide
LC	Lignocellulosic
L:W	Liquid-to-wood ratio (L/kg)
Mn	Number average molecular weight, g/mol
MO	Ash in bamboo
Mw	Weight average molecular weight, g/mol
NaOH	Sodium hydroxide
Na_2S	Sodium sulfide
Na_2SiO_3	Sodium silicate
ND	Not detected
NH_4OH	Ammonia hydroxide
NREL	National Renewable Energy Laboratory
OH^-	Hydroxide ion
o.d.	Oven dried

PDI	Polydispersity index
r	Reaction rate
r^2	Regression coefficient
R	Radius of silica particle, m
RSM	Response surface methodology
s	Solid phase
T	Temperature, ^oC
t	Time, min
w/w	Weight by weight
WVP	Water vapour permeability
WVTR	Water vapour transfer rate
X	Xylose unit
k_i	Reaction rate constant
K_i	Equilibrium constant, unitless
α	Fraction of residual silica, unitless
β	Reaction order the hydroxide ion concentration, unitless
ρ	Density of silica, kg/m^3

Acknowledgements

In the first place, I would like to express my sincerest gratitude to my supervisors, Prof. D. Mark Martinez and Prof. Rodger P. Beatson for their invaluable guidance and support throughout my Ph.D. study. Above all and the most needed, they provided me support and friendly help in various ways. I deeply grateful to Dr. Nuwan Sella Kapu for his guidance, suggestions and valuable discussions throughout the course of this research.

In addition, I am deeply thankful to Xue Feng Chang for his helpful guidance, discussions and critical comments. My special thanks go to George Soong for his assistance with all types of technical problems, Lingfeng Zhao for friendship and enlarging my vision about pulp and paper.

I am grateful to my committee members, Dr. Heather L. Trajano, Dr. Richard Chandra and Dr. Valdeir Arantes for their great comments and input about my research. I offer my heartfelt thanks to my departed committee member, Prof. Carl Douglas, for his comments and suggestions through the initial phase of my research.

Specially thanks are given to my family and friends for their constant love and support. At finally, I would like to specially thank Chunyu for her constant support and always being by my side.

Chapter 1

Introduction

Concerns over climate change have driven the development of a bio-based economy in which energy and numerous consumer products are manufactured from renewable lignocellulosic feedstocks. Among the feedstocks, non-wood materials are attracting attention for use in conventional pulp and papermaking, and as a feedstock for the biorefinery applications (Farrell et al. (2000); Machmud et al. (2013); Salmela et al. (2008)). Of the non-woods, bamboo, a perennial woody grass, has received substantial attention due to its chemical composition (similar to wood), fast-growth that becomes harvest-ready in 3-5 years, and high abundance in many Asian countries (Luo et al. (2013); Okubo et al. (2004)). While bamboo is already used for the commercial manufacture of numerous products, there is interest in expanding its use for producing dissolving pulp (Ma et al. (2011)), transportation fuels (Leenakul and Tippayawong (2010)) and various chemicals (Liu et al. (2011); Littlewood et al. (2013)).

Production of dissolving grade pulp (*i.e.* pulp with > 92 $w/w\%$ α-cellulose with very low quantities of "impurities" such as hemicellulose, ash and lignin) generally requires a pre-hydrolysis step in which the lignocellulosic material is subjected to hydrothermal (water/steam) or dilute acid treatment to remove hemicellulose and increase the accessibility of substrate to chemicals used in subsequent processes (Sixta (2006); Agbor et al. (2011); Öhgren et al. (2007)). Pre-hydrolysis is also referred to

'pretreatment' in the lignocellulosic fuels literature (Chandra et al. (2016); Chandra et al. (2015); Trajano and Wyman (2013); Fengel and Wegener (1983)). One of the open remaining questions in the literature is the incomplete understanding of the kinetics of this process. This could facilitate more efficient process optimization and scale-up in these areas.

Indeed, there are difficulties to adopt bamboo in traditional processes. Compared to wood, bamboo contains a much higher level of silica (0.5-5%). Silica creates various downstream challenges during the industrial utilization of bamboo. For example,

(a) The high silica level creates problems such as scaling of evaporators and decreasing the causticizing efficiency in the causticizer in the recovery cycle of the conventional kraft pulping process.

(b) During the production of dissolving grade pulp, high amounts of residual silica causes poor filterability and interferes with the downstream conversion of dissolving pulps into other products (Liese (1987); Salmela et al. (2008); Tsuji et al. (1965)).

(c) During the industrial applications of lignin obtained from bamboo pulping or ethanol fermentation residues, the silica stays in the residual lignin hindering thermal motions (softening, decomposition or degradation) and preventing thermal processing of lignin into value-added bio-products such as emulsion stabilizers and dispersing agents (Kadla et al. (2002); Pye (2008))

(d) Silica in the water stream also causes several complications such as membrane fouling and pipeline scaling (Le et al. (2015); Negro et al. (2001)).

Thus, the ideal method to solve the silica issues encountered in processing bamboo for industrial processes is that silica should be separated completely from the raw material prior to processing. The extracted silica could then be recovered as a by-product for further utilization, for example as a filler in cement or for the production of catalysts and absorption agents. Therefore, understanding the pre-extraction of hemicellulose and silica from bamboo and their subsequent recovery is critical in expanding bamboo usage.

In this work, hydrothermal pretreatment, using water as the media with/without the addition of chemicals (acid or alkali), was used to extract hemicellulose and silica from bamboo biomass. The thesis is presented in two distinct yet complimentary parts. In the first study, a mathematical model was developed to describe the proton concentration evolution during auto- and dilute-acid pretreatment of bamboo chips. The proposed model provides guidelines to evaluate the effect of temperature, acid addition and time on the H^+ generation during pre-hydrolysis.

In the second study, we proposed a novel methodology to pre-condition bamboo to transform it to a useful feedstock for dissolving pulp or kraft pulp. This proposed method of solving the silica associated problems will be a guide to improving chemical recovery of kraft mills using non-wood materials as well as optimizing present dissolving pulp or kraft pulping processes in order to obtain high quality pulp products at high yield.

The hypotheses of this work are as follows:

1. A proton evolution model that covers auto- and dilute acid pre-hydrolysis of bamboo can be generated to guide the acidic pre-treatment of lignocellulosic

biomass.

2. NaOH can selectively remove silica and hemicellulose from bamboo.

3. Extracted silica and hemicellulose can be recovered in an economical and environmentally friendly way for further applications.

4. The process of combination of pre-extraction and recovery of silica and hemicellulose is suitable for the production of high-grade kraft pulp from bamboo while resolving the silica associated challenges.

This thesis is organized into 5 chapters. The motivation of this work is given in Chapter 1. Chapter 2 presents the evolution of proton concentration during auto- and dilute-acid pretreatment of bamboo biomass. Chapter 3 presents alkaline pre-extraction of silica and hemicellulose from bamboo prior to pulping. The study on the the effect of alkaline pretreatment on kraft pulping of bamboo and the recovery of extracted silica and hemicellulose from the spent liquor of alkaline pre-extraction as byproducts are presented in Chapter 4 and a mass balance for the proposed modification to a typical kraft pulping process is also given. The highlights of this work are summarized in Chapter 5 and recommendations for future research are given.

Chapter 2

Evolution of the Proton Concentration During Auto- and Dilute Acid Hydrolysis of Hemicellulose

2.1 Introduction

In this chapter the kinetics of proton generation during pre-hydrolysis of bamboo chips in a batch reactor is examined. Bamboo is a perennial species belonging to the Gramineae family and Bambuseae subfamily. It is highly abundant worldwide and encompasses over 1250 species within 75 genera (Scurlock et al. (2000)). In China alone, there are approximately 300 species in 44 genera, occupying 33000 km^2 of the country's total forest area (Littlewood et al. (2013)). Bamboo plantations also have several advantages such as limiting soil erosion in cropping systems, improving water quality, and requiring relatively low chemical and nutrients during growing (García-Aparicio et al. (2011)). Moreover, compared to woods, most bamboo species need less time (3-5 years) to mature (Gratani et al. (2008); Krzesińska et al. (2009)).

Moreover, bamboo is considered a promising species for cultivation on marginal land for biofuels and bio-products (Littlewood et al. (2013)). Belonging to the family of grass, bamboo has a stem structure with numerous vascular bundles scattered in a matrix of parenchyma storing cells, all of which are surrounded by a strong and dense epidermis. Vascular bundles are commonly known as bamboo fibres (Amada (1995)).

The three main components of bamboo are cellulose, hemicellulose and lignin, and are found at levels comparable to those of hardwoods and softwoods (Table 2.1) (Luo et al. (2013); Peng et al. (2009); Jun et al. (2012); Huang and Ragauskas (2013)). Cellulose is a linear polymer of repeating sugar units of glucose linked by $\beta - 1,4$ glycosidic bonds and has cyrstalline and paracrystalline regions (Hallac and Ragauskas (2011)). Hemicelluloses are branched, amorphous polysaccharides composed of short lateral chains consisting of several different monosaccharides and functional groups such as xylose, mannose, galactose, arabinose, acetyl groups and glucuronic acid groups (Scheller and Ulvskov (2010)). Like agricultural residuals, such as wheat-straw and rice-straw, the hemicellulose of bamboo is primarily glucuronoarabinoxylan which has a xylose backbone with arabinose, glucuronic acid and acetyl side-groups (Pauly et al. (1999); Scheller and Ulvskov (2010)). Lignin, which is hydrophobic in nature, is an amorphous polyphenol of the primary monolignols: coumaryl, coniferyl, and sinapyl alcohol (Saake and Lehnen (2007)). Within the cell wall, lignin is tightly bound to cellulose and hemicellulose through hydrogen bonds, lignocellulosic complexes and covalent bonds. Biomass also contains some compounds known collectively as extractives (soluble in water or organic solvent). In bamboo, the extractives are mainly composed of resins, fats, nonstructural sugars, nitrogenous material, chlorophyll, and waxes (He and Yue (2008)). The extractives often have

Table 2.1: Chemical composition of bamboo, hardwood and softwood (Huang and Ragauskas (2013); Saka (2004); Dence (1992); Li et al. (2012); Song et al. (2013); Torelli and Čufar (1995)).

	Cellulose (%)	Hemicellulose (%)	Lignin (%)	Silica (%)	Pectin, starch, etc. (%)
Bamboo	38-51	24-28	21-31	0.5-5	1-5.5
Hardwood	42-51	23-35	19-26	0-0.05	1-3
Softwood	41-47	23-31	27-33	0-1.2	1-2

protective biological and anti-microbial activities and aid in the chemotaxonomic division of plant species by their specific biosynthetic pathways (Torssell (1997)). Other common extractives include phenolics, terpenes, aliphatic acids and alcohols (Fengel and Wegener (1983)). Besides these organics, bamboo also contains inorganic minerals, which is commonly referred to as ash, and includes both plant structural components and inorganic materials such as in soil picked up in harvesting operations. The ash content is composed of salts and oxides containing elements such as potassium, calcium, magnesium, sodium and silicon. As a non-wood, bamboo ash contains high level of silica content of up to 70% of total ash (Liese (1987)).

Cellulose is the main component of dissolving grade pulp and both cellulose and hemicellulose can be readily hydrolyzed into fermentable sugars for the production of biofuels and chemicals. Therefore, from the pulping or biorefinery perspective, the total content of cellulose and hemicellulose of bamboo is about 65-75% of the raw biomass, which indicates that it is a suitable candidate as an alternative feedstock for pulp and paper industry and biorefineries.

With regards to the structure of the biomass, the hemicellulose-lignin matrix and structural proteins are thought to serve as a physical barrier and adheres to, and tethers, cellulose macrofibrils through hydrogen bonds and van der Waal's interactions,

see Fig. 2.1 (Altaner and Jarvis (2008); Dammström et al. (2008); Cosgrove et al. (2012)). The strong barrier has high stability and hinders degradation of biomass components. Altering the biomass structure and increasing cell wall accessibility is essential during the utilization of lignocellulosic biomass for the production of fuels, chemicals, pulps and other bio-based materials. Different precondition methods, which can be categorized as physical, chemical, biological and hydrothermal, have been developed to solubilize and remove hemicellulose and/or a fraction of lignin, and increase pore volume and surface area of the biomass (Xu and Huang (2014)).

Among the practical precondition technologies, acidic pretreatment is regarded to be an essential unit operation and has been commercially applied in the production of dissolving pulp and biofuels from lignocellulosic biomasses. This is because this treatment method takes advantage of the high moisture content within the biomass. It can also efficiently convert the polysaccharides into monomeric sugars and their corresponding degradation products in a low energy and environmentally friendly manner. During the production of dissolving grade pulp, acidic pretreatment is also referred to pre-hydrolysis, which includes both auto-hydrolysis (using water/steam as the media) and dilute acid hydrolysis.

Pre-hydrolysis refers to the reaction pathway to remove hemicellulose from lignocellulosic materials prior to subsequent chemical or enzymatic treatment (Littlewood et al. (2013); Sixta (2006); Trajano and Wyman (2013)). During acidic pre-hydrolysis, an acid catalyzes the breakdown of the long hemicellulose chains to form shorter chian oligomers and sugar monomers in the presence of water or steam. The production of dissolving pulp and nanocrystalline cellulose (NCC) (a product made from dissolving pulp) requires the removal of more than 70% of hemicellulose during

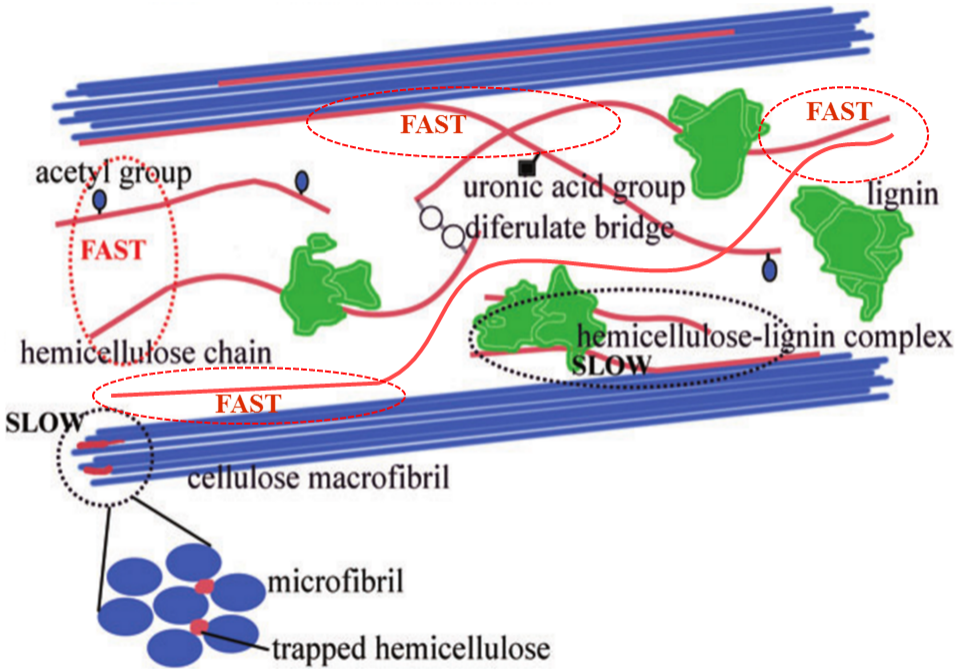

Figure 2.1: A simplified, hypothertical model of bamboo/grass secondary cell wall illustrating molecular interactions of hemicellulose with cellulose and lignin. This figure is reproduced from Sella Kapu and Trajano (2014).

pre-hydrolysis. Lignocellulosic ethanol production uses acid hydrolysis to generate an enzymatically digestible cellulose-fraction. The hydrolyzed hemicellulose-derived oligomers and monomers can be used in food applications or in the textile, paper, explosives, cosmetic, petroleum, and mining industries (González-Muñoz et al. (2012)). In addition, hemicellulose oligomers can also be used to produce gels, films, coatings, and adhesives (González-Muñoz et al. (2012); Sella Kapu and Trajano (2014)).

Pre-hydrolysis is different from torrefaction wherein biomass is treated at 200-300 ^oC in an inert gas environment (Neupane et al. (2015)). During hemicellulose torrefication, it is degraded into volatile organic compounds including CO_2 and CO, and char (Neupane et al. (2015)). Pre-hydrolysis of lignocellulosic biomass is normally conducted between 120-220 ^oC in the presence of water or steam with/without

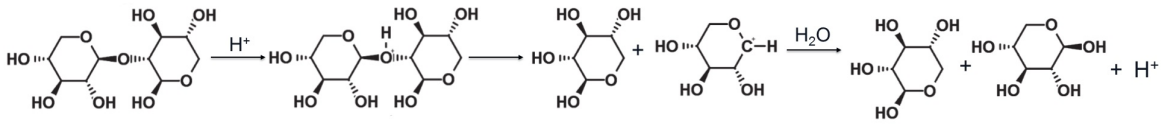

Figure 2.2: Hydrolysis of hemicellulose during acidic pre-hydrolysis process.

the addition of acid (Sanchez and Cardona (2008); Borrega et al. (2013); Rissanen et al. (2014a); Rissanen et al. (2014b); Yan et al. (2014)). The breaking of glycosidic linkages between monomers in the polymeric chains of hemicellulose and cellulose is the fundamental hydrolysis mechanism (Fengel and Wegener (1983)). Hydrolysis of the glycosidic linkage is initiated by the protonation of either glycosidic oxygen or ring oxygen to form a carbonium cation and an end chain product, *i.e.* glucose in the depicted case. Further, a water molecule is added to the carbonium cation, the reaction teminates, resulting in the formation of two monomeric sugars and a proton (Grénman et al. (2011); SriBala and Vinu (2014)). The protons, released by the dissociation of water at high temperature, the added acid and the cleavage of acetyl groups from hemicellulose, subsequently catalyze the hydrolysis of hemicellulose (Grénman et al. (2011)). Fig. 2.2 shows the hemicellulose hydrolysis reaction process.

In acidic pre-hydrolysis process, monomeric pentoses and hexoses released during the hydrolysis of hemicellulose and cellulose may undergo subsequent dehydration reactions to form furfural and hydroxymethylfurfural (HMF), respectively (Rogalinski et al. (2008)). Increasing the hydrolysis temperature or prolonging the residence time will increase the generation of hemicellulose and cellulose degraded byproducts such as furfural, HMF and other light organics (Pu et al. (2013)). Furfural and HMF may further react to generate formic or levulinic acid (Pu et al. (2013)). Using birch wood, Borrega et al. (2011) reported a 7-10% yield of furfural during auto-hydrolysis between

200-240 ^oC using a batch reactor. Bamboo exhibits the same trend as wood during acidic hydrolysis: an increase in monomeric or polymeric sugar yield with increasing temperature/time followed by a decrease due to increased degradaded byproducts production. For example, when the temperature of steam treatment of bamboo was increased from 186 to 200 ^oC, the xylose yield in the liquid phase increased by more than 50% (García-Aparicio et al. (2011)). However, above 200 ^oC, the xylose content in the liquid phase decreased by about 25% (García-Aparicio et al. (2011)). In addition, during acidic pretreatment, the addition of acid accelerates the hemicellulose hydrolysis through the availability of proton catalyst (Larsson et al. (1999); Gütsch et al. (2012)).

Both auto-hydrolysis and dilute acid hydrolysis are considered viable pretreatment options in the production of dissolving pulp and lignocellulosic ethanol. However, kinetic modelling still remains at the forefront and the evolution of concentration of the acid catalyst [H^+] is one of the longstanding unanswered questions (Sella Kapu and Trajano (2014)). One major reason might be the chemical complexity of biomass.

The literature on the kinetics of the removal of hemicellulose is substantial. The modelling approach was built upon the approach used for dilute acid hydrolysis of cellulose (Saeman (1945)). For hemicellulose, complex behavior is evident and numerous groups consider that two fractions of hemicellulose are distributed spatially over two separate domains in the solid matrix to help simplify the analysis (Kobayashi and Sakai (1956)). Each fraction reacts with available protons at differing rates due to differences in reaction activation energy. This model has been adopted widely and is commonly referred to as the "biphasic model". It consists of two solid species, fast and slow hemicellulose, denoted as $X_i(s)$, which hydrolyze following first-order

kinetics

$$X_i(s) \xrightarrow[\mathrm{H^+}]{k_i} X(aq) \qquad r_i = k_i[X_i] \tag{2.1}$$

where r_i and k_i are defined as the rate of reaction and the rate constant, respectively, to form a set of soluble products, $X(aq)$, which are susceptible to further hydrolysis or decomposition reactions. The subscript i represents either fast or slow. The initial values for X_i are considered to be intrinsic for the biomass (Esteghlalian et al. (1997); Ma et al. (2011)). Variations on this approach are available in the literature to describe subtle effects such as the formation of oligomeric intermediates or mass transfer rates (Cahela et al. (1983); Conner and Lorenz (1986); Tillman et al. (1990); Carrasco and Roy (1992); Garrote et al. (2001); Kim and Lee (2002); Brennan and Wyman (2004); Hosseini and Shah (2009); Morinelly et al. (2009); Mittal et al. (2009); Shen and Wyman (2011); Visuri et al. (2012); Liu et al. (2012); Luo et al. (2013); Zhao et al. (2012); Aguilar et al. (2002)). However, no physical or chemical attributes have been identified to differentiate fast and slow hemicellulose.

One of the open remaining questions in this literature is an understanding of the evolution of the concentration of the acid catalyst. What makes this problem particularly challenging is that there are competing pathways governing proton evolution and neutralization. Although difficult to substantiate, a number of authors have advanced rate constants k_i of the form

$$k_i = k_{oi} \exp(-\frac{E_{ai}}{RT}) f(t, [\mathrm{H^+}]) \tag{2.2}$$

where k_{oi} is the pre-exponential factor; and E_{ai} is the activation energy. The function $f(t, [H^+])$ is determined empirically and is found to vary greatly in the literature. This function is included to allow for different reaction rates with different acid levels. In one extreme we find that this function varies linearly in time while in the other extreme it is considered as a constant and set to its initial value. We summarize these forms as

$$f(t, [H^+]) = \begin{cases} a + bt & \text{autohydrolysis} \\ [H^+]_o^n & \text{dilute acid} \end{cases} \tag{2.3}$$

depending upon if the experiment is conducted under dilute-acid or autohydrolysis conditions. Here *a, b* and n are empirical constants and $[H^+]_o^n$ is the initial concentration of the acid catalyst. n is typically found to be between 0.8-1.3 and we note that Shen and Wyman (2011) set $n = 1$ for corn stover. The utility of this functional form has been questioned and it is evident that there is no theoretical basis for the form of the assumed functions (Esteghlalian et al. (1997); Conner and Lorenz (1986); Morinelly et al. (2009); Maloney et al. (1985); Malester et al. (1992); Lloyd and Wyman (2004); Lloyd and Wyman (2005); Hong et al. (2013)). In this chapter we attempt to gain insight into the assumed form of Equation 2.3. We do so by examining the evolution of the proton concentration during reaction through experiment and mathematical modelling.

2.2 Model Development

The analysis presented in this section is aimed at understanding the evolution of $[H^+]$ during the reaction. The goal is to develop a qualitative understanding of this

form by posing a hypothetical reaction scheme which, at some level of approximation, represents the true reaction scheme. It is done at a level in which the analysis is mathematically transparent and of sufficient detail to capture the dominant mechanisms. As a result the approach is referred to as a "toy model".

One of the many complicating factors hindering the modelling process is that there is a large number of chemical species such as cellulose, hemicellulose, lignin and different ash components, which are distributed throughout the cell wall in a complex manner. To simplify, classes of species which behave similarly are grouped together and represented as one hypothetical species. For example, we represent the ash constituents as a lumped parameter MO, that is, the ash is an oxide of the hypothetical species M with a valence state of 2^+; this hypothetical species serves to neutralize the available protons. This can be reposed at another valence state or with secondary effects, such as precipitation from solution, included. In a similar manner the hemicellulose constituents have been reduced to a linear xylose polymer, denoted by X, fast and slow, having arabinose (Ar) side chains (Fig. 2.3). Protons are represented by H^+ and the hydroxyl groups by OH^-; both of these species are considered to be in the aqueous phase and the (aq) notation has been dropped. We have included the potential of an acid being added to the system and denote this species as H_2A because sulfuric acid is most commonly used in the literature. The acetyl group Ac is defined as $H_3C{-}C(=O){-}$. Mass transfer effects are neglected.

We consider four primary reactive pathways in Fig. 2.4 and each individual reaction is assumed to follow elementary kinetics. In the first of these, shown on the far left of Fig. 2.4, we consider deacetylation where Ac is cleaved from the hemicellulose

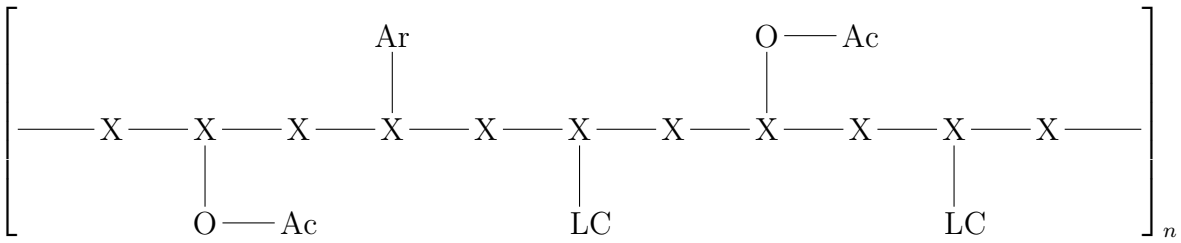

Figure 2.3: A schematic of the idealized hemicellulose - lignocellulose (LC) substrate considered in this work. Although xylan is hypothesized to be comprised of fast and a slow reacting fractions, we do not distinguish these in this figure. The species Ac and Ar, which represent the acetyl and arabinose groups, are initially bound to the xylan chain but are released through acid hydrolysis. The ash (MO) is not shown in this figure but is considered to be *physically* embedded in the LC portion of the matrix.

backbone through an acid hydrolysis of the ester.

$$\mathrm{XOAc} + \mathrm{H_2O} \xrightarrow[\mathrm{H^+}]{\mathrm{k_1}} \mathrm{XOH(s)} + \mathrm{AcOH(aq)} \qquad r_1 = k_1[\mathrm{XOAc}][\mathrm{H^+}] \tag{2.4}$$

This reaction may occur with acetyl groups which are attached to either soluble or solid phases of the hemicellulose. For simplicity, any differences in rate between the deacetylation reaction occurring in the solid or liquid phases are ignored. As the product AcOH(aq), acetic acid, behaves as a weak acid, it adopts the following equilibrium in solution

$$\mathrm{AcOH(aq)} \overset{\mathrm{K_{AcOH}}}{\rightleftharpoons} \mathrm{AcO^-} + \mathrm{H^+} \qquad K_{AcOH} = \frac{[\mathrm{AcO^-}][\mathrm{H^+}]}{[\mathrm{AcOH}]} = 1.8 \times 10^{-5} \tag{2.5}$$

where K_i, from this point forward is defined as the equilibrium constant and the value quoted is at room temperature. Both Garrote et al. (2001) and Aguilar et al. (2002) have used similar modelling approaches to describe deacetylation. Aguilar et al. (2002), for example, explicitly indicates that this reaction follows first order

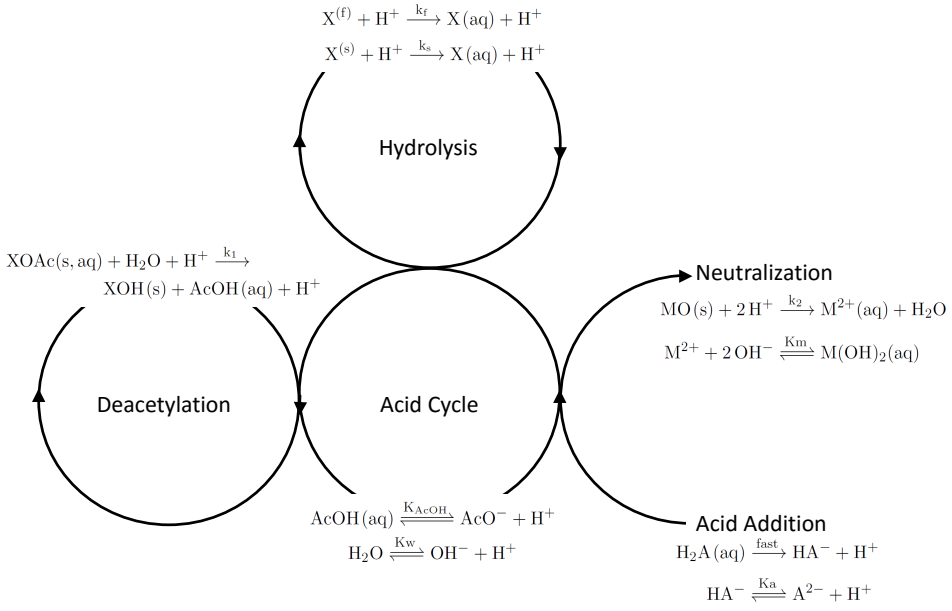

Figure 2.4: A schematic of the idealized reaction scheme. The chemical reactions shown form the basis of the toy mathematical model of the proton concentration.

kinetics (Aguilar et al. (2002)). We build upon these studies by including the effects of the weak-acid behavior of acetic acid (see Equation 2.5).

To continue, water disassociation demands

$$\mathrm{H_2O} \overset{\mathrm{Kw}}{\rightleftharpoons} \mathrm{OH^-} + \mathrm{H^+} \qquad K_w = [\mathrm{OH^-}][\mathrm{H^+}] = 1 \times 10^{-14} \tag{2.6}$$

and this serves as an additional source of $\mathrm{H^+}$. Because of these equilibria, $\mathrm{H^+}$ is available for both the neutralization and hydrolysis reactions.

In addition to this, protons may also be available if acid is added to the system. We capture the reaction scheme as if the added acid is sulfuric acid, as this is the most common addition in the literature:

$$\mathrm{H_2A\,(aq)} \overset{\mathrm{fast}}{\longrightarrow} \mathrm{HA^-} + \mathrm{H^+} \tag{2.7}$$

$$\mathrm{HA^-} \overset{\mathrm{Ka}}{\rightleftharpoons} \mathrm{A^{2-}} + \mathrm{H^+} \qquad K_a = \frac{[\mathrm{A^{2-}}][\mathrm{H^+}]}{[\mathrm{HA^-}]} = 1 \times 10^{-2} \tag{2.8}$$

Like others in the literature, we consider the disassociation give in Equation 2.7 to be instantaneous. The final aspect to consider is the neutralization of the protons by the ash. As mentioned above the reaction scheme depends upon the species involved. As discussed, we consider that MO reacts according to the following scheme

$$\mathrm{MO\,(s)} + 2\,\mathrm{H^+} \overset{\mathrm{k_2}}{\longrightarrow} \mathrm{M^{2+}(aq)} + \mathrm{H_2O} \qquad r_2 = k_2[\mathrm{MO(s)}][\mathrm{H^+}] \tag{2.9}$$

$$\mathrm{M^{2+}} + 2\,\mathrm{OH^-} \overset{\mathrm{Km}}{\rightleftharpoons} \mathrm{M(OH)_2(aq)} \qquad K_m = \frac{[\mathrm{M^{2+}(aq)}][\mathrm{OH^-}]^2}{[\mathrm{M(OH)_2}]} \to 0 \tag{2.10}$$

As the equilibrium constant K_m is unknown, we simply assign this value to be a

very small number to reduce the number of free parameters. It should be noted that we do not characterize a number of potential secondary reactions in solutions, even though they may affect the proton levels to small degree. For example, we ignore the potential reaction between M^{2+} and A^{2-} for mathematical transparency as these do not affect the proton concentration.

Having established the chemistry of the toy model, we now construct the mathematical model. We build the model upon two conservation laws: conservation of mass of each of the species found in solution and an overall charge neutrality of the solution. Conservation of mass expresses that the initial moles of a certain species must sum to total moles of the species in the reaction products. For example, the initial moles of M in $[MO]_o$, must balance the number of moles of M, in the species [MO], $[M^{2+}]$, and $[M(OH)_2]$ at any time throughout the course of the reaction. This can be expressed as

$$[MO]_o = [MO] + [M^{2+}] + [M(OH)_2] = [MO] + [M^{2+}]\left(1 + \frac{[OH^-]^2}{K_m}\right) \tag{2.11}$$

through use of the equilibrium relationship given in Equation 2.10. In a similar manner, conservation of mass for the species Ac can be expressed as

$$[XOAc]_o = [XOAc] + [AcOH] + [AcO^-] = [XOAc] + [AcO^-]\left(1 + \frac{[H^+]}{K_{AcOH}}\right) \tag{2.12}$$

and A as

$$[H_2A]_o = [HA^-] + [A^{2-}] = [A^{2-}]\left(1 + \frac{[H^+]}{K_a}\right) \tag{2.13}$$

with use of Equations 2.5 and 2.8, respectively. To continue, charge neutralization is invoked, i.e.

$$[\mathrm{AcO^-}] + [\mathrm{OH^-}] + [\mathrm{HA^-}] + 2[\mathrm{A^{2-}}] = [\mathrm{H^+}] + 2[\mathrm{M^{2+}}] \tag{2.14}$$

which can be expressed as

$$\left(\frac{[\mathrm{XOAc}]_o - [\mathrm{XOAc}]}{\left(1 + \frac{[\mathrm{H^+}]}{K_{AcOH}}\right)} \right) + \frac{K_w}{[\mathrm{H^+}]} + [\mathrm{H_2A}]_o \left(\frac{[\mathrm{H^+}] + 2K_a}{[\mathrm{H^+}] + K_a} \right) = [\mathrm{H^+}] + 2 \left(\frac{[\mathrm{MO}]_o - [\mathrm{MO}]}{\left(1 + \frac{\mathrm{K_w}^2}{K_m[\mathrm{H^+}]^2}\right)} \right) \tag{2.15}$$

through use of Equations 2.11-2.13. This equation indicates that the proton concentration in the solution is governed by charge neutralization and is related to moles of acetic acid formed (first term on LHS of equation), the amount of ash neutralized (second term on RHS of equation), three different equilibria found in solution (K_m, K_a, K_{AcOH}), and the amount of acid initially added $[\mathrm{H_2A}]_\mathrm{o}$. To complete this description, we use the rate expressions given in Equations 2.4 and 2.9

$$\frac{d}{dt}[\mathrm{XOAc}] = -k_1[\mathrm{XOAc}][\mathrm{H^+}] \qquad [\mathrm{XOAc(0)}] = [\mathrm{XOAc}]_\mathrm{o} \tag{2.16}$$

$$\frac{d}{dt}[\mathrm{MO}] = -k_2[\mathrm{MO}][\mathrm{H^+}] \qquad [\mathrm{MO(0)}] = [\mathrm{MO}]_\mathrm{o} \tag{2.17}$$

where the subscript o represents the initial concentration of the species. Equations 2.15-2.17 represent the toy model to describe the proton concentration during reaction. The utility of this set of equations will be tested experimentally in three limiting cases, i.e.

(a) at long reaction times where the reactions with XOAc and MO are nearly complete.

(b) with the reaction occurring at room temperature in order to examine the proposed ash neutralization scheme.

(c) at typical reaction temperatures found for pre-hydrolysis.

as a function of initial pH.

2.3 Materials and Methods

Bamboo chips, prepared from $3-7$ year old trees, were provided by the Lee & Man Paper Manufacturing Ltd. China. The obtained chips were stored at 4 ^oC until used for experimentation. The chips were air dried for approximately 24 h and re-chipped using a Wiley mill (Thomas Scientific, NJ, USA) and screened with a 45-16-9.5 mm stacked sieve system. Chips retained on the 9.5 mm were designated as accepts for experimentation. The accepts were then washed with deinoized water at 35 ^oC for 10 min at a liquid-to-wood ratio of 20 L/kg using a laboratory mixer to remove impurities, such as soil and sand (see Appendix A1 and A2). The washed chips were air dried for approximately 24 h and then stored at 4 ^oC until used for subsequent experiments. The chips were analyzed with respect to lignin content, carbohydrate composition, extractives, ash and silica content. All chemicals used in this study were reagent grade and purchased from Fisher Scientific, Canada.

The moisture content of solid samples was measured by drying at 105 ± 2 ^oC to constant weight. The contents of water and solvent extractives of bamboo chips were

determined using a Soxhlet extractor according to TAPPI T 204 cm-97.

Carbohydrates and lignin contents of the solids were determined after air drying according to National Renewable Energy Laboratory (NREL) standard protocols (Sluiter et al. (2012)). Briefly, the chips were air-dried and ground to pass through a 40-mesh screen of a Wiley mill. The samples were then subjected to a two-step H_2SO_4 hydrolysis protocol to digest the polysaccharides into monomeric sugars. After hydrolysis, Klason lignin was separated through filtration and measured gravimetrically. Acid soluble lignin in the hydrolysate (after removing Klason lignin) was determined at wavelength 205 nm using a UV-vis spectrophotometer (Dence (1992)). Acid hydrolysates were then filtered using 0.2 μm syringe filters (Chromatographic Specialties, Inc. ON, Canada) and analyzed for monomeric sugars using a Dionex ICS 5000+ HPLC (high performance liquid chromatography) system equipped with an AS-AP autosampler and an electrochemical detector (Thermo Fisher Scientific, MA, USA). The monomeric sugars were separated on a Dionex CarboPac SA10 analytical column (Thermo Fisher Scientific, MA, USA) at 45 ^oC using 1 mM NaOH as the mobile phase, and the sugars were quantified using electrochemical detection and Chromeleon software (Thermo Fisher Scientific, MA, USA). High purity monomeric sugar standards, arabinose, galactose, glucose, xylose and mannose were purchased from Sigma-Aldrich (ON, Canada). Fucose was used as the internal standard.

Total ash content of the raw bamboo chips was determined according to TAPPI T211 om-02. Silica content of bamboo chips and pulp was measured gravimetrically, using a method modified from (Ding et al. (2008)). Briefly, about 5 g of dried and powdered bamboo sample was completely ashed at 550 ^oC. After cooling, 10 mL of HCl (6 mol/L) was added to the ash to precipitate silica and dissolve acid-soluble

Table 2.2: Composition of the bamboo chips used in this study. The values reported in this table are based upon the total mass of the bamboo chips.

Composition	% od, Bamboo
Hemicellulose as:	21.8
Xylan	20.3
Arabinan	0.8
Galactan	0.7
Ash as:	2.1
SiO_2	1.12
CaO	0.37
K_2O	0.28
Al_2O_3	0.15
Cellulose as:	48.7
α-cellulose	47.3
β-cellulose	1.4
Lignin as:	25.1
Acid Soluble	0.9
Acid Insoluble	24.2
Extractives as:	4.6
Water	3.4
Solvent	1.2
Acid groups as:	3.6
Acetyl group	2.7
Uronic acid	0.9

ash. The resultant solution was gently boiled to near dryness in a boiling water bath. HCl treatment was repeated three times in about 30 min, after which another 15 mL of HCl (6 mol/L) was added to the solution. After 2 more minutes, the solution was filtered off through No. 42 ashless filter paper (Fisher Scientific, Canada). The precipitate was rinsed 5-6 times with 1 mol/L HCl solution and 5-6 times with hot deionized water ($\approx$ 50 ^oC). Both the filter paper with the precipitate was ashed at 700 ^oC and calcined at 1000 ^oC in a muffle furnace to reach a constant weight. The resultant silica residue was weighed to determine silica and ash content. All measurements were run at least in triplicate. Detailed analysis of the metal composition

of ash was done using inductively coupled plasma time of flight mass spectrometry (ICP-TOFMS) (Benkhedda et al. (2000)). During the ash composition analysis, high purity ($> 99.9\%$) nitric acid (HNO_3) was used as the dissolution agent. All chemicals used were analytical grade. A summary of the compositional analysis is shown in Table 2.2.

Four separate studies were conducted in this work, as summarized in Table 2.3. In all cases bamboo chips and water were mixed at defined liquor to wood ratios (see Table 2.3) and placed in a 300 mL stainless steel reactor. The total mass of the chips and water for all liquid-to-wood ratios was kept constant at 217 g; this slurry filled about 80% of the available volume of the reactor. The purpose of the first study (Series 1-10) was to characterize the reactor temperature response over time. The reactor was immersed in an oil bath set at a defined temperature, T_b. The temperature of the mixture was continually monitored with two thermocouples mounted in the middle of the reactor, on the central plane but at two different radial positions. Upon completion of a run, the reactor was cooled by immersion in an ice-water bath.

In the second study (Series 11 and 12), conducted to investigate the equilibrium proton concentration after a long period of time, the pH of bamboo chips-liquid mixture having a liquor-to-wood ratio of 6.5 L/kg was measured as a function initial acid content after a minimum of 315 min (in some cases 10 h). In the third study, the second study was repeated but at room temperature (Series 13-16). In the fourth series, the time evolution of the proton concentration was measured as a function of time, temperature and initial acid addition (Series 17-21). In this case the liquid-to-wood ratio was 6.5 L/kg.

Table 2.3: A summary of the experimental conditions tested.

Experiment	Series	$L:W$ (L/kg)	$[H^+]_o$ (pH)	T_b (^oC)	t (min)
Temp. Measurement	1	water only	7.1	120	$0 < t < 45$
	2	water only	7.1	150	$0 < t < 45$
	3	6.5	7.1	140	$0 < t < 45$
	4	6.5	7.1	150	$0 < t < 45$
	5	6.5	7.1	160	$0 < t < 45$
	6	6.5	7.1	180	$0 < t < 45$
	7	8	7.1	120	$0 < t < 45$
	8	8	7.1	150	$0 < t < 45$
	9	10	7.1	120	$0 < t < 45$
	10	10	7.1	150	$0 < t < 45$
Long time behavior	11	6.5	1.3-6.8	160	$t > 315$
	12	6.5	1.5-7.1	180	$t > 315$
Room Temperature	13	6.5	1.5	23	$0 < t < 1155$
	14	6.5	2.9	23	$0 < t < 1155$
	15	6.5	5.0	23	$0 < t < 1155$
	16	6.5	6.0	23	$0 < t < 1155$
Elevated Temperature	17	6.5	1.7	160	$0 < t < 360$
	18	6.5	1.5	160	$0 < t < 390$
	19	6.5	7.2	160	$0 < t < 390$
	20	6.5	7.2	180	$0 < t < 390$
	21	6.5	3.5	160	$0 < t < 360$

Footnotes: In Series 1 through 10, the temperature was sampled at a frequency of 1 Hz. In Series 11-12 a total of 18 samples were measured at times ranging from 315 to 390 min. In Series 13-14, four different initial pH were tested and approximately 11 samples, obtained at different times, were measured. In this case T_b is defined as the oil bath temperature. "$L:W$" and "t" refer to liquid-to-wood ratio and time.

2.4 Results and Discussion

Before proceeding to the main findings, it is instructive to first examine the temperature profile in the reactor after immersion in the oil bath. For each experimental condition, the temperature of the reaction mixture (chips and liquid phases) was recorded using two temperature transducers located at different radial positions in the reactor. For all conditions (Series 1-21) there was no significant difference between the two transducer signals, and the reactor seemingly behaved as if there were no spatial gradients in the system. Two results representative of all the runs are shown in Fig. 2.4. For each experimental condition, the signals from both temperature transducers, located at different radial positions in the reactor are reported. What is evident in this figure is that there is no significant difference in the signals and the reactor seemingly behaves as if there are no spatial gradients in the system, i.e. it is at a uniform temperature. The trend with all the data sets is that the heat up period is about $\sim 15 - 20\, min$ *i.e.* the heat-up rate was essentially the same. The cool-down rate is approximately $\sim 25\, ^oC/min$.

It is curious that there are no strong radial temperature gradients in the system. This result is evident in both the pure water case (Series 1-2) and cases with liquid-to-wood ratio as low as 6.5 L/kg (Series 3-6). Two speculative arguments are proposed to explain this. In the first case we argue that the thermal mass of the steel reactor, i.e. the product of its mass and heat capacity, to be significantly larger than the reactants. As a result, the temperature response of the reactants is dictated by the heating or cooling of the reactor. The second argument is somewhat more delicate. It is also possible that convection occurs due to difference in density of the fluid near

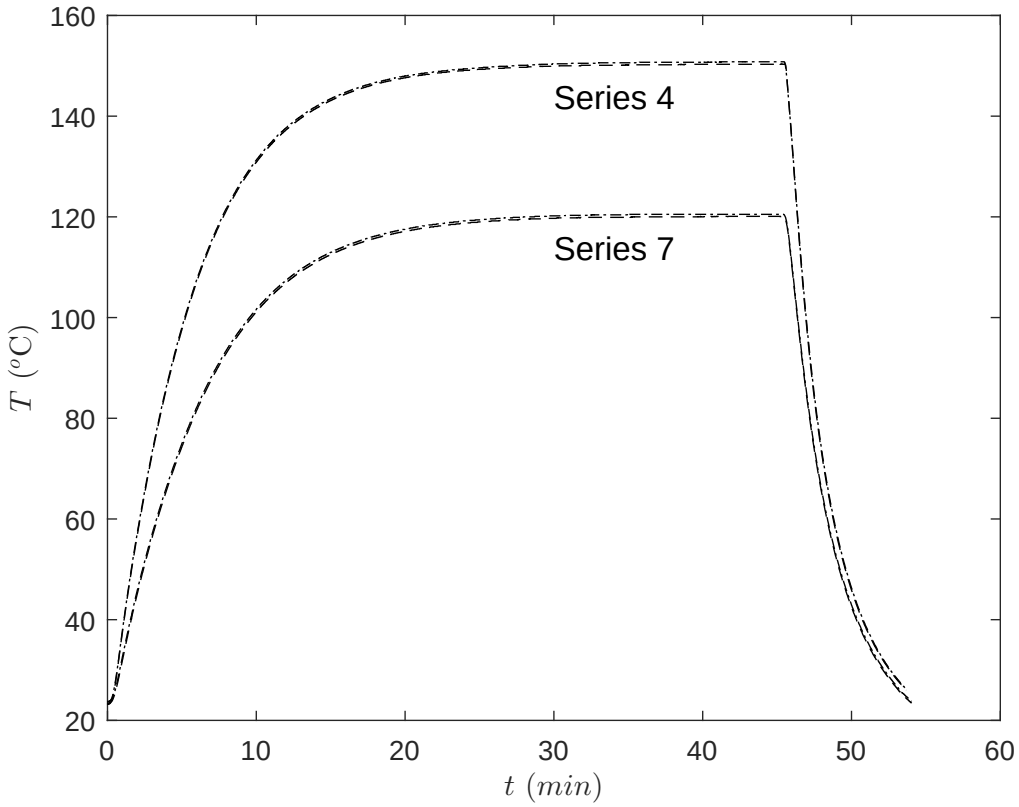

Figure 2.5: Temperature evolution for two representative cases. Both thermocouple signals are presented and replicate runs are shown but the difference between them is not perceptible on this scale. The thermocouples are placed at the same elevation in the reactor but at two different radial positions.

the outer wall in comparison to the bulk. Convective currents in the reactor would tend to diminish the radial gradients.

With the notion of uniform spatial temperature gradients, we examine the temperature evolution throughout the reaction. We propose the temperature profile follows an equation of the form

$$c\frac{dT}{dt} = h(T_b - T) \quad \Rightarrow \quad \bar{T} = \frac{T_b - T}{T_b - T_o} = \exp(-\frac{h}{c}t) \tag{2.18}$$

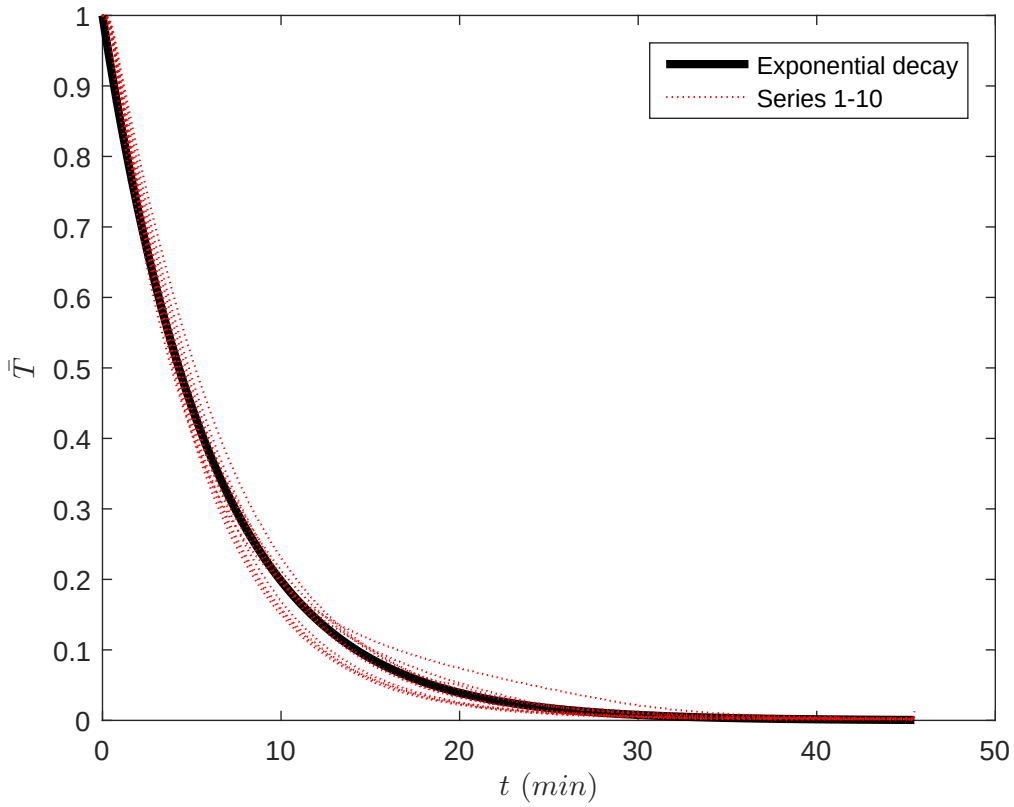

Figure 2.6: The temperature evolution during the heat up period for Series 1-10. The results have been scaled using the form advanced in Equation 2.18 with h/c set to be 0.15 min^{-1}.

where c is the product of the effective mass and heat capacity of the reactor and reactants; h is the overall heat transfer coefficient; and T and T_b are temperature and oil bath temperature, respectively. The utility of this equation is tested by plotting Series 1-10, shown in Table 2.3, in Fig. 2.6 using the scalings indicated in Equation 2.18. What is evident in this figure is that the system displays nearly exponential behavior as the experimental data (the red dotted lines) somewhat follow Equation 2.18, shown as the thick black line. However, we were unable to achieve a similar scaling during the cool-down period.

At this point we begin to explore the utility of the toy model (Equations 2.15-2.17). The first aspect of the model that we will explore is the long-time behavior and examine if a steady state proton concentration is possible. Experimentally the pH was measured at long-time by simply allowing the reaction to proceed for at least 315 minutes at an elevated temperature. From the toy model, we see that a steady state concentration for $[H^+]$ exists and can only be achieved when both the deaceytlyation and neutralization reactions are complete, i.e.

$$\frac{d[\mathrm{XOAc}]}{dt} = \frac{d[\mathrm{MO}]}{dt} = 0, \quad \text{thus,} \quad [\mathrm{XOAc}] = [\mathrm{MO}] = 0 \tag{2.19}$$

Indeed, at steady state the proton concentration may be estimated directly from Equation 2.15, i.e.

$$\frac{[\mathrm{XOAc}]_o}{\left(1 + \frac{[\mathrm{H}^+]}{K_{AcOH}}\right)} + \frac{K_w}{[\mathrm{H}^+]} + [\mathrm{H_2A}]_o \left(\frac{[\mathrm{H}^+] + 2K_a}{[\mathrm{H}^+] + K_a}\right) = [\mathrm{H}^+] + 2\frac{[\mathrm{MO}]_o}{\left(1 + \frac{\mathrm{K_w}^2}{K_m[\mathrm{H}^+]^2}\right)} \tag{2.20}$$

which is a sixth-order polynomial in $[H^+]$. The steady state concentration is given by the roots of this polynomial and the behavior of this function is given in Fig. 2.7. This equation was solved for $[H^+]$ in MATLAB using the built-in root finding procedure. Superimposed on this is the experimental data given as Series 11 and 12. Two observations are clearly evident. The first observation that can be made is that we find a remarkably similar trend with the toy model. The second observation is that there two distinct regions. Under autohydrolysis conditions, i.e. the right hand portion of the graph, the steady state (or long-time) pH is independent of the initial pH. Here, the steady state pH is governed by the weak-acid equilibrium and by ash

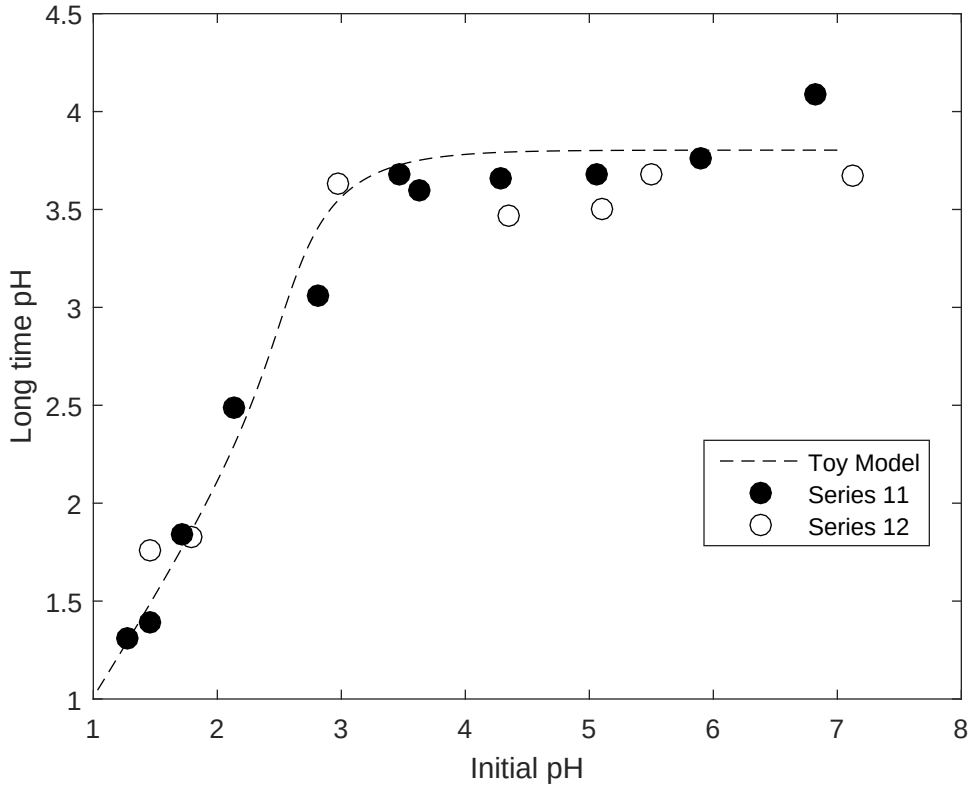

Figure 2.7: The effect of initial pH on the steady state pH measured after long term pre-hydrolysis. The dashed line represents the toy model with the equilibrium constant given in the text previously. The value of K_m is not stated in the text and is taken to be small. For practical purposes we set $K_m = 10^{-17}\,M$ for this calculation. The two remaining parameters are set to be $[\mathrm{XOAc}]_o = 0.025\,M$ and $[\mathrm{MO}]_o = 0.001\,M$ and determined through regression. Although defined previously, Series 11 represents the reaction at 160 ^oC and Series 12 at 180 ^oC.

neutralization or buffering. With increasing levels of added acid, we find that the long time pH approximately equals the initial pH. This is shown on the left hand portion of Fig. 2.7.

These results support the kinetic modelling for xylan removal under dilute acid conditions. As discussed in Section 2.1, a number of authors have assigned the proton concentration to be constant and equal to its initial value (see Kobayashi and Sakai (1956); Esteghlalian et al. (1997); Wyman et al. (2005); Shen and Wyman (2011) for

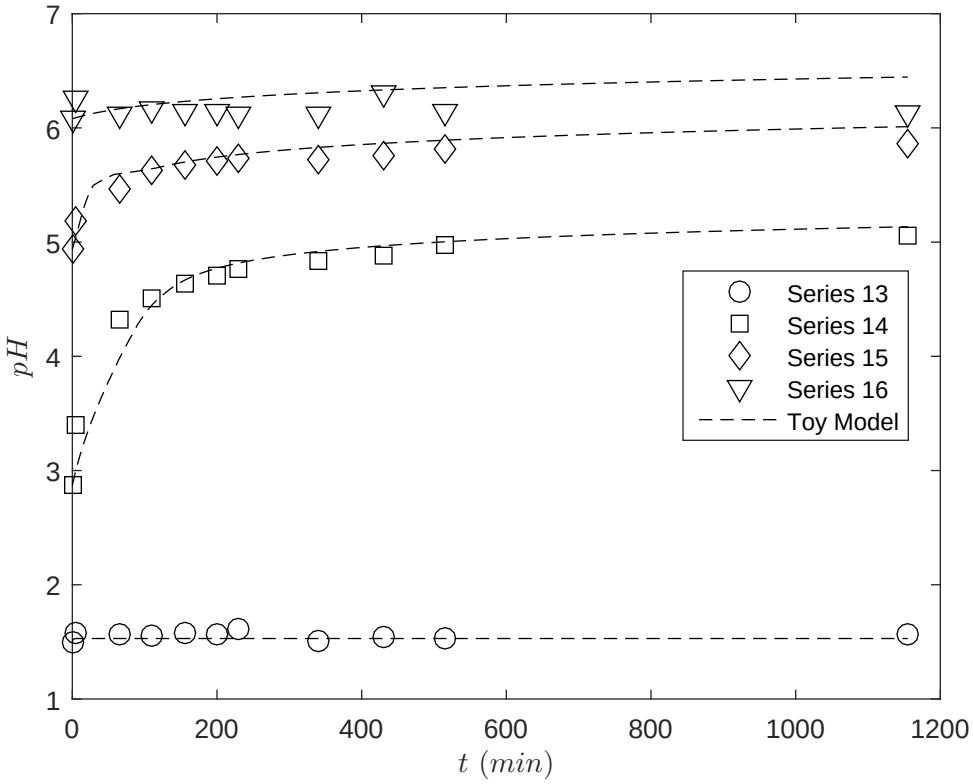

Figure 2.8: Examination of the pH when the reaction proceeds at room temperature. To evaluate the toy model, the same values for the constant given in the caption of the previous Figure are used. In addition, we set $k_2 = 10M^{-1}min^{-1}$ as determined by regression.

example). However, under autohydrolysis conditions, this does not occur. There is a vast difference between the initial and steady state pH of the system.

We continue the discussion of the toy model and examine a second limiting case when the reaction proceeds at room temperature, see Fig. 2.8. Here, four cases were examined in which the amount of acid added initially was varied. At room temperature it can be assumed that the deacetylation reaction proceeds at a much slower rate in comparison to the ash neutralization scheme. Under this assumption,

the toy model reduces to

$$\frac{d}{dt}[\mathrm{MO}] = -k_2[\mathrm{MO}][\mathrm{H}^+] \tag{2.21}$$

$$\frac{K_w}{[\mathrm{H}^+]} + [\mathrm{H_2A}]_o \left(\frac{[\mathrm{H}^+] + 2K_a}{[\mathrm{H}^+] + K_a} \right) = [\mathrm{H}^+] + 2 \left(\frac{[\mathrm{MO}]_o - [\mathrm{MO}]}{\left(1 + \frac{\mathrm{K_w}^2}{K_m[\mathrm{H}^+]^2}\right)} \right) \tag{2.22}$$

which has been solved numerically in MATLAB using a Runge-Kutta scheme (ODE23s) coupled with root finding procedure for the proton concentration. The equations are solved simultaneously. As shown in Fig. 2.8, at low initial pH (Series 13), pH is constant as the concentration of added acid is in excess of the neutralization potential of the ash. With decreasing initial added acid (Series 14-15), the neutralization reaction proceeds until all the ash is reacted. With Series 16, no added acid, the pH varies weakly with time. We interpret this result through the toy model, and advance the argument that the neutralization reaction proceeds but the kinetics are extremely slow due to the low proton concentration.

We now move to perhaps the main findings in this chapter and examine the evolution of pH during pre-hydrolysis treatment. In our final set of experiments, we examined the evolution of the proton concentration at elevated temperatures. Here we must include the effect of deacetylation and as a result, the full toy model must be solved numerically using MATLAB. We treat Equations 2.16 and 2.17 as a system of equations and solve this initial value problem in conjuction with a root finding procedure to estimate $[\mathrm{H}^+]$ from Equation 2.15. The results are shown in Fig. 2.9. Again at low initial pH, proton concentration varies weakly with time (Series 17 and 18) and remains essentially at its initial value. This was the expected result as

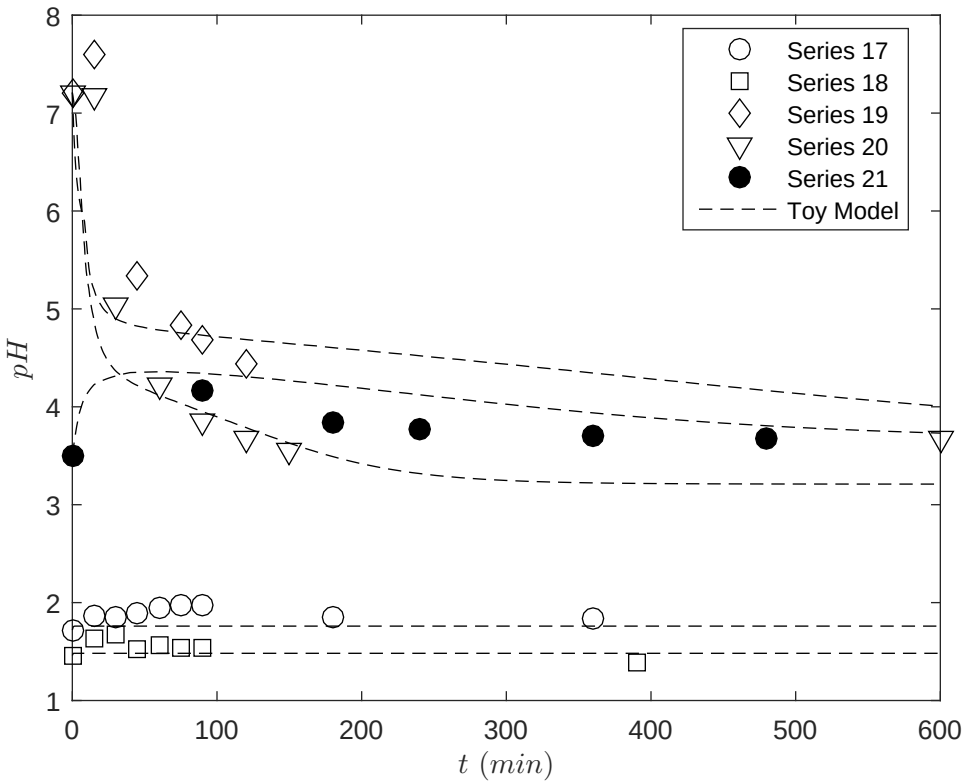

Figure 2.9: A evolution of pH under prehydrolysis conditions. To help understand this we related the lowest initial pH experiments to the added acid: Series 17 0.25% (w/w) and Series 18 0.5 % (w/w).

demonstrated earlier through steady state analysis under excess acid conditions, the pH should remain essentially constant. Below this limit complex behavior is observed. Under autohydrolysis conditions (Series 19 and 20), there is a rapid initial drop in pH followed by a diminished rate at longer times. However, the most curious result is given by Series 21 where non-monotonic behavior, i.e. the pH initially rises and then falls, is observed. We base our interpretation on the toy model which indicates that the neutralization reaction is initially proceeding faster than deacetylation. At longer times, the ash is completely reacted and the pH diminishes from deacetylation.

These results can now be used to interpret the form of the rate constant used for xylan removal. As seen in Equation 2.3, the rate constant under dilute acid conditions is related to the initial pH. This is quite reasonable as we have shown that the pH should be essentially constant during the course of the reaction. However, we cannot make any comment on the value of n in this equation. Below this limit, the behavior of $[H^+]$ is very complex. Simple linear functions may indeed apply for a particular systems of interest. However, this can not be generalized as the pH response depends strongly on the rate of ash neutralization in comparison to the rate of deacetylation.

2.5 Summary

In this chapter the evolution of the proton concentration was examined during the hydrolysis of bamboo chips. At issue was the seemingly disparate model descriptions in the literature which treat dilute acid differently than autohydrolysis conditions. We have attempted to address this issue by posing a "toy model" in which we have included a number of chemical components to help describe the reaction. We advance

that the proton concentration is governed by a charge neutrality in the solution and influenced by the:

(a) weak acid equilibrium formed from the deaceytlation of the acetyl group from the xylan

(b) equilibrium created by water dissociation

(c) ash neutralization and the associated equilibrium in solution

(d) added acid

There are a number of outcomes from the toy model which have been tested experimentally. The first, and perhaps most significant outcome, is that the toy model predicts the existence of a steady state solution. The steady state value is dictated by the equilibrium constants, and the initial added acid and acetyl group levels. The model qualitatively follows the trend given by experiment. It is difficult to perform a quantitative comparison as auxiliary relationships, such the variation of the equilibrium constant with temperature are not known. The model was tested at room temperature to examine the changes in pH when ash neutralization is the dominant mechanism. Under these conditions we find, surprisingly, that the pH remains essentially constant both at low initial pH and under autohydrolysis conditions. Acid is likely in excess of the neutralization potential of the ash, in the former case, and the kinetics of neutralization become exceedingly small in the latter case due to the low proton concentration. Finally, when the hydrolysis reaction proceeded at elevated temperatures, we found one case of non-monotonic behaviour in which the pH initially increased, and then decreased at longer times. This is attributed to the difference in

rates between the neutralization and deacetylation reactions.

As described in the introduction the evolution of the proton concentration during pre-hydrolysis is poorly modeled using empirical functions (Equation 2.3) which are not rooted in a proper chemical reaction scheme. With our toy model we propose a chemical reaction pathway that satisfactorily describes experimentally determined proton concentration under both auto- and dilute-acid hydrolysis conditions. Accurate modeling of the proton concentration would significantly improve the existing kinetic models of hemicellulose hydrolysis and facilitate more efficient process optimization and scale-up in pulping and biorefinery areas.

Chapter 3

Alkaline Pre-extraction of Silica and Hemicellulose from Bamboo

As discussed in Chapter 1, silica creates downstream processing problems for pulping and bioconversion processes. Considerable effort has been expended in trying to solve this silica issue. These efforts have been mainly focused on retaining silica in the final pulp or desilication of black liquor (Jahan et al. (2006); Kopfmann and Hudeczek (1988); Pan et al. (1999); Tsuji et al. (1965)). Unfortunately, until now, none of this work has led to a commercial process. Recently, the proposed integrated forest biorefinery concept (IFBR) has been advanced as a means of addressing concerns over energy security and climate change. According to the IFBR concept, hemicellulose is partially pre-extracted prior to the pulping stages for the generation of value added products such as bioethanol, furfural, acetone, or to be used as papermaking additives (Bai et al. (2012); Hamzeh et al. (2013); Liu et al. (2013); Mao et al. (2008)). Moreover, pre-extraction of lignocellulosic biomass has been shown to be an efficient way of extracting biomass components while also improving the digestibility of the residual biomass and preserving pulp quality (van Heiningen (2006)). Thus, a novel way to solve the silica problems encountered when pulping bamboo could involve pre-extraction of silica along with hemicellulose prior to pulping processes.

In this chapter, alkali was used as the reagent for the dissolution of silica from bamboo biomass. To understand the reaction mechanism during alkaline pre-extraction of bamboo, four separate experiments were conducted and presented, i.e.

(a) dissolution of pure amorphous silica particles with different sizes to investigate the mechanism of silica reaction.

(b) alkaline treatment of bamboo powder to study the chemical reactions occurring during alkaline treatment.

(c) alkaline treatment of bamboo chips to understand the mass transfer effects during the removal of silica and other bamboo components .

(d) with response surface methodology in order to examine the mechanisms of alkaline treatment of bamboo chips and implement the proposed technology into an industrial scale process.

3.1 Dissolution of Pure Amorphous Silica in Sodium Hydroxide Solution

3.1.1 Introduction

Silicon (Si) is the second-most abundant element after oxygen in the Earth's crust and is critical to many geochemical and biochemical processes. Plants of Equisetaceae, Cyperaceae and Poaceae are rich in silica compared to hardwoods and softwoods. Belonging to the family Poaceae, bamboo takes up the monomeric silicic acid, $Si(OH)_4$,

from the soil during the growth (Sangster and Parry (1981)). Most of silica is accumulated as amorphous hydrated silica ($SiO_2 \cdot nH_2O$) in the plant body with little crystalline phases (Motomura et al. (2006); Sterling (1967)). Once deposited, the silica in the tissue is immobile and the process appears to be irreversible. Three types of silica deposits have been recognized in vascular plants (bamboo included), which are silica incrustations of cell walls, silica infilling of the interior of cells (cell lumen) and silica extracellular deposits such as the silica layer associated with outer cuticle of leaf or stem of plant (Fauteux et al. (2005); Le et al. (2015); Richmond and Sussman (2003)). These deposits have been suggested to play a role in mechanical strength and stability of tissues, protection against fungi, insects and herbivores, resistance to drought, improvement of light interception, alleviation of problems caused by nutrient deficiency and excess, and increase of photosynthetic efficiency (Raven (1983); Prychid et al. (2003); Ma and Yamaji (2006)).

One of the key steps to efficiently implement bamboo in the traditional pulp and paper industry is to remove silica. In order to understand the extraction mechanism of silica from bamboo, understanding the reaction kinetics between pure amorphous silica and NaOH is of great importance.

The term silica refers to the chemical compound silicon dioxide, with the chemical formula SiO_2, but as a monomer it is never found in this form. In nature, silica consists of three different forms *viz.*, crystalline silica, vitreous silica , and amorphous silica. In most forms of silica and silicate minerals, the basic chemical structural unit is the tetrahedral arrangement of four oxygen atoms surrounding a central silicon (Si) atom, shown as Fig. 3.1 (Bergna and Roberts (2005)). Silica found in nature is made up of three-dimensional branched chains of alternating silicon and oxygen atoms

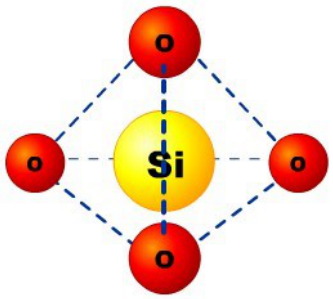

Figure 3.1: Basic structural unit of silica

(tetrahedrons or octahedrons), in which the chains terminate in hydroxyl groups linked to the silicon atom (Cox (1993)). Different arrangements of tetrahedrons or octahedrons in silica yield different structures and thereby properties. For example, the random packing of tetrahedrons in amorphous silica makes it less stable than the ordered dense packing of tetrahedrons in quartz (Bergna and Roberts (2005); Le et al. (2015)).

At ordinary temperatures silica is chemically stable and resistant to many common reagents, especially acids such as sulfuric acid (H_2SO_4) and hydrochloric acid (HCl) (Cox (1993)). However, it undergoes a wide variety of chemical transformations under harsh conditions such as high temperature and high pH (Brückner (1970)). Moreover, the reactivity of silica is greatly dependent on the crystalline structure, treatment conditions, and state of subdivision of the particular sample investigated. For example, finely divided amorphous silica is considerable more reactive than other forms of silica (Sierka and Sauer (1997)).

With regards to the solubilization of silica in water (solubility), it is reported to

be in accordance to the reversible reaction (Niibori et al. (2000)), as

$$SiO_2(s) + 2\,H_2O \rightleftharpoons Si(OH)_4(aq) \tag{3.1}$$

where s and aq represent solid and aqueous phases, respectively. The solubility of soluble $Si(OH)_4$ in water is affected by various factors such as silica structure, temperature and pH (Wirth and Gieskes (1979)). Quartz is the thermodynamically stable form of silica below 870 ^oC (Bergna and Roberts (2005)) and is essentially water-insolubile with a solubility of around 10 *ppm* at 25 ^oC (Lier et al. (1960)). On the contrary, amorphous silica has a higher solubility, which is about 100 *ppm* at room temperature (Iler (1979)). The solubility also increases with increasing the temperature, which in the case of amorphous silica increases to about 900 *ppm* at 200 ^oC (Gunnarsson and Arnórsson (2000)). Moreover, the presence of impurities such as sodium sulfate (Na_2SO_4) and sodium chloride (NaCl) in the solution increases the solubility of silica (Chen and Marshall (1982)). In addition, both low and high *pH* values increase the solubility of silica (Fleming and Crerar (1982)). At very low *pH* (< 2) the solubility increases by the reaction of $Si(OH)_4$ with H^+. The solubility appears relatively constant from *pH* 2 to *pH* 9 at room temperature, but increases considerably above *pH* 9 with more than a six-fold increase in solubility realized at *pH* 11 due to the formation of silicate ion in addition to $Si(OH)_4$ (Alexander et al. (1954); Iler (1979)).

Ordinary acids do not react with silica except for hydrofluroic acid (HF) and phosphoric acid (H_3PO_4) (at elevated temperatures) (Talvitie (1951); Blumberg (1959)). In contrast, silica shows an acidic character by its reaction with a large number of

basic oxides to form silicates (Zaitsev et al. (2000)). For example,

$$2\,Na_2O + SiO_2 \longrightarrow Na_4SiO_4 \tag{3.2}$$

$$Na_2O + SiO_2 \longrightarrow Na_2SiO_3 \tag{3.3}$$

$$Na_2O + 2\,SiO_2 \longrightarrow Na_2Si_2O_5 \tag{3.4}$$

Silica is known to dissolve in both sodium hydroxide (NaOH) and sodium carbonate (Na_2CO_3) solutions. The reaction rates increase with increasing the reaction temperature. The reactions are occurring according to following schemes

$$SiO_2 + 2\,NaOH \longrightarrow Na_2SiO_3 + H_2O \tag{3.5}$$

$$SiO_2 + Na_2CO_3 \longrightarrow Na_2SiO_3 + CO_2\uparrow \tag{3.6}$$

The formed sodium silicate is soluble in aqueous solution. However, when the pH of the alkali solution is reduced from above pH 11 to between pH 9-10, sodium silicate will be converted into insoluble silicic acid. This pH adjustment step can be achieved by the use of mineral acids such as sulfuric acid (H_2SO_4) or carbon dioxide (CO_2) gas. As an example, with using CO_2 treatment, the reaction can be expressed as

$$Na_2SiO_3 + 2\,CO_2 + 2\,H_2O \longrightarrow H_2SiO_3\downarrow + 2\,NaHCO_3 \tag{3.7}$$

In addition, during the dissolution of silica in alkaline solutions, the presence of

some polyvalent cations such as Ca^{2+}, Mg^{2+}, Fe^{3+}, Al^{3+} and Cu^{2+} will interact with silica causing co-precipitation and forming insoluble deposits (Le et al. (2015); East et al. (2013)), in turn reducing the dissolution of silica particles.

Since the silica in bamboo is mainly in amorphous phase (Motomura et al. (2006)), we review and study the chemistry of amorphous silica in this work. Several research groups have studied the kinetics and mechanisms of the dissolution of pure amorphous silica in aqueous solutions of alkali. They assumed the dissolution of silica to follow equilibrium reaction kinetics and assumed that the dissolution rate is as a function of the reactive surface area (Anatskii and Ratinov (1969); Greenberg and Price (1957); Iler (1979); Okunev et al. (1999); Thornton et al. (1988)). The dissolution rate was modeled as dependent on temperature, time, and hydroxide ion (OH^-) and silica concentrations according the spherical shrinking core model. The reaction order with respect to $[OH^-]$ in the proposed models remains an open question. Therefore, the objective of this part of work was to examine whether the dissolution of silica in NaOH solution follows the spherical shrinking core model under the studied conditions.

3.1.2 Materials and Methods

Amorphous silica particles with three diameters (0.2-0.3, 250-400, and 850-1000 μm) were purchased from Sigma-Aldrich (Saint Louis, MO, USA) with a purity higher than 99%. All chemicals used in this study were reagent grade and solutions were prepared with purified deionized water.

The experiments on the dissolution of amorphous silica in NaOH solution were carried out in a round bottomed three-necked flask, equipped with a stirrer, thermometer

Table 3.1: A summary of the experimental conditions tested for the dissolution of pure amorphous silica.

Silica particle size (μm)	Temperature (^oC)	$[OH^-]_o$ (mol/L)	time (min)
0.2-0.3	70	0.45	$0 < t < 90$
250-400	70	0.15	$0 < t < 100$
250-400	70	0.30	$0 < t < 100$
250-400	70	0.45	$0 < t < 100$
850-1000	70	0.45	$0 < t < 130$

Note: $[OH^-]$ and t refer to NaOH concentration and reaction time.

and pH meter, immersed in a laboratory-scale heated oil bath. The experimental conditions used for the dissolution of pure amorphous silica particles are summarized in Table 3.1. In all cases, the liquid to silica ratio was kept constant at 100:1.12 ($L : kg$). A flask with 0.5 g pure amorphous silica particles and the calculated volume of water was placed in the bath for 15 min to heat up to 70 ^oC. Then, the calculated volume of NaOH solution (stock concentration of 100 g/L) was added into the mixture to maintain the target NaOH concentrations (0.15-0.45 mol/L) and the desired liquid-to-silica ratio. During the reaction process, he stirring rate was fixed at 100 rpm. At the end of the experimental run, the samples in the reactor were filtered with the membrane filter of pore size of 0.02 μm, the dissolved silica in the filtrate was determined photometrically by the yellow silicomolybdate method (Tong et al. (2005)). Undissolved silica particles on the membrane were collected and oven dried at 105 $\pm$ 2 ^oC to constant weight. The weight of the solids was determined with an analytical balance. The particle size distribution of the silica particles of various times (0-130 min) during the reaction was measured by a Mastersizer 2000 (Malvern, United Kingdom). The residual alkali concentration of the filtrate was measured. All experiments were completed in triplicate.

After the NaOH treatment, the residual fraction of silica particles was calculated as

$$\alpha = \frac{\text{the amount of residual silica}}{\text{the amount of initial silica introduced into the alkaline reaction system}} \quad (3.8)$$

where α is the fraction of residual silica during the dissolution process.

3.1.3 Results and Discussion

In this section, the goal of alkaline dissolution of pure amorphous silica is to determine the reaction rate between silica and NaOH in the absence of competing reactions and mass transfer effects created by bamboo biomass. It is well known that the basic chemical structural unit of silica is the tetrahedral arrangement of four oxygen atoms surrounding a central silicon (Si) atom. When silica is put into a NaOH solution, several reactions take place simultaneously (Wirth and Gieskes (1979)), i.e.

$$\mathrm{SiO_2(s) + H_2O \rightleftharpoons H_4SiO_4(aq)} \qquad K_{sp} = 5.32 \times 10^{-4}\, M \quad (3.9)$$

$$\mathrm{mSiO_2(s) + 2\,NaOH \rightarrow Na_2O \cdot mSiO_2(aq) + H_2O} \qquad m = 1 - 4 \quad (3.10)$$

Fig. 3.2 shows the mass fraction of residual silica (α) against the reaction time. As shown, under the same NaOH concentration (0.45 mol/L) decrease the particle size of initial silica powders resulted in the faster dissolution of silica particles. For example, the times needed for the dissolution of 98% of initial silica particles with the size ranges of 0.2-0.3, 250-400 and 850-100 μm were 30, 80 and 110 min, respectively. This could be attributed to the fact that silica particles with smaller particle size

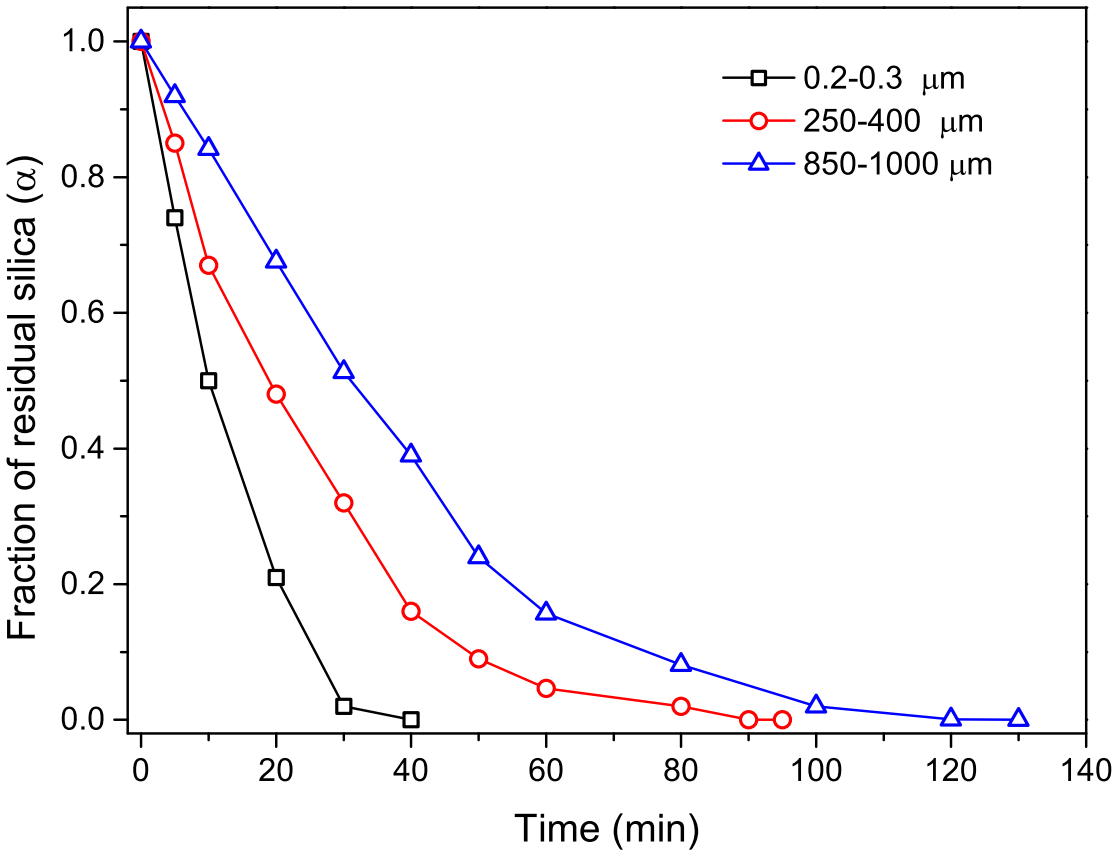

Figure 3.2: Effect of particle size on the dissolution rate of silica (temperature = 70 ^oC and NaOH = 0.45 mol/L).

have a larger total reaction surface area than that of silica with larger particle size at the same mass in the reaction system (Mgaidi et al. (2004)).

To study the effect of NaOH concentration on the dissolution of pure amorphous silica. Silica powder with particle size of 250-400 μm was used (Fig. 3.3). Increasing the NaOH concentration resulted in faster dissolution of the silica. For example, when treating 250-400 μm silica powder with NaOH solution having a concentration of 0.15 mol/L, 89% of initial silica was dissolved in 60 min, whereas, increasing the NaOH concentration to 0.45 mol/L, 95% of silica was dissolved in 60 min. One likely reason is that the contact probability of silica and hydroxide ion is increased with more hydroxide ion in the reaction system, resulting in faster depolymerization of silica.

To interpret the experimental data and describe the silica dissolution in NaOH solution, the classic shrinking core model was applied, where the reaction rate is considered to be proportional to the surface area of the unreacted silica particles (Niibori et al. (2000); Mgaidi et al. (2004)). In applying the spherical shrinking core model, the surface of silica particle is assumed to have the equal reactivity and a smooth reaction interface. Thus, the rate of reaction was assumed as

$$r_1 = k_1 A[\mathrm{OH}^-]^{\beta} \tag{3.11}$$

where r_1 is the reaction rate of silica (mol/min), k_1 is the reaction rate constant per unit surface area [$mol/(m^2 \cdot min)$], A is the reactant surface area for the reaction (m^2), [OH^-] is the concentration of hydroxide ion (mol/L), and β is the reaction order with respect to hydroxide ion concentration ([OH^-].

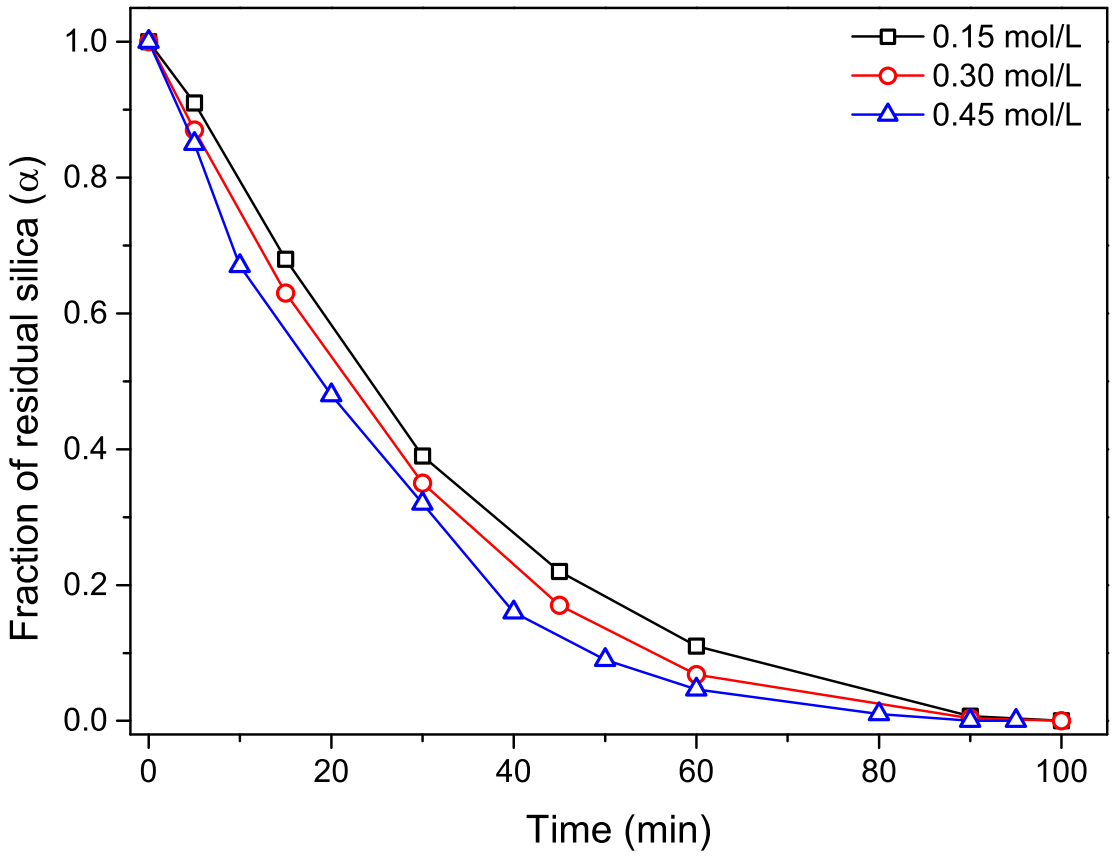

Figure 3.3: Effect of NaOH concentration on the dissolution rate of pure amorphous silica (temperature = 70 ^oC and silica particle size = 250-400 μm).

Based on Equation 3.11, the dissolution rate can be obtained as a function of undissolved silica (α)

$$\frac{d(1-\alpha)}{dt} = \frac{3M}{R_o\rho}k_1[\mathrm{OH}^-]^\beta\alpha^{2/3} \tag{3.12}$$

where M is the molecular weight of SiO_2 (kg/mol), R_o is the radius of the initial silica particles (m), respectively, and ρ is the density of silica (kg/m^3).

Since the NaOH charge used for the silica dissolution is in stoichiometrically largely excessive ($\geq$ 5:1), [OH^-] could be considered to be constant during the reaction process. The time required for the conversion $(1-\alpha)$ is given by

$$1-\alpha^{1/3} = k_2 t \qquad k_2 = \frac{Mk_1}{R_o\rho}[\mathrm{OH}^-]^\beta \tag{3.13}$$

Experimental data shown in Figs. 3.2 and 3.3 were tested with Equation 3.13. The utility of Equation 3.13 was shown in Figs. 3.4 and 3.5. Straight lines passing through the origin were obtained for each particle size and NaOH concentration, indicating that Equation 3.13 could describe the silica dissolution process under the studied conditions. The results of the nature of the rate-controlling mechanism was a function of the extent of dissolution with the reaction order of $\frac{2}{3}$ with respect to silica concentration, which is in agreement with the reported results of 0.6-0.8 on the dissolution of silica aerogel into NaOH solution (Okunev et al. (1999)). Table 3.2 shows the rate constants k_2 obtained from Figs. 3.4 and 3.5. As a reaction rate constant, k_1 is independent of silica particle size. Based on the values of k_2, it can be deduced that the value of k_1 ranging from 5.8-6.5 ($mol^{0.36}L^{0.64}m^{-2}min^{-1}$) was obtained.

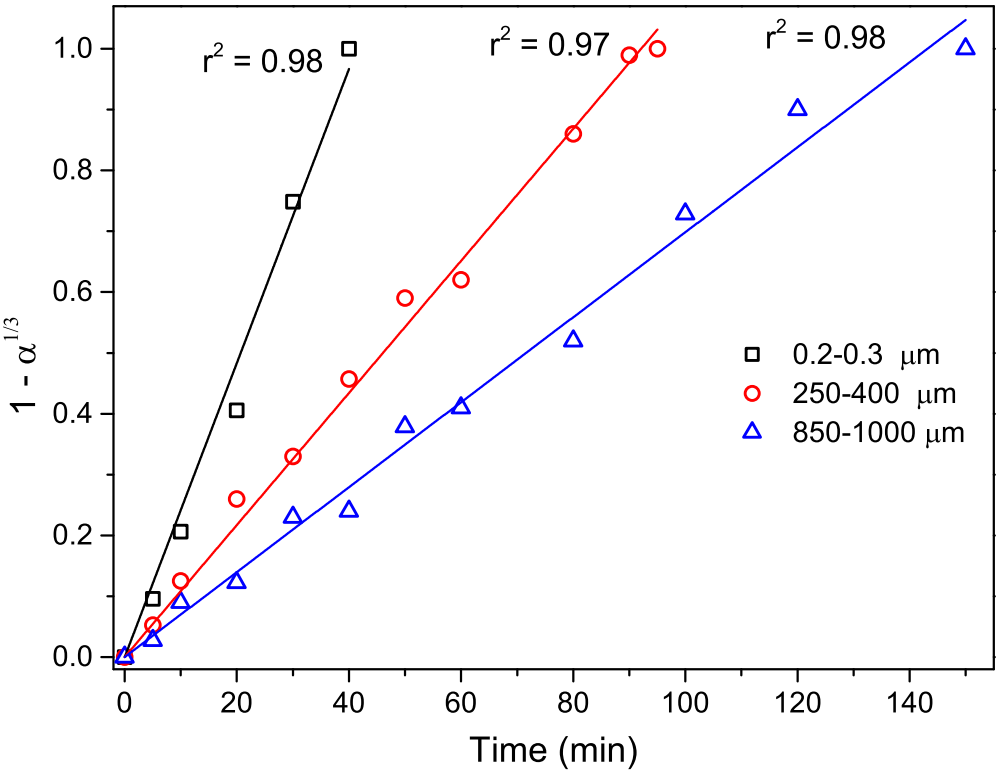

Figure 3.4: Plot of $1 - \alpha^{1/3}$ versus reaction time (t) with different silica particle sizes (temperature=70 ^oC; $[OH^-]_o = 0.45\ mol/L$).

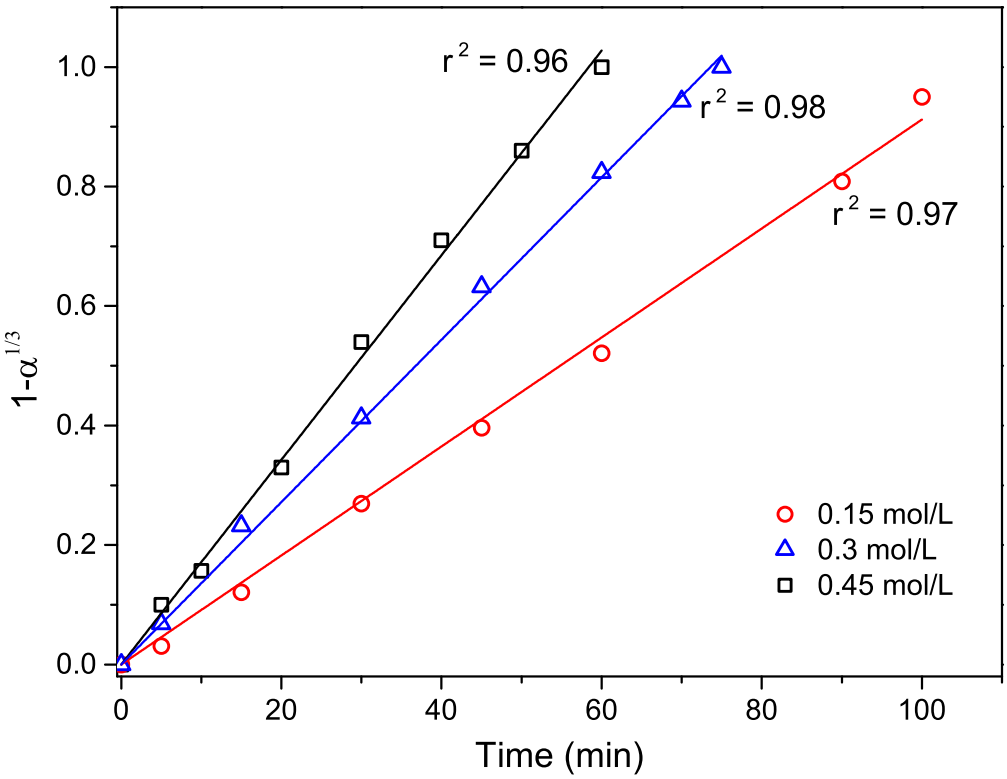

Figure 3.5: Plot of $1 - \alpha^{\frac{1}{3}}$ versus reaction time (t) with different initial NaOH concentrations (0.15-0.45 mol/L). Experiments were carried out with initial silica particle size of 250-400 mum and at 70 ^oC.

Table 3.2: Reaction rate constant (k_2) calculated by experimental data fitting

Silica particle size (μm)	[NaOH] (mol/L)	k_2 (min^{-1}))
0.2-0.3	0.45	0.024
250-400	0.15	0.0091
250-400	0.3	0.014
250-400	0.45	0.018
850-1000	0.45	0.0071

For silica with the same particle size, the value of k_1 should be constant. Thus, the relationship between k_2 and k_1

$$k_1 = \frac{k_2 R_o \rho}{3M[\mathrm{OH}^-]^\beta} \tag{3.14}$$

gives an approach to estimate the value of β. With the values of k_2 of experimental results with the same silica particle size (250-400 μm) (table 3.2), we could estimate the value of $\beta = 0.64$ by assuming the $[\mathrm{OH}^-]$ is constant during the reaction process. From above results (Figs. 3.4, 3.5 and Table 3.2), it can be concluded that the shrinking core model is able to describe silica dissolution in NaOH solution.

Moreover, during the dissolution of pure amorphous silica in NaOH solution, the residual alkali concentration is given by the following equation

$$[\mathrm{OH}^-] = [\mathrm{OH}^-]_o - \frac{2}{m}\left([\mathrm{SiO_2}]_o - [\mathrm{SiO_2}]\right) + \frac{K_w}{[\mathrm{OH}^-]} \quad K_w = 10^{-14} \tag{3.15}$$

which is a second-order polynomial in $[\mathrm{OH}^-]$. Clearly, the residual OH^- concentration is given by the root of the polynomial. This equation was solved numerically for $[\mathrm{OH}^-]$ in MATLAB using the built-in root finding procedure. Fig. 3.6 presents the comparison of calculated $[\mathrm{OH}^-]$ values against experimental data for the dissolution

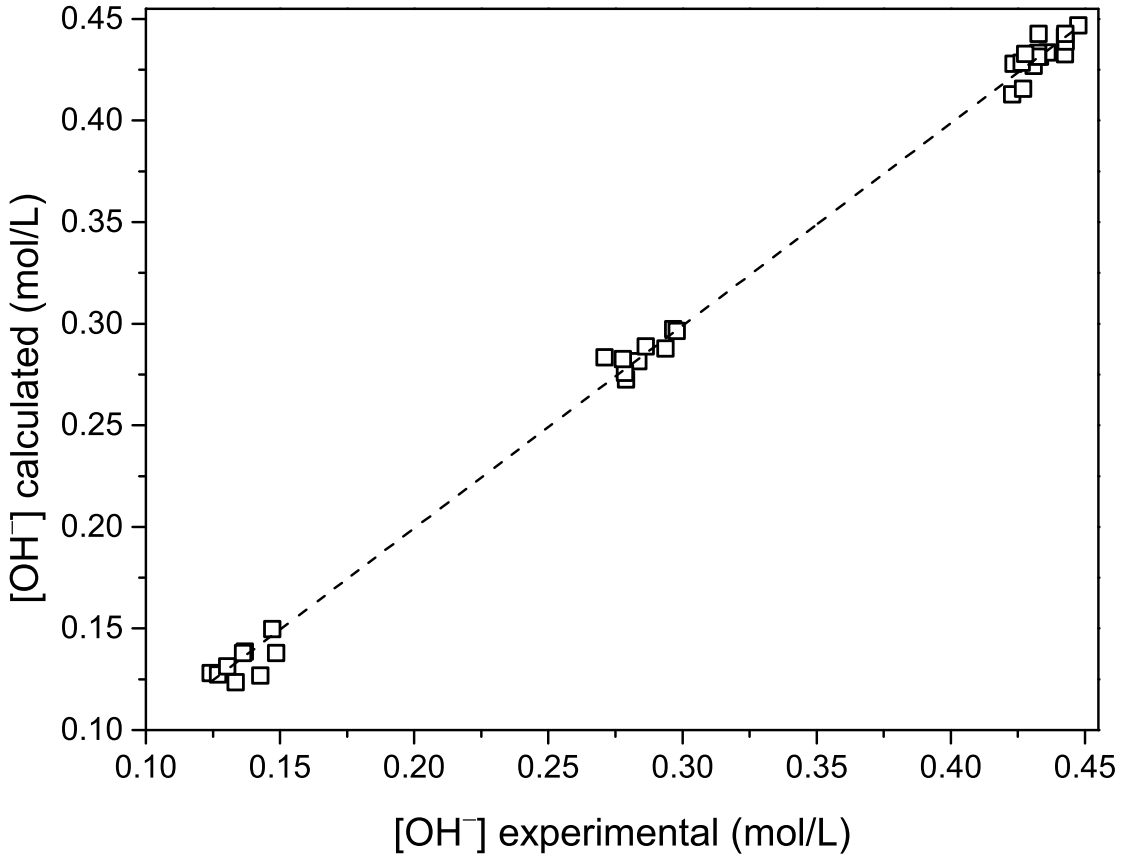

Figure 3.6: Comparison between the experimental data and the predictions by Equation 3.15 for OH^- concentration. The parameter is set m = 1 for the calculation. Data points are from experimental results.

of amorphous silica in NaOH solutions. By using a linear regression, it was found that the model prediction is very good, with a regression coefficient (r^2) of 0.982. Additionally, m = 1 was obtained from the plot of predicted $[OH^-]$ against experimental $[OH^-]$.

One of the limitations of the classic shrinking model is that it does not consider particle size distribution during the dissolution process. Taking the silica particles range 250-400 μm as an example, the particle size distribution during the reaction at an initial NaOH concentration of 0.15 mol/L was determined (Fig. 3.7). After heat-

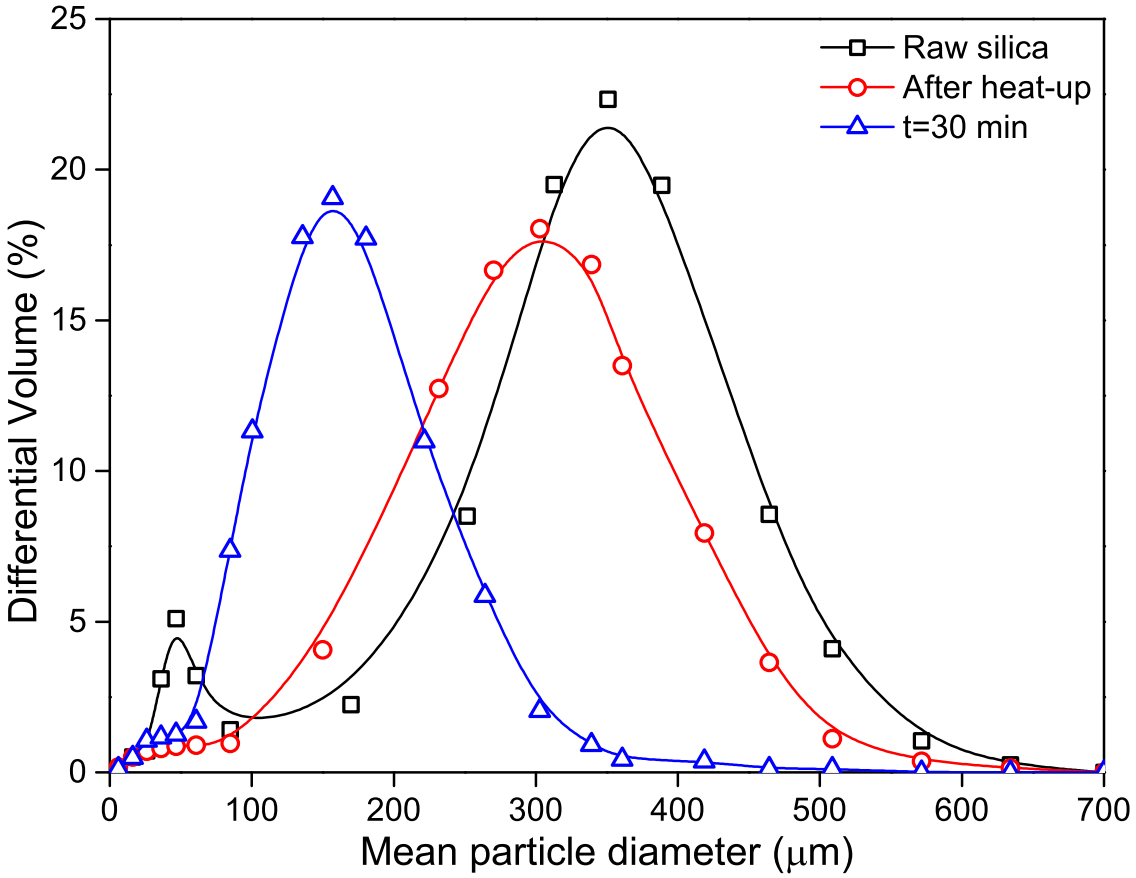

Figure 3.7: Particle size distribution of the solid particles at different reaction times (initial silica particle size = 250-400 μm, temperature = 70 ^oC, initial [OH^-] = 0.15 mol/L).

up period, about 15% of the volume of raw silica materials with particle diameter less than 60 μm disappeared and the volume diameter was decreased to about 300 μm. As the chemical reaction proceeded, the volume diameter of silica particles was further reduced. The volume diameter was about 150 μm after 30 min. These results confirmed that silica with smaller particle size dissolves faster compared to larger size. Thus, from the results obtained, it was reasonable to conclude that the dissolution rate of amorphous silica in NaOH solution is controlled by the reactant surface area.

3.1.4 Summary

Experimental results on the dissolution of pure amorphous silica particles in NaOH solution demonstrated that the classic shrinking core model could be used to describe the silica dissolution rate under the alkali concentrations studied in this work. With the decrease of initial silica particle size, the dissolution of silica particles into NaOH solution was much faster compared to that of silica with large larger particle sizes. The reaction order with respect to OH^- concentration of 0.64 was obtained under the studied conditions. This is helpful to understand the removal of silica from bamboo biomass or other high-silica biomasses following alkaline extraction to resolve the silica associated challenges during biorefinery applications.

3.2 Alkaline Pre-extraction of Silica and Hemicellulose from Bamboo Powder

3.2.1 Introduction

The degree of silica accumulation is quite different among various tissues of bamboo tree; distribution can vary even within the same tissue. The silica content in bamboo increases from the stem, through the branches, to the leaves (Lux et al. (2003); Ding et al. (2008)). In the leaf, silica is mainly accumulated in epidermal cells, with the highest levels in specialized idioblasts (silica cells) and lower levels in the mesophyll cells and vascular bundles; silica in the bamboo root is accumulated exclusively in the endodermal cells (Bennett and Sangster (1981); Motomura et al. (2000); Lux et al. (2003)). In the stem of bamboo, silification mainly takes place as infillings of

the interior epidermis cells, which are located as the outmost layer of plant tissues (Piperno (2014)). Other tissues in the bamboo culm, such as hypodermal and vascular tissue, may also be silicified, but to a lesser degree than the epidermal tissue (Le et al. (2015); Motomura et al. (2000)).

Silica content of the bamboo stem ranges from 0.5-5% (w/w) (Liese (1992)). In contrast, the silica content of wood is usually less than 0.01% (w/w), with few species, however, having higher silica content (up to 1%) (Song et al. (2013); Torelli and Čufar (1995)). Thus, bamboo silica takes up a considerable part of the biomass.

During the utilization of bamboo biomass in biorefineries, rather than taking silica as a complication, silica in the raw material can be used as a sustainable feedstock for various high-value products such as for the production of catalysts, thixotropic agents, pharmaceuticals, film substrates, or used as mescoporous structured silica for adsorption processes and as fillers in cement (Kalapathy et al. (2002); Liou and Yang (2011); Klapiszewski et al. (2015)). Accordingly, similar to the pre-extraction of hemicellulose and lignin from biomass, the pre-extraction of silica along with lignocellulosic components from raw materials prior to pulping and biofuels production could be a promising method to resolve the silica problems.

Alkali can be used to dissolve silica and transfer the generated soluble silicates into the bulk liquor; this provides a means of extracting silica prior to subsequent processing steps (Section 3.1). Alkali dissolution of silica from lignocellulosic biomass can also be referred as alkaline pretreatment of biomass. Alkaline pretreatment is another chemical/hydrothermal pretreatment technology that has been used to extract hemicellulose from biomass. Several alkaline reagents, including sodium hydroxide (NaOH), calcium hydroxide ($Ca(OH)_2$), potassium hydroxide (KOH), aqueous ammo-

nia, ammonia hydroxide (NH_4OH), and NaOH incombination with hydrogen peroxide (H_2O_2), have been investigated for the pretreatment of lignocellulosic feedstocks (Kumar et al. (2009); Jun et al. (2012); Walton et al. (2010); Alvarez-Vasco and Zhang (2013)). Although the type of alkali had little effect on the extraction efficiency of hemicellulose from lignocellulosic feedstocks, it did affect the extent of lignin removal (Jin et al. (2010)). For example, NaOH and KOH have been reported to be more effective in lignin removal while NH_4OH has little effect (Huang et al. (2008)). Moreover, different from the pretreatment under acidic conditions, the alkaline pretreatment can be carried out at relative low temperatures (room temperature) and wide range of times (from seconds to days) (Mosier et al. (2005)).

Hydrolysis under alkaline conditions also causes the cleavage of lignin bonds and glycosidic hemicellulose bonds as well as disruption of ester bonds crosslinking lignin and hemicellulose, resulting in the removal of hemicellulose and lignin. The most important alkali-catalyzed reactions include polysaccharides dissolution, deacetylation of hemicellulose, peeling reactions of carbohydrates, and random hydrolysis followed by secondary peeling reactions (Jin et al. (2010); Lehto and Alén (2013)). The alkaline peeling reaction removes terminal anhydro-sugar units to generate new reducing end groups until a competitive stopping reaction begins and forms a stable saccharide acid end group. At the same time, dissolution or/and degradation of lignin, removal of extractives, and saponification of esters (fats and waxes) are occurring (Lehto and Alén (2013)). Alkaline pretreatment also removes acetyl and uronic substitutents on hemicellulose by alkaline saponification (Zhang and Lynd (2004)).

Alkaline pretreatment of biomass results in the reduction in the degree of polymerization and crystallinity of cellulose and swelling of fibres, which increases the

surface area and accessibility of treated solids to enzymes and chemicals used during subsequent processing. In addition, compared to the pretreatments with other alkalis, NaOH pretreatment can also cleave the ester bonds between lignin and/or hemicellulose and hydroxycinnamic acids, such as p-coumaric and ferulic acids (Spencer and Akin (1980)), thereby enhancing the removal of hemicellulose and lignin.

Compared with acid and autohydrolysis, alkaline treatment is more effective method at breaking ester bonds between lignin, hemicellulose and cellulose, and limiting fragmentation of hemicellulosic polymers; many of the sodium salts of organic acids can be recovered and/or regenerated (Gáspár et al. (2007); Xu and Huang (2014)). Under alkaline conditions, softwood glucomannan is rapidly degraded by the peeling reaction while most of xylan in hardwood, bamboo and cereal straw is solubilized in the oligomer form (van Heiningen (2006); Jin et al. (2010)). Moreover, it has been reported that alkaline pretreatment is regarded to be more effective at removing hemicellulose from xylan-rich lignocellulosic biomasses (hardwoods, bamboo and agricultural residues) than softwoods (van Heiningen (2006); Huang et al. (2010); Yoon and van Heiningen (2010)).

Increasing severity by increasing temperature, time, or alkali charge facilitated solids dissolution from lignocellulosic biomass (Yoon and van Heiningen (2010); Vena et al. (2013)). Vena et al. (2013) investigated the alkaline pre-treatment of hardwoods prior to pulping. They reported that the maximum xylan recovery yield of 16% (based on dry wood mass) could be obtained by increasing the temperature, time and NaOH concentration to 90 ^oC, 240 min and 2 mol/L, respectively (Vena et al. (2013)). However, high temperature, long reaction time and high alkaline charge facilitate generation of carboxylic acids. For example, Lehto and Alén (2015) investigated

NaOH treatment of softwood chips at 130 and 150 ^oC with 1-8% alkali charge for 30-120 min and these treatments resulted in 2.0-13.6% removal of the original dry wood material with the main constituents in the dissolved organic fraction being various carboxylic acids (volatile formic and acetic acids and non-volatile hydroxy monocarboxylic and hydroxy dicarboxylic acids). The lower alkali charges were found to favor the formation of the carboxylic acids.

Yoon and van Heiningen (2010) investigated the green liquor hydrolysis of Loblolly pine chips at temperature of 170-190 ^oC with green liquor charge of 2-6% (w/w) (as Na_2O) and compared to pure water extraction with final pH of about 4 at 170-190 ^oC (Yoon and van Heiningen (2008); Yoon and van Heiningen (2010)). The results demonstrated that the sugar yields of xylose and mannose were both lower with alkali addition; the mannose yield after green liquor hydrolysis was approximately 92.7% lower than that of the autohydrolysis yield. A similar green liquor pretreatment of mixed hardwood chips dissolved approximately 60% of initial mannan using an alkali charge of 8% (w/w) at 160 ^oC (Jin et al. (2010)). Xylan dissolution increased with alkali charge, however, it was difficult to remove more than 25% of the initial xylan even at an alkali charge of 20% (w/w). Nearly 100% cellulose could be preserved during alkaline pretreatment. The low extent of polysaccharides removal could be due to the pH being too low to start random hydrolysis and secondary peeling reactions (Jin et al. (2010)).

The monomer concentration in the alkaline hydrolysate is lower than that of acidic hydrolysate (Yoon and van Heiningen (2010); Lehto and Alén (2013)). Low alkali charge ($< 6\%$ of biomass) favors the monomer production (Lehto and Alén (2013)). Walton et al. (2010) compared hydrolysis of mixed southern hardwood chips with hot

water and alkali (alkali charge of 2-8%) at the same conditions of 160 ^oC for 1-2 h. Xylose concentration in alkaline hydrolysate did not show as strong correlation with the severity of treatment as that was found for water hydrolysis (Walton et al. (2010)). During alkaline pretreatment, glucose units are liberated by alkaline hydrolysis or peeling reaction from cellulose chains. Due to the high crystallinity and degree of polymerization (DP), cellulose is more resistant towards alkaline media and suffers less degradation than hemicellulose. For example, less than 2% of cellulose was removed during alkaline treatment of wheat straw with the utilization of 1.5% NaOH at 20 ^oC for up to 144 h while up to 90% of hemicellulose was extracted (Sun et al. (1995)).

Several studies have also been conducted with bamboo. Yamashita et al. (2010) investigated alkaline peroxide pretreatment to improve the enzymatic saccharification of treated bamboo chips. They found that the combination of 1% NaOH with 1% (v/v) H_2O_2 could yield 399 mg/g (initial dry sample) of glucose without using severe conditions such as high NaOH concentration or high temperature. Li et al. (2014) subjected bamboo powder (2.0 mm) from different bamboo layers (bamboo green, bamboo timber and bamboo yellow) to alkaline pretreatment with 6-12% NaOH (w/w) at 180 ^oC for 30 min. These treatments removed 54.5% of xylose and 60.2% of lignin from bamboo when treating with 12% NaOH (w/w) at 180 ^oC for 30 min (Li et al. (2014)). This study showed that the dissolution of lignin and hemicellulose was mainly dependent on the loading of NaOH (Li et al. (2014)). During alkaline pretreatment, the separated and fully exposed micro-fibrils increased the external surface area and the porosity, thereby facilitating subsequent enzymatic and chemical processing for the production of dissolving grade pulp and lignocellulosic fuels.

However, previous studies on the alkaline pretreatment of bamboo chips prior to

pulping were mainly focused on the extraction of hemicellulose/lignin for the production of kraft pulp, high-grade dissolving pulp or fermentable sugar (Leenakul and Tippayawong (2010); Luo et al. (2013); Yamashita et al. (2010); Li et al. (2014); Sathitsuksanoh et al. (2010)). Limited investigation has been conducted in extracting silica from bamboo. Additionally, the extracted silica can also be an excellent resource for silica-derived products (Zhang et al. (2013)). Thus, it would be useful to fabricate nanosilica from renewable silica-containing biomass material in a cost-effective way.

In addition, alkaline pretreatment of lignocellulosic materials can be well-integrated with an existing alkaline process such as kraft pulping, since it can lower the alkali charge required in subsequent cooking or bleaching step and hence preserve the pulp quality (Jun et al. (2012); Huang et al. (2008); Huang et al. (2010); Helmerius et al. (2010)). Moreover, the hemicellulose extracted during the alkaline pre-extraction process can be used for the generation of value-added products such as bioethanol, furfural, acetone or papermaking additives (Bai et al. (2012); Liu et al. (2013); Mao et al. (2008); Hamzeh et al. (2013)). In addition, for the production of dissolving grade pulp, near-complete removal of hemicellulose is required (Sixta (2006)). Alkaline pre-extraction of hemicellulose also promises an alternative way to produce dissolving pulp from high silica biomasses by pre-extracting silica and hemicellulose prior to pulping.

Among different alkali reagents investigated for the removal of silica from bamboo or other high silica biomasses, NaOH is considered to be a better choice as it is readily available in the form of white liquor in kraft pulping operations and the co-precipitation caused by the interaction of silica with some polyvalent alkali cations

(Ca^{2+}, Mg^{2+}, Fe^{3+}, Al^{3+} and Cu^{2+}) can be significantly alleviated (Le et al. (2015)). Within this context, the pre-extraction of silica prior to subsequent commercial pulping may not only be able to solve the silica problems of using bamboo in kraft pulping but also would add value and increase revenue to the mill.

Moreover, it has been suggested that chip size play an important role in the extraction of hemicellulose or other products from wood chips (Brennan and Wyman (2004); Rissanen et al. (2014a)). Thus, to minimize the mass transfer effects on the extraction of silica from bamboo, alkaline pretreatment of bamboo powder was evaluated. In the work presented in this section, alkaline pretreatment was carried out to completely extract silica and partially separate hemicellulose from bamboo powder. The effects of pretreatment conditions (NaOH concentration, temperature and time) on silica and hemicellulose pre-extraction were investigated. The comparison of the dissolution of silica from bamboo powder and pure amorphous silica was made to understand the mechanism for silica extraction. Moreover, chemical reactions involved in alkaline treatment of bamboo biomass are proposed and a toy model to describe the evolution of OH^- concentration is given.

3.2.2 Materials and Methods

The washed commercial bamboo chips used in Chapter 2 were taken as the raw feedstock. Some dried bamboo chips were ground using a Wiley Mill and sieved to a particle size of 40-60 mesh. The bamboo powder was collected in glass jars for further use. All chemicals used were reagent grade and solutions were prepared with purified deionized water.

Table 3.3: A summary of experimental conditions investigated for alkaline treatment of bamboo powder.

Temperature (^oC)	time (min)	$[OH^-]_o$ (mol/L)
70	$0 < t < 180$	0.15-0.525
80	$0 < t < 180$	0.15, 0.45
90	$0 < t < 180$	0.15, 0.45
100	$0 < t < 180$	0.15, 0.45

$[OH^-]_o$ and t refer to initial NaOH concentration and time.

Alkaline pre-extraction experiments on bamboo powder (40-60 $mesh$) were carried out in 4 silicate glass bottles of 500 mL capacity immersed in a laboratory-scale heated oil bath. A series of isothermal pre-extraction experiments were conducted over various temperatures (70-100 ^oC), times (5-180 min) and initial NaOH concentrations (0.15-0.45 mol/L) at constant liquid-to-wood ratio (10 L/kg) (Table 3.3). For an alkaline pre-extraction run, bamboo powder of 20 g oven dried (o.d.) and the calculated volume of deionized water and NaOH solution (stock concentration of 100 g/L) were mixed and placed in a reactor. Subsequently, the reactor was placed in the oil bath pre-heated to the target temperature. After the treatment, the vessels were rapidly cooled down in an ice/water bath. The pre-treated bamboo powder was separated from the liquor through filtration. The liquor was collected and then stored at 4 ^oC for the compositional analysis. The treated powder was washed thoroughly with deionized water to remove dissolved substances and collected for component analysis. All experiments were performed in triplicate.

The chemical composition was determined according to the NREL standard protocol described in Chapter 2. The ash and silica content of the solid samples were measured based on the methods described in Chapter 2. The silica content of the liquor was measured by using the silicon molybdenum blue photometric method (Tong

et al. (2005)). Briefly, 1 mL APEL was dissolved in 10 mL HNO_3 solution. After shaking, 10 mL ammonium molybdate ($(NH_4)_6Mo_7O_{24}$) was added into the solution. The solution was gently heated at 30 ^oC for 12 min in a shaking water bath (75 rpm). After cooling, 40 mL ammonium ferrous sulfate ($(NH_4)_2Fe(SO_4)_2 \cdot 6\,H_2O$) was added to the solution. The resultant solution was made up to 250 mL with a volumetric flask. The silica content was measured at wavelength 813 nm with a UV-vis spectrophotometer. The residual alkali concentration in the liquor was determined by titration with hydrochloric acid (HCl) according to TAPPI T 625 cm-85.

3.2.3 Results and Discussion

Application of Shrinking Core Model in Silica Removal from Bamboo Powder

The composition of the bamboo feedstock used in this study has been determined and shown in Table 2.2 in Chapter 2. In this section, the main purpose of alkaline pre-extraction of bamboo powder is to understand the reaction kinetics on alkaline pre-extraction of bamboo biomass by minizing the mass transfer effects. The other goal is to preserve lignin and cellulose in the pretreated biomass. This is because the presence of lignin in the spent pre-extraction liquor hampers its utilization in bioethanol or xylitol production as lignin degradation products inhibit the growth and metabolic activity of micro-organisms used in bioconversion processes. Moreover, silica recovery through lowering the pH of alkaline pre-extraction liquor is also negatively affected due to the co-precipitation of lignin (Minu et al. (2012); Shi et al. (2011)). Since pre-extraction processes using high temperature and low alkali concentration have

several drawbacks such as high capital investment cost and low molecular-mass of the extracted hemicellulose (Jun et al. (2012); Yoon and van Heiningen (2010)), high alkali concentration and relatively lower reaction temperatures were investigated in this work.

To minimize the mass transfer limitations, bamboo powder (250-400 μm) was used for the alkaline treatment. To verify the utility of shrinking core model in modelling the extraction of silica from bamboo powder, alkaline treatment was carried out at the same temperature (70 ^oC) as used for the dissolution of pure amorphous silica under various NaOH concentrations (Fig. 3.8). As shown, the extraction of silica increased with the increase of NaOH concentration.

Fig. 3.9 shows the results of the application of Equation 3.13 to describe the dissolution of silica from bamboo powder. Here, it can be observed that large deviations were obtained when plotting $(1 - \alpha^{\frac{1}{3}})$ against reaction time t (min) at lower NaOH concentrations ($< 0.45\ mol/L$), indicating that the removal of silica from bamboo powder does not follow the fitting of standard shrinking core model. This might be due to competing reaction for the NaOH by wood components such as such as acetyl and uronic acid groups, xylan, and other extractives. When increasing the NaOH concentration, straight lines with $r^2 > 0.95$ passing through the origin were obtained, which means that the shrinking core model works at the high OH^- concentration. One explanation for this is that when using high OH^- concentration, the stoichiometric ratio of OH^- to silica is excessively large throughout the reaction process. Thus, it can be concluded that the increase of NaOH concentration could increase the silica dissolution rate from bamboo powder.

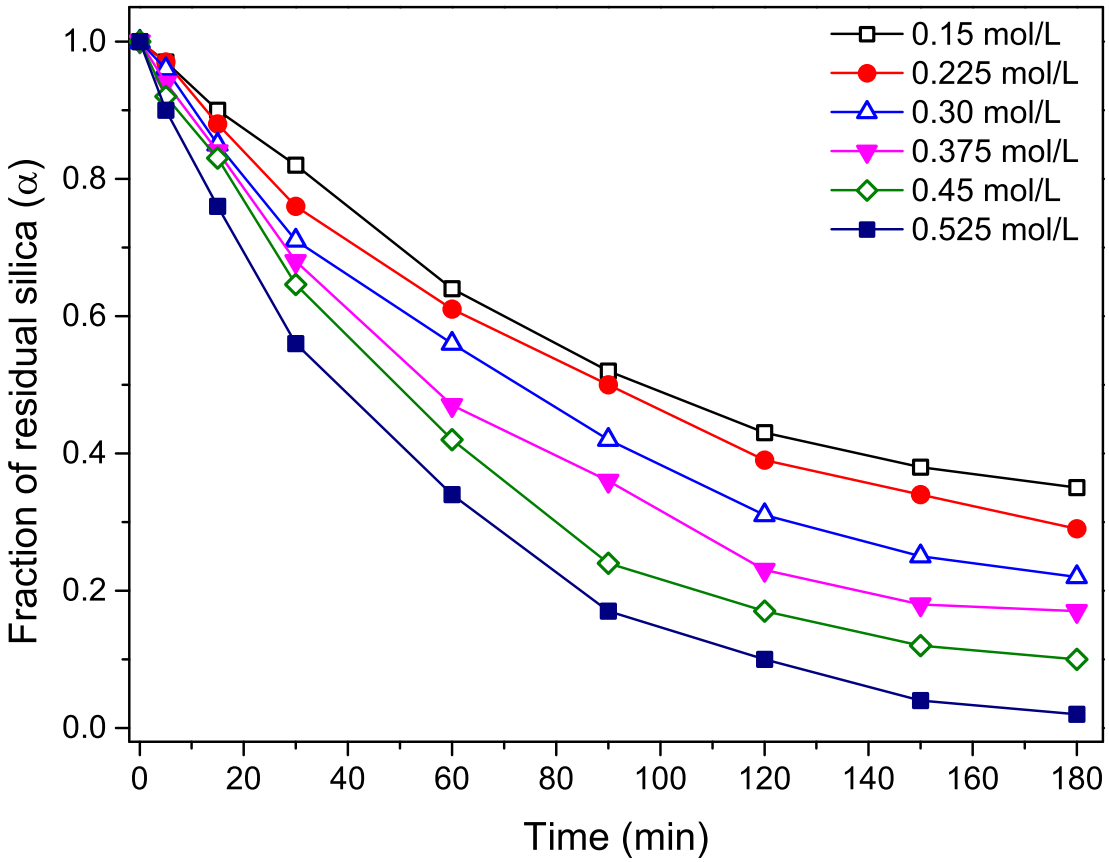

Figure 3.8: Effect of NaOH concentration on the extraction of silica from bamboo powder at 70 ^oC.

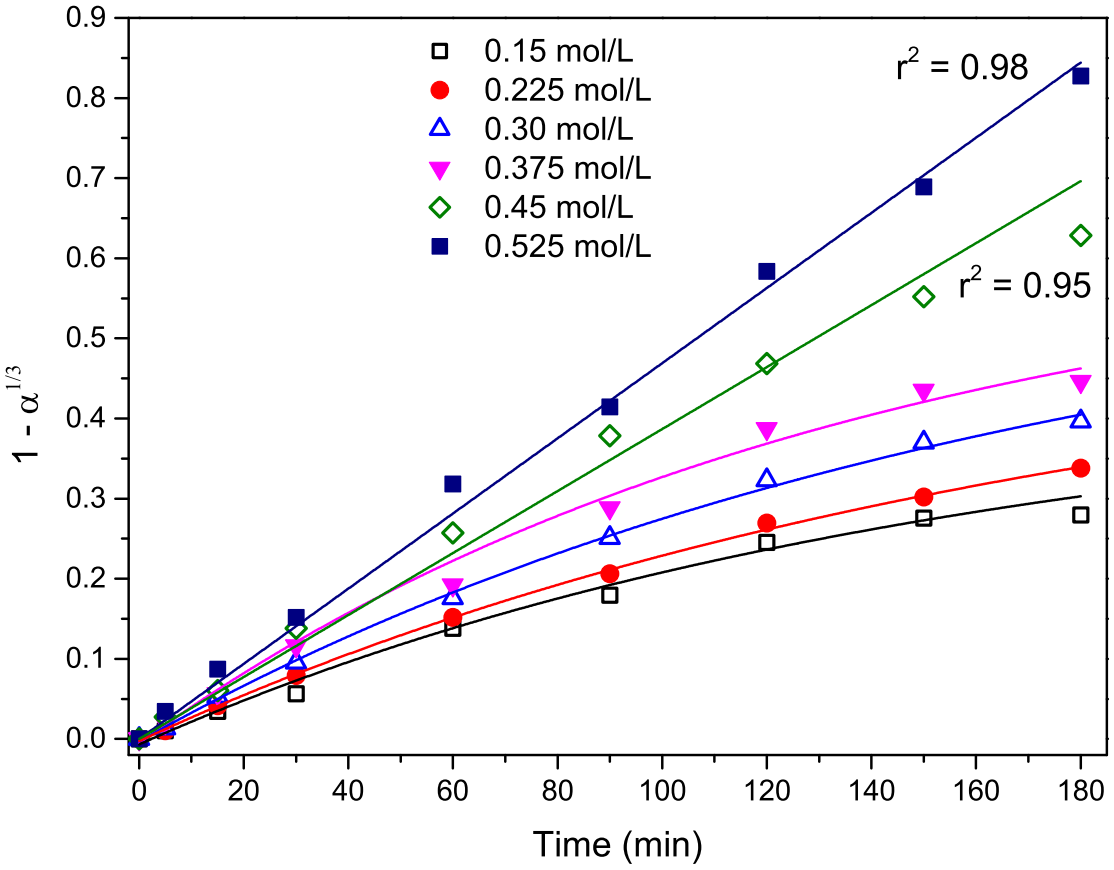

Figure 3.9: Application of shrinking core model on silica removal from bamboo powder (temperature = 70 ^oC).

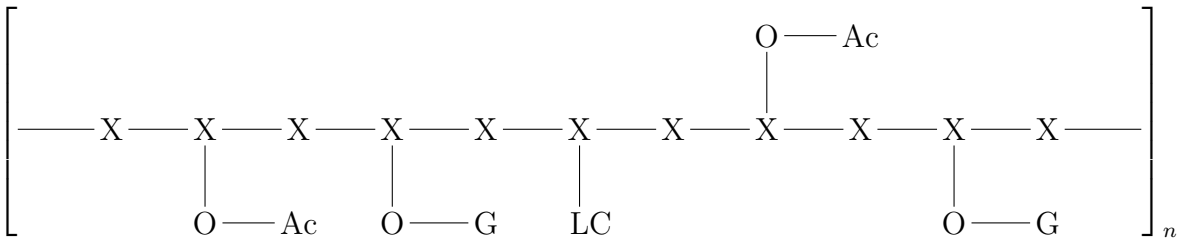

Figure 3.10: A schematic of the idealized hemicellulose - lignocellulose (LC) substrate considered in this work. X-X-X-X represents the backbone of the xylan structure. The species Ac, Ar and G, which represent the acetyl, arabinose and glucuronic acid groups, are initially bound to the xylan chain but are released through alkaline treatment. Silica and other ash components (MO) are not shown in this figure but are considered to be *physically* embedded in the LC portion of the matrix.

Toy Model

During alkaline pretreatment of bamboo biomass, the behavior of NaOH is complex. There are a number of pathways governing OH^- consumption and generation. Based on the discussion and definition in Chapter 2, an idealized hemicellulose structure for use in modelling the alkaline pretreatment is proposed and shown in Fig. 3.10.

For establishing the chemistry of the toy model, hydroxyl groups are represented by OH^- and protons by H^+; both of these species are considered to be in aqueous phase and the *aq* notation has been dropped. Sodium hydroxide (NaOH) is the alkali being added to the system. The acetyl group Ac and glucuronic acid G are defined as $H_3C{-}C(=O){-}$ and $C_5H_9O_5COOH$. During the alkaline pre-extraction of silica from bamboo, several reactions take place simultaneously.

As disscussed in Section 3.1, when silica is put into the NaOH solution, several reactions take place simutaneously (Wirth and Gieskes (1979)). The dissolution rate of silica in NaOH is considered to be a function of total reactant surface area of silica partciels (Niibori et al. (2000)). For simplicity, we consider the dissolution of silica

follows Equation 3.10 and the dissolution rate is given with Equation 3.11, in which r_i and k_i are defined as the chemical reaction rate and rate constant, respectively, A is the total surface area of silica particles, β is the reaction order with respect to $[OH^-]$.

We consider alkali consumption by Ac and G, which are cleaved from the hemicellulose backbone through an alkaline saponification of the ester bonds. Based on the stoichiometry, the reactions between NaOH and acetic and glucuronic acid follow first order kinetics.

$$\begin{aligned} \mathrm{XOAc} + \mathrm{NaOH} \xrightarrow{\mathrm{k_2}} \mathrm{Ac{-}O^-Na^+(aq)} + \mathrm{XOH(s)} \\ r_2 = k_2[\mathrm{XOAc}][\mathrm{OH^-}] \end{aligned} \tag{3.16}$$

$$\begin{aligned} \mathrm{XOG} + \mathrm{NaOH} \xrightarrow{\mathrm{k_3}} \mathrm{G{-}O^-Na^+(aq)} + \mathrm{XOH(s)} \\ r_3 = k_3[\mathrm{XOG}][\mathrm{OH^-}] \end{aligned} \tag{3.17}$$

where r_i and k_i are defined as the chemical reaction rate and rate constant, respectively.

These two reactions may occur with acetyl and glucuronic groups which are attached to either soluble or solid phases of the hemicellulose. For simplicity, any differences in rate between the alkaline saponification reaction occurring in the solid or liquid phases are ignored. As the products AcONa(aq) and GONa(aq), sodium acetate and sodium glucuronate, behave as salts with strong alkaline base; they adopt

the following equilibria in solution

$$\begin{gathered}\mathrm{Ac{-}O^{-}Na^{+}(aq) + H_2O \overset{K_{AcONa}}{\rightleftharpoons} Ac{-}OH + OH^{-} + Na^{+}} \\ K_{AcONa} = \frac{[\mathrm{AcOH}][\mathrm{OH^{-}}]}{[\mathrm{AcONa}]} = 5.56 \times 10^{-10}\end{gathered} \tag{3.18}$$

$$\begin{gathered}\mathrm{G{-}O^{-}Na^{+}(aq) + H_2O \overset{K_{GONa}}{\rightleftharpoons} G{-}OH + OH^{-} + Na^{+}} \\ K_{GONa} = \frac{[\mathrm{GOH}][\mathrm{OH^{-}}]}{[\mathrm{GONa}]} = 8.51 \times 10^{-12}\end{gathered} \tag{3.19}$$

where K_i, from this point is defined as the equilibrium constant and the value quoted is at room temperature (Avdeef et al. (1993); Wang et al. (1991)).

We consider xylan dissolution under mild alkaline conditions ($< 140\ ^oC$) is mainly derived from the peeling reaction (Sixta (2006)). Although the stopping reaction also occurs, but compared to peeling reaction, the stopping reaction rate is much slower, which is ignored in this modelling process. The degradation of xylan is assumed to follow the mechanism

$$\begin{gathered}\mathrm{X}_n(\mathrm{s}) \xrightarrow[\mathrm{OH^{-}}]{\mathrm{k}_{p1}} \mathrm{X}_{n-1}(\mathrm{s}) + \mathrm{DCOOH\,(aq)} \qquad n = 2, 3... \\ r_{p1} = k_{p1}[\mathrm{X}_n][\mathrm{OH^{-}}]\end{gathered} \tag{3.20}$$

$$\begin{gathered}\mathrm{DCOOH + NaOH \xrightarrow{k_4} DCOO^{-}Na^{+} + H_2O} \\ r_4 = k_4[\mathrm{DCOOH}][\mathrm{NaOH}]\end{gathered} \tag{3.21}$$

where DCOOH is the degradation product of xylan (xyloisosaccharinic acid). The neutralization of the formed degradation acid (Equation 3.21) consumes the alkali in the pretreatment liquor. Since the rate of neutralization reaction is fast, the degradation rate of xylan is mainly controlled by Equation 3.20. The disassociation of

$DCOO^-Na^+$ in solution (Perrin et al. (1981))

$$\begin{aligned} DCOO^-Na^+ + H_2O &\overset{K_D}{\rightleftharpoons} DCOOH + OH^- + Na^+ \\ K_D &= \frac{[DCOOH][OH^-]}{[DCOO^-Na^+]} = 1 \times 10^{-9} \end{aligned} \tag{3.22}$$

serves as a source of OH^-.

In a similar manner, cellulose, a linear polymer of repeating sugar units of glucose, also undergoes degradation to some extent by the peeling reaction

$$\begin{aligned} C_n(s) \xrightarrow[OH^-]{k_{p2}} C_{n-1}(s) + ECOOH(aq) \qquad n = 2, 3... \\ r_{p2} = k_{p2}[C_n][OH^-] \end{aligned} \tag{3.23}$$

where ECOOH is the degradation product of cellulose (glucoisosaccharinic acid). The neutralization of ECOOH

$$\begin{aligned} ECOOH + NaOH &\xrightarrow{k_5} ECOO^-Na^+ + H_2O \\ r_5 &= k_5[ECOOH][NaOH] \end{aligned} \tag{3.24}$$

$ECOO^-Na^+$ adopts the following equilibrium in solution (Käkölä and Alén (2006))

$$\begin{aligned} ECOO^-Na^+ + H_2O &\overset{K_E}{\rightleftharpoons} ECOOH + OH^- + Na^+ \\ K_E &= \frac{[ECOOH][OH^-]}{[ECOO^-Na^+]} = 1.58 \times 10^{-11} \end{aligned} \tag{3.25}$$

Since the neutralization reaction takes place fast, we consider the reactions given in Equations 3.21 and 3.24 to be instantaneous. To continue, lignin might also be

removed to some extent

$$\begin{aligned} \mathrm{Lignin\,(s)} + \mathrm{b[OH^-]} &\xrightarrow{\mathrm{k_L}} \mathrm{Lignin\,(s)} + \mathrm{P\,(aq)} \\ r_L &= k_L[\mathrm{Lignin}][\mathrm{OH^-}]^{\mathrm{b}} \end{aligned} \tag{3.26}$$

where b is the stoichiometry parameter with respect to NaOH and P is the degradation product of lignin. Since alkaline delignification of biomass starts at temperature higher than 100 ^oC (Sixta (2006)), the dissolved lignin could be mainly mono- or oligo-lignols (Arato et al. (2005)).

In the reaction system, water disassociation demands

$$\mathrm{H_2O} \overset{\mathrm{K_w}}{\rightleftharpoons} \mathrm{OH^-} + \mathrm{H^+} \qquad K_w = [\mathrm{OH^-}][\mathrm{H^+}] = 1 \times 10^{-14} \tag{3.27}$$

and this serves as an additional source of $\mathrm{OH^-}$.

In addition to these equilibria, the disassociation of NaOH is the main source of $\mathrm{OH^-}$ in the reaction system

$$\mathrm{NaOH} \xrightarrow{\mathrm{fast}} \mathrm{Na^+} + \mathrm{OH^-} \tag{3.28}$$

As NaOH is a strong alkali, we consider the disassociation given in Equation 3.28 to be instantaneous. The final aspect to consider is the dissolution of ash in water. As mentioned above the reaction scheme depends upon the species involved. Here, we consider a hypothetical oxide MO which reacts according to the following scheme

$$\mathrm{MO\,(s)} + \mathrm{H_2O} \rightleftharpoons \mathrm{M(OH)_2\,(aq)} \tag{3.29}$$

The dissolution of ash (MO) in the solution is assumed to be instantaneous.

$$\begin{aligned} \mathrm{M(OH)_2(aq)} &\overset{\mathrm{K}_m}{\rightleftharpoons} \mathrm{M^{2+}} + 2\,\mathrm{OH^-} \\ K_m &= \frac{[\mathrm{M^{2+}}(aq)][\mathrm{OH^-}]^2}{[\mathrm{M(OH)_2}]} \rightarrow 0 \end{aligned} \tag{3.30}$$

As the equilibrium constant K_m is unknown, we simply assign this value to be a very small number to reduce the number of free parameters. It should be noted that we do not characterize a number of the potential secondary reactions in solutions, even though they may affect the OH^- levels to a small degree. For example, we ignore the stopping reactions of xylan and glucan with NaOH for mathematical transparency as these have much slower reaction rate compared to that of the peeling reaction. The precipitation of metal hydroxides was also ignored for mathematical transparency.

Since the alkaline treatment temperature used in this study was low ($\leq 100\ ^oC$), the degradation of cellulose and lignin can be ignored. Thus, reactions shown in Fig. 3.11 can be used to describe the dominant mechanisms during alkaline treatment of bamboo.

Having established the chemistry of the toy model, we now construct the mathematical model. We build the model upon two conservation laws: conservation of mass of each of the species found in solution and an overall charge neutrality of the solution. Conservation of mass expresses that the initial moles of a certain species must sum to the total moles of the species in the reaction products. For example, the initial moles of M is $[\mathrm{MO}]_\mathrm{o}$, must balance the number of moles of M, in the species of [MO], $[\mathrm{M^{2+}}]$, and $[\mathrm{M(OH)_2}]$ at any time throughout the courses of the reaction. This

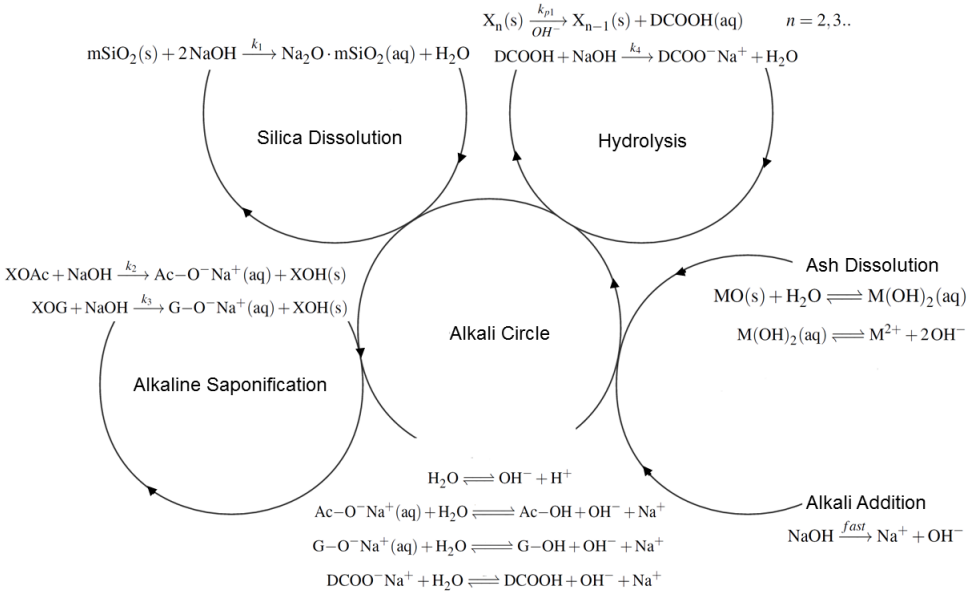

Figure 3.11: A schematic of the idealized reaction scheme. The chemical reactions shown present the dominant reaction mechanisms during alkaline treatment of bamboo biomass.

can be expressed as

$$\begin{aligned}[MO]_o &= [MO] + [M^{2+}] + [M(OH)_2] \\ &= [MO] + [M^{2+}]\left(1 + \frac{[OH^-]^2}{K_m}\right)\end{aligned} \tag{3.31}$$

through use of the equilibrium relationship given in Equation 3.30. In a similar manner, conservation of mass for the species Si, Ac, G, Na^+ can be expressed as

$$[SiO_2]_o = [SiO_2] + [H_4SiO_4] + m[Na_2O \cdot mSiO_2] \tag{3.32}$$

$$\begin{aligned}[\mathrm{XOAc}]_o &= [\mathrm{XOAc}] + [\mathrm{AcO^-Na^+}] + [\mathrm{AcOH}] \\ &= [\mathrm{XOAc}] + [\mathrm{AcONa}]\left(1 + \frac{K_{AcONa}}{[\mathrm{OH^-}]}\right)\end{aligned} \tag{3.33}$$

$$[\mathrm{XOG}]_o = [\mathrm{XOG}] + [\mathrm{GO^-Na^+}] + [\mathrm{GOH}] = [\mathrm{GOAc}] + [\mathrm{GONa}]\left(1 + \frac{K_{GONa}}{[\mathrm{OH^-}]}\right) \tag{3.34}$$

$$\begin{aligned}[\mathrm{NaOH}]_\mathrm{o} &= 2[\mathrm{Na_2O \cdot mSiO_2}] + [\mathrm{AcONa}] + [\mathrm{GONa}] \\ &\quad + [\mathrm{DCOONa}] + [\mathrm{Na^+}] \\ &= 2[\mathrm{Na_2O \cdot mSiO_2}] + \left(\frac{[\mathrm{AcOH}][\mathrm{OH^-}]}{K_{AcONa}}\right) + \left(\frac{[\mathrm{GOH}][\mathrm{OH^-}]}{K_{GONa}}\right) + \\ &\quad \left(\frac{[\mathrm{DCOOH}][\mathrm{OH^-}]}{K_D}\right) + [\mathrm{Na^+}]\end{aligned} \tag{3.35}$$

with use of Equations 3.10, 3.11, 3.18, 3.19, and 3.22. To continue, the charge neutralization conservation equation is invoked, i.e.

$$[\mathrm{Na^+}] + [\mathrm{H^+}] + 2\,[\mathrm{M^{2+}}] = [\mathrm{OH^-}] \tag{3.36}$$

Thus, Equation 3.36 can be expressed as

$$\begin{aligned}[\mathrm{OH^-}] = [\mathrm{OH-}]_o - \frac{2}{m}\left([\mathrm{SiO_2}]_o - [\mathrm{SiO_2}]\right) - \left(\frac{[\mathrm{XOAc}]_o - [\mathrm{XOAc}]}{\left(1 + \frac{K_{AcONa}}{[\mathrm{OH^-}]}\right)}\right) \\ - \left(\frac{[\mathrm{XOG}]_o - [\mathrm{XOG}]}{\left(1 + \frac{K_{GONa}}{[\mathrm{OH^-}]}\right)}\right) - \left(\frac{[\mathrm{X}]_o - [\mathrm{X}]}{\left(1 + \frac{K_D}{[\mathrm{OH^-}]}\right)}\right) + \frac{K_w}{[\mathrm{OH^-}]} + 2\left(\frac{[\mathrm{MO}]_o - [\mathrm{MO}]}{1 + \frac{[\mathrm{OH^-}]^2}{K_m}}\right)\end{aligned} \tag{3.37}$$

through use of Equations 3.31-3.35. This equation (Equation 3.37) gives the residual OH^- concentration in the reaction system during the process of alkaline treatment of bamboo powder. This equation also indicates that the residual alkali concentration in the solution is governed by silica dissolution, alkaline saponification of acetyl and glucuronic acid groups, the amount of neutralization by the formed degradation products from xylan and cellulose, five different equilibria found in solution (K_m, K_{AcONa}, K_{GONa}, K_D), and the amount of alkali initially added ($[NaOH]_0$).

Removal of Silica and Hemicellulose from Bamboo Powder

A series of experiments were carried out over a wide range of reaction conditions (see Material and Methods Section). The chemical composition of the treated samples was analyzed. As an example, the composition of bamboo powder obtained from the extraction at 100 ^oC is shown in Table 3.4. The yields are reported in percentage and related to original oven-dried bamboo mass. As can be observed from Table 3.4, the treatment yield decreased with increasing the extraction severity. For example, at 100 ^oC, the use of 0.15 mol/L NaOH resulted in biomass yields between 89% and 99% while the yield decreased to 82%-97% with initial NaOH concentration of 0.45 mol/L. Results in Table 3.4 also showed that alkaline extraction under low temperatures ($<$ 100 ^oC) resulted in little loss of cellulose and lignin while significantly reducing the hemicellulose (mainly xylan) and silica contents. On the basis of the powder yield and compositional analysis, the actual loss of the different bamboo components during the alkaline extraction was calculated (calculation not shown). At 100 ^oC, by increasing the initial NaOH concentration from 0.15 to 0.45 mol/L and reaction time from 5 to 180 min, the calculated cellulose and lignin mass fraction losses were 0.4-5.1% and

0.3-6.4% (based on initial starting raw material), respectively. The high crystallinity and limited accessibility towards chemicals make cellulose very recalcitrant towards degradation under mild conditions such as those utilized in this study (Engström et al. (2006)). Low amounts of extracted lignin would benefit the recovery of silica from alkaline pre-extraction liquor (APEL) by reducing lignin co-precipitation, resulting in high purity silica particles. The loss of galactan and arabinan, did not contribute much to yield loss as the content in the starting material was low (total mass fraction less than 1.5% in raw chips); the majority of the extracted hemicellulose was xylan.

Fig. 3.12 shows the fraction of residual xylan remaining in the extracted bamboo powder as a function of reaction time. The error bars are calculated from the average values from triplicate experiments at 100 ^oC with the standard deviation (95% confidence interval). As shown in Fig. 3.12, the amount of residual xylan decreased with increasing reaction time, treatment temperature and NaOH concentration. During initial alkaline treatment, xylan solubilization is rapid and solubilization slows down with increasing time, especially at low initial NaOH loading. This is probably because the consumption of NaOH by bamboo components such as silica, acetyl and glucuronic acid groups lower the hydroxyl ions (OH^-) available for the attack of the hemicellulose structure. For example, at the initial NaOH concentration of 0.15 mol/L and the treatment time of 180 min, increasing the temperature from 70 to 100 ^oC only resulted in the removal of about 7-18% of initial xylan (Fig. 3.12a). Approximately 20% of the original xylan mass was extracted by treating bamboo powder at 70 ^oC with initial NaOH concentration of 0.45 mol/L for 180 min. In contrast, at 100 ^oC with the same initial NaOH concentration (0.45 mol/L), up to 56% of xylan was extracted in 180 min (Fig. 3.12b).

Table 3.4: Chemical composition of bamboo powder after pre-extraction with NaOH at 100 ^oC.

NaOH (mol/L)	Time (min)	Yield (%)[a]	Glucose (%)[b]	Xylose (%)[b]	Galactose (%)[b]	Arabinose (%)[b]	Lignin (%)[b]	Silica (%)[b]
0.15	5	98.9	47.63±0.78	20.05±0.15	0.65±0.05	0.71±0.04	24.38±0.14	1.01±0.02
	15	97.4	47.78±1.26	19.56±0.24	0.68±0.03	0.54±0.10	24.34±0.18	0.85±0.02
	30	95.6	48.79±0.45	18.86±0.29	0.58±0.06	0.63±0.07	24.55±0.25	0.68±0.01
	60	92.8	50.07±0.96	18.09±0.32	0.62±0.04	0.56±0.06	25.04±0.37	0.45±0.03
	90	91.6	50.36±0.85	17.63±0.18	0.65±0.06	0.39±0.12	25.21±0.49	0.32±0.02
	120	90.3	50.62±1.12	17.16±0.36	0.48±0.10	0.55±0.08	25.36±0.66	0.26±0.02
	150	89.2	50.71±0.72	16.85±0.27	0.36±0.12	0.62±0.04	25.69±0.68	0.21±0.03
	180	88.7	50.83±0.66	16.65±0.31	0.43±0.08	0.52±0.09	25.81±0.32	0.19±0.01
0.45	5	97.2	48.43±0.88	19.84±0.25	0.68±0.04	0.74±0.05	24.82±0.14	0.89±0.03
	15	95.6	48.94±1.02	18.47±0.32	0.73±0.02	0.70±0.04	24.98±0.25	0.48±0.02
	30	92.2	50.14±0.57	17.39±0.27	0.69±0.06	0.64±0.10	25.56±0.47	0.21±0.03
	60	87.1	52.17±1.34	15.62±0.44	0.64±0.04	0.57±0.08	26.7±0.86	0.05±0.02
	90	85.6	52.96±1.86	14.70±0.24	0.52±0.10	0.48±0.12	26.97±0.74	0.01±0.006
	120	84.5	52.57±1.67	13.45±0.38	0.36±0.12	0.53±0.06	27.23±0.95	ND
	150	83.4	53.48±0.94	13.63±0.25	0.57±0.22	0.64±0.09	27.44±0.83	ND
	180	82.2	53.93±0.72	13.33±0.43	0.49±0.14	0.42±0.14	27.56±0.72	ND

[a] Calculations were based on initial o.d. chip mass. [b] Values were calculated based on treated o.d. chip mass. ND-not detected.

The other goal of the alkaline pre-extraction was to extract silica prior to pulping. With alkaline extraction, the amount of silica removal from bamboo powder increased with increasing NaOH charge and temperature. Fig. 3.13 shows the fraction of residual silica remaining in the extracted solids as a function of time. The error bars are calculated from the average values from triplicate experiments at 100 ^oC with the standard deviation (95% confidence interval). Results shown in Fig. 3.13 clearly illustrate that faster removal of significant amounts of silica requires either increasing the initial NaOH concentration or treating at higher temperature for longer times. For example, alkaline treatment of bamboo powder for 180 min with the initial NaOH concentration of 0.15 mol/L at 70 and 100 ^oC resulted in the extraction of about 65% and 84% of initial silica, respectively. One reason has been discussed in Section 3.1, which is that increasing the treatment temperature increases the reaction rate between silica and NaOH. The other likely reason for the less effectiveness of silica removal at lower initial NaOH concentration such as 0.15 mol/L might be that some alkali is consumed or neutralized by bamboo components such as acetyl and uronic acid groups (Gossett et al. (1982); Pavlostathis and Gossett (1985)), resulting in much reduced [OH^-] in later stages for the reaction. In contrast, using initial NaOH concentration of 0.45 mol/L at 100 ^oC, nearly 95% of silica could be extracted from bamboo powder in 45 min. Moreover, after the removal of 96% of silica mass, the silica content of treated material was about 0.04% or even less (based on treated o.d. solid mass), which means that even the silica impact on the production of high purity dissolving-grade pulp can be eliminated (Sixta (2006)). With such low amount of silica ($\leqslant$ 0.04%, w/w) in the treated bamboo sample, the adverse effect of silica on the chemical recovery process of kraft pulping can be significantly reduced.

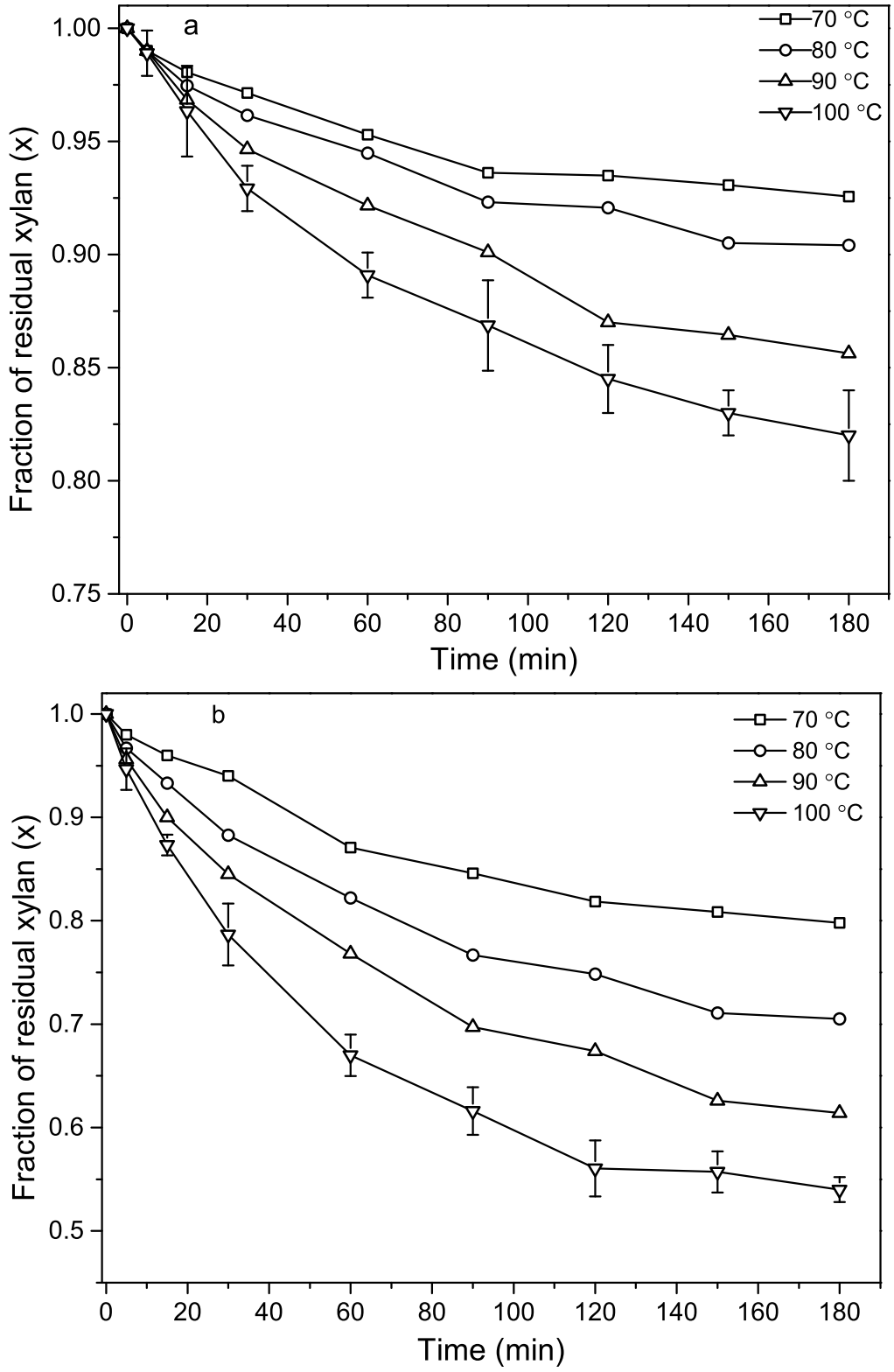

Figure 3.12: Experimental yields of xylan remaining in the extracted milled bamboo powder at alkaline pre-extraction temperatures of 70-100 ^oC (initial NaOH concentration: a = 0.15 mol/L; b = 0.45 mol/L).

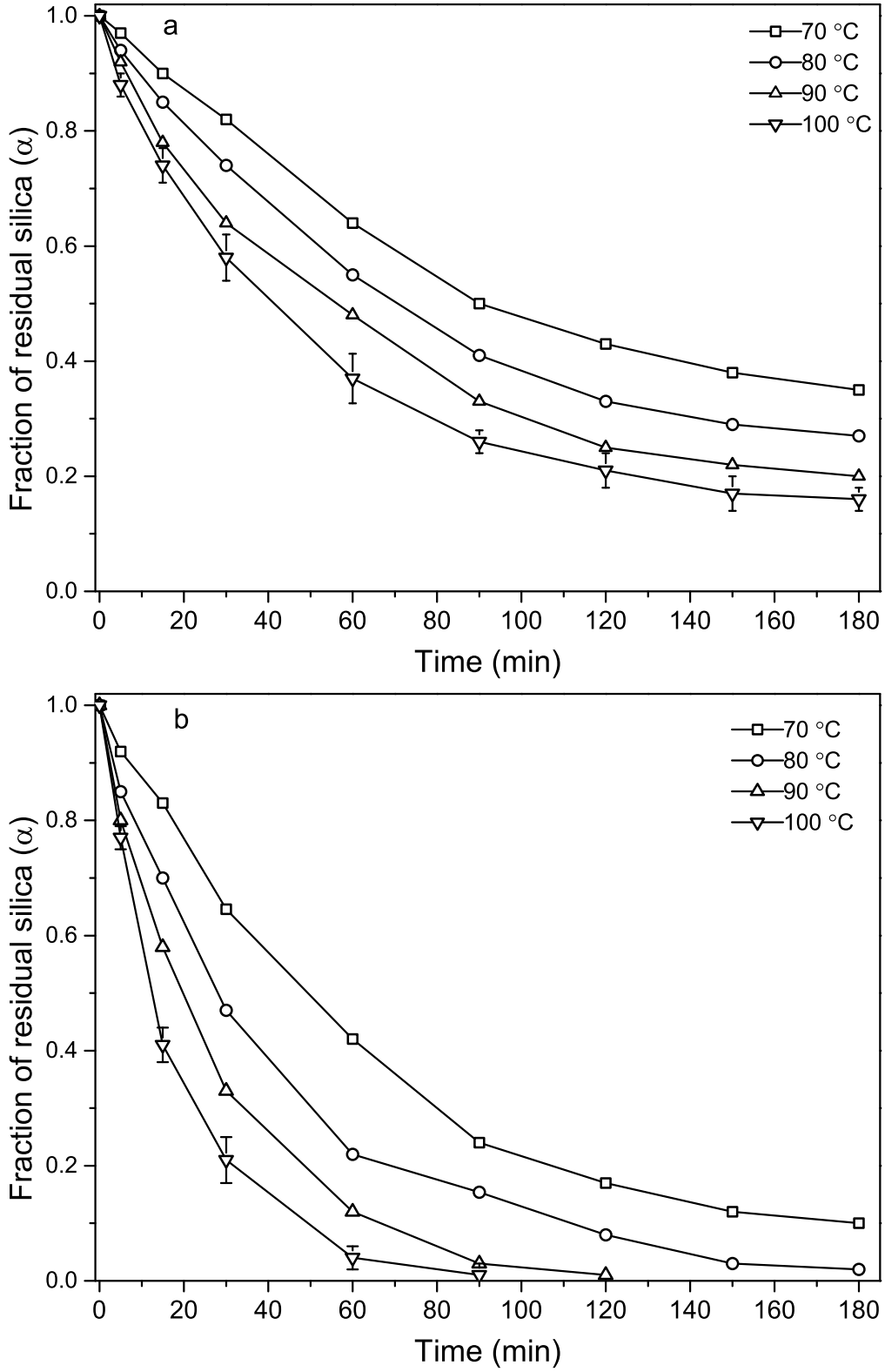

Figure 3.13: Experimental yields of silica remaining in the extracted milled bamboo powder at alkaline pre-extraction temperatures of 70-100 ^oC (initial NaOH concentration: a = 0.15 mol/L; b = 0.45 mol/L).

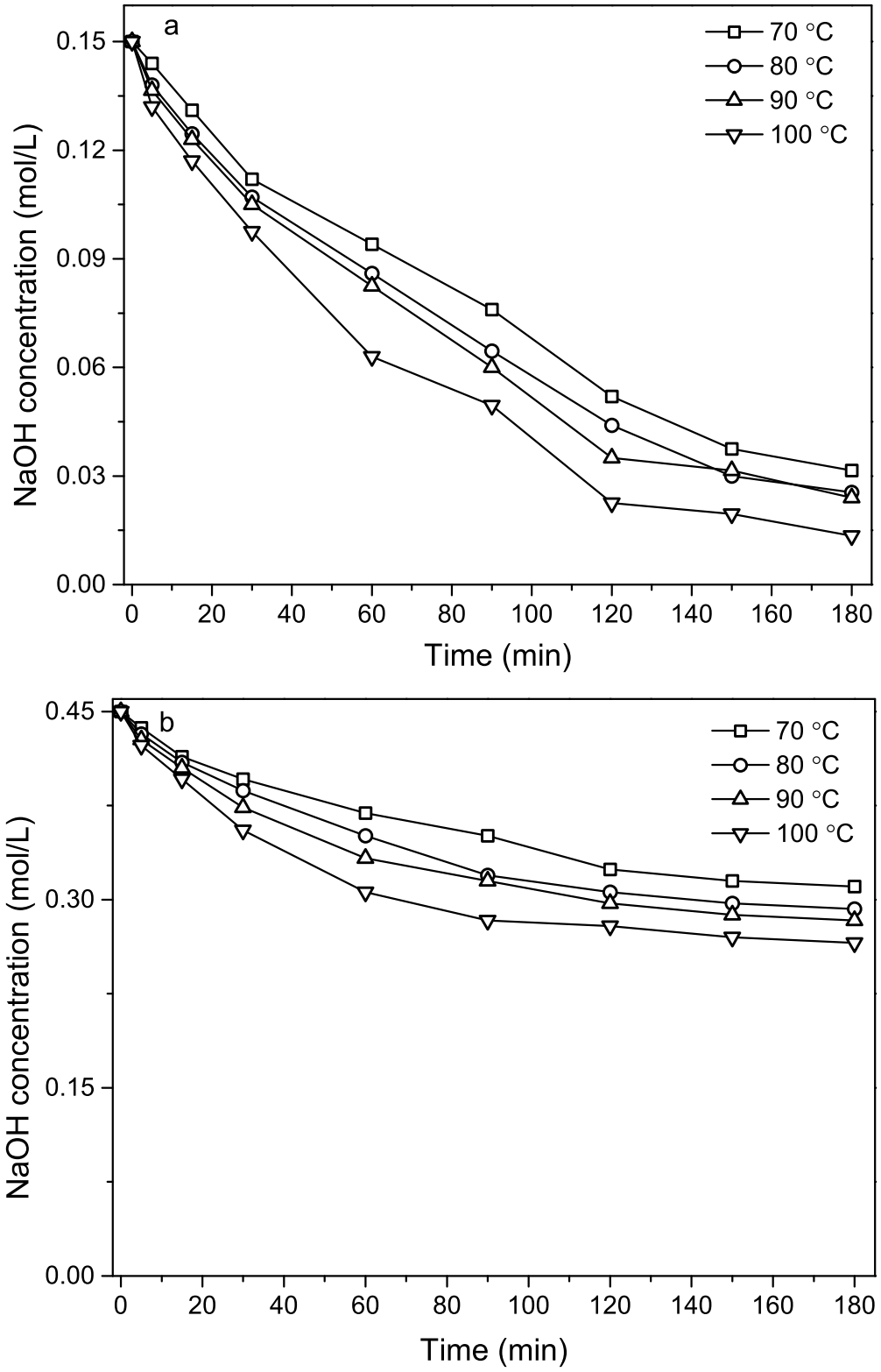

Figure 3.14: NaOH concentration during alkaline pre-extraction of bamboo powder at temperatures of 70-100 ^oC (initial NaOH concentration: a = 0.15 mol/L; b = 0.45 mol/L).

To further assess the effects of alkaline pre-extraction on the dissolution of bamboo components, the sugars, soluble lignin and silica in the extract liquors were analyzed. Table 3.5 shows the chemical composition of liquors obtained from the alkaline pre-extraction at 100 ^oC with initial NaOH concentration of 0.45 mol/L. The yields are reported in weight percentage of original o.d. wood mass. An interesting observation is that the sum of powder yield (Table 3.4) and solid contents of the alkaline pre-extraction liquor (APEL) (Table 3.5) was larger than 100% in the treatment experiments. The excess values of the mass balance might be partly due to the sodium ions bound to dissolved components such as acetic or glucuronic acid. On the other hand, the weight of extraneous inorganic compounds dissolved in the alkaline extracts such as NaOH also contributed to the total solid content. As shown in Table 3.5, varying the severity of the pre-treatment had little effect on the extraction of glucan and lignin from bamboo powder into the APEL. In contrast, a large portion of silica and hemicellulose in the raw material were extracted. In addition, the silica content at the maximum silica removal (120-180 min) was calculated to be in the range of 1.10-1.13% (based on original o.d. mass of bamboo biomass), indicating almost all silica in bamboo was extracted during alkaline pre-treatment (Table 3.5). At extraction conditions that resulted in the removal of more than 97% of initial silica, the xylan content in the APEL reached up to 7% (based on the original o.d. bamboo powder). Moreover, data in Tables 3.4 and 3.5 also show that the sum of xylan content in both biomass residuals and APELs was 88.3-96.6% of the initial xylan in raw material, revealing a reasonable mass balance. The 4-12% xylan not accounted for might be lost during sample washing after the pre-extraction or through xylan degradation into products undetected by the methodology used. Moreover, as shown in Table

Table 3.5: Composition of hydrolysates (based on initial o.d. bamboo powder) obtained from alkaline treatment at 100 ^oC with NaOH concentration of 0.45 mol/L.

	time (min)					
Products	30	60	90	120	150	180
Xylose (%)	3.36±0.24	5.54±0.31	6.25±0.27	7.12±0.51	7.07±0.46	6.97±0.34
Galactose (%)	0.05±0.2	0.02±0.02	0.16±0.2	0.14±0.04	0.17±0.05	0.10±0.02
Arabinose (%)	0.15±0.02	0.15±0.03	0.17±0.04	0.13±0.06	0.21±0.04	0.27±0.02
Glucose (%)	0.98±0.12	1.23±0.73	1.19±0.65	1.36±0.52	1.26±0.81	1.55±0.79
Lignin (%)	0.45±0.14	0.51±0.61	0.53±0.22	0.68±0.17	0.70±0.56	0.84±0.67
Silica (%)	0.90±0.03	1.04±0.02	1.07±0.02	1.10±0.03	1.10±0.03	1.10±0.03
Total solids (%)	26.54	29.77	30.67	31.08	32.39	32.61

The values are expressed as percentage of the initial o.d. chip mass.

3.5, the content of total xylose (both monomers and oligomers) initially increased with treatment severity, thereafter it decreased a little. This is probably due to the peeling reaction of the reducing end groups of xylooligomers into xyloisosaccharinic acid via α and β benzilic acid rearrangement, which confirmed the assumption that xylan could be degraded during alkaline pre-treatment of bamboo biomass.

Equation 3.37 illustrates the consumption of NaOH by different bamboo components during alkaline pre-extraction of bamboo. To further confirm this, alkali concentration of the APEL was determined and shown in Fig. 3.14. It can be observed that at lower initial NaOH concentration (0.15 mol/L), the residual alkali concentration after treatment for 180 min ranged from 0.014-0.03 mol/L, corresponding to the fact that more than 80% of initial NaOH was consumed during the reaction (Fig. 3.14a). In contrast, when using initial NaOH concentration of 0.45 mol/L and treatment temperature of 100 ^oC, the lowest NaOH concentration after alkaline treatment was 0.26 mol/L (Fig. 3.14b), which still had high concentration of OH^- available for the dissolution of silica. These results to some extent explain the deviations obtained

during the fitting of shrinking core model in the removal of silica from bamboo powder (Fig. 3.9).

3.2.4 Summary

NaOH concentration plays an essential role in the dissolution of silica from bamboo powder. During alkaline pretreatment of bamboo powder, several reactions between bamboo components and NaOH take place in parallel and consuming a significant amount of OH^-, resulting in a silica dissolution rate in bamboo powder slower than that found for pure amorphous silica particles under the same alkaline dissolution conditions. The treatment parameters such as temperature, time and NaOH concentration had a positive effect on the removal of silica and xylan during the alkaline pre-extraction of bamboo powder. All silica and up to 60% of xylan in bamboo powder could be extracted under the conditions investigated in this work. A toy model that describes the evolution of OH^- concentration and the extraction of silica and xylan in the reaction process was proposed.

3.3 Alkaline Pre-extraction of silica and Hemicellulose from Bamboo Chips

3.3.1 Introduction

During the pre-extraction of biomass for the removal of hemicellulose or other components, particle size of the raw biomass also plays an important role. It has been suggested that the reduction of the particle size accelerates the removal of wood com-

ponents from lignocellulosic feedstocks (Chundawat et al. (2007); Zhao et al. (2008)). In the previous section, we described the work on alkaline pre-extraction of bamboo powder (250-400 mesh). Results demonstrated that almost all silica and up to 60% of hemicellulose could be extracted under the studied conditions.

In the pulp and paper industry, commercial bamboo chips, which have a larger size ($\approx 1{\times}2{\times}3\ cm$) than bamboo powder, are used as the raw material. Thus, mass transfer effects might affect the transportation of treatment chemicals and the diffusion of solubilized degradation products. Thus, the work presented in the section was to evaluate the mass transfer effects on the removal of silica and hemicellulose from bamboo chips during alkaline pre-extraction. Understanding of the underlying mechanisms of alkaline treatment of commercial bamboo chips also favors the process scale-up and optimization.

3.3.2 Materials and Methods

Bamboo chips used for alkaline pre-extraction were the same as that used in Chapter 2. All chemicals were reagent grade and solutions were prepared with purified deionized water.

Alkaline pre-extraction of bamboo chips were carried out in 4 silicate glass reactors of 2 L capacity immersed in a laboratory-scale oil bath. Before using for the experiments, bamboo chips were placed in a bucket with deionized water and soaked for 72 h to allow uniform penetration of treatment chemicals into the chip during alkaline treatment process. The alkaline pre-extraction temperature and NaOH concentration were the same as that used in the treatment of bamboo powder. To extract more

silica and hemicellulose from bamboo chips, longer reaction time was investigated compared to that used for the treatment of bamboo powder. For each experiment, 100 g o.d. bamboo chips and the calculated NaOH solution (stock concentration of 100 g/L) and deionized water were mixed and placed in a reactor. The treatment process and the sample collection were the same as previous described (see Section 3.2). All experiments were performed in triplicate.

Chemical composition of insoluble solids and liquid samples were analyzed according to the NREL standard protocol (Chapter 2). Silica in the liquor was measured according to Tong et al. (2005) (Section 3.2).

3.3.3 Results and Discussion

To understand mass transfer effects on the extraction of silica and hemicellulose from bamboo, alkaline pre-treatment of commercial bamboo chips was carried out under the same conditions used for the treatment of bamboo powder. Figs. 3.15 and 3.16 show the experimental data for alkaline pre-extraction of bamboo chips obtained in the laboratory at 70-100 ^oC with initial NaOH concentrations of 0.15 and 0.45 mol/L for up to 300 min. Similar to the trends obtained from the alkaline pre-extraction of bamboo powder, the extraction of xylan and silica increased with enhancing the treatment intensity, such as higher temperature, increased NaOH loading and longer time. However, when comparing the data obtained from bamboo chips (Figs. 3.15 and 3.16) to that of bamboo powder (Figs. 3.12 and 3.13), it can be observed that the amounts of solubilized xylan and silica with bamboo chips were generally lower than bamboo powder under the same alkaline treatment conditions. For example, alkaline

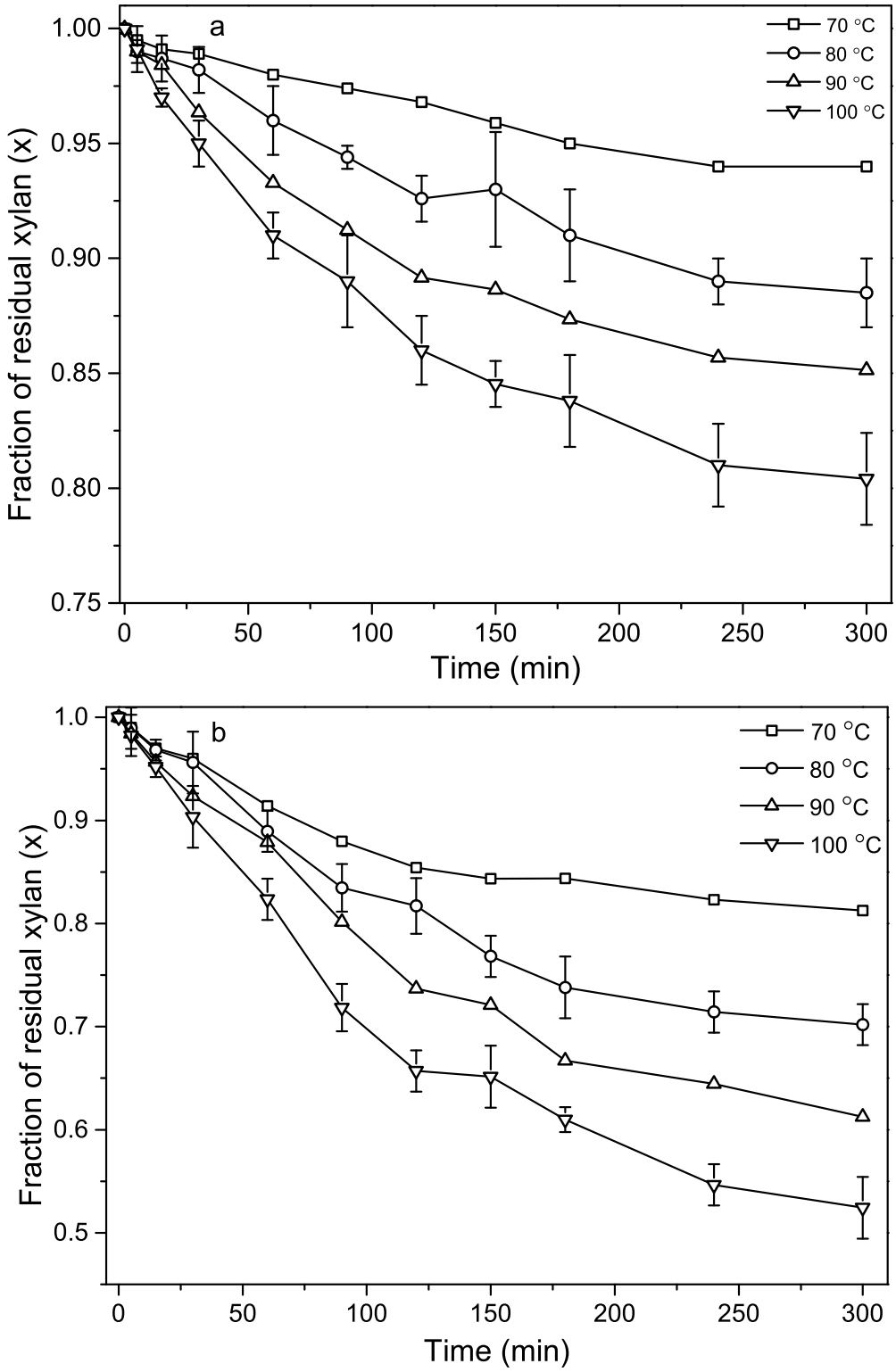

Figure 3.15: Experimental yields of xylan remaining in the extracted bamboo chips at alkaline pre-extraction temperatures of 70-100 ^oC (initial NaOH concentration: a = 0.15 mol/L; b = 0.45 mol/L).

treatment of bamboo biomass at 90 ^oC and NaOH concentration of 0.45 mol/L for 100 min, about 34% of xylan and 97% of silica were extracted from bamboo powder while the extracted xylan and silica from bamboo chips were 18% and 92%, respectively (Figs . 3.12, 3.13, 3.15 and 3.16). This might be attributed to the mass transfer effects play an important role in the solubilization of silica and xylan from bamboo chips. During alkaline pretreatment of bamboo biomass, NaOH molecules penetrate into the inside of bamboo mainly through the lumen. Therefore, the decrease of the particle size can improve the transportation of chemicals into the inside of the bamboo chip. Moreover, since bamboo powder has a smaller particle size and a larger specific surface area than bamboo chips, more silica molecules and ester linkages are accessible for dissolution and hydrolysis by OH^-, resulting in higher silica and xylan solubilization under the same extraction conditions (Mittal et al. (2009)). In contrast, when treating bamboo chips, not only hydroxide ions (OH^-) have to penetrate into inside bamboo chip pores to dissolve silica and hydrolyze xylan, but also the dissolved silica and solubilized xylan products also have to transport from the inside of chip pores to the bulk liquor. The limited accessibility of bamboo components to chemicals and the recalcitrant nature of bamboo biomass negatively affect the extraction of silica and xylan from bamboo chips compared to bamboo powder.

Since the goal of alkaline pre-extraction of bamboo chips was to extract the most silica and hemicellulose while minimizing the loss of cellulose and lignin to preserve the final pulp yield and the heating value of the generated black liquor. Longer treatment time (up to 300 min) was used than bamboo powder (180 min). Figs. 3.15b and 3.16b illustrate that at 80-100 ^oC using initial NaOH concentration of 0.45 mol/L, about 30-50% of xylan and all silica in bamboo chips could be removed within

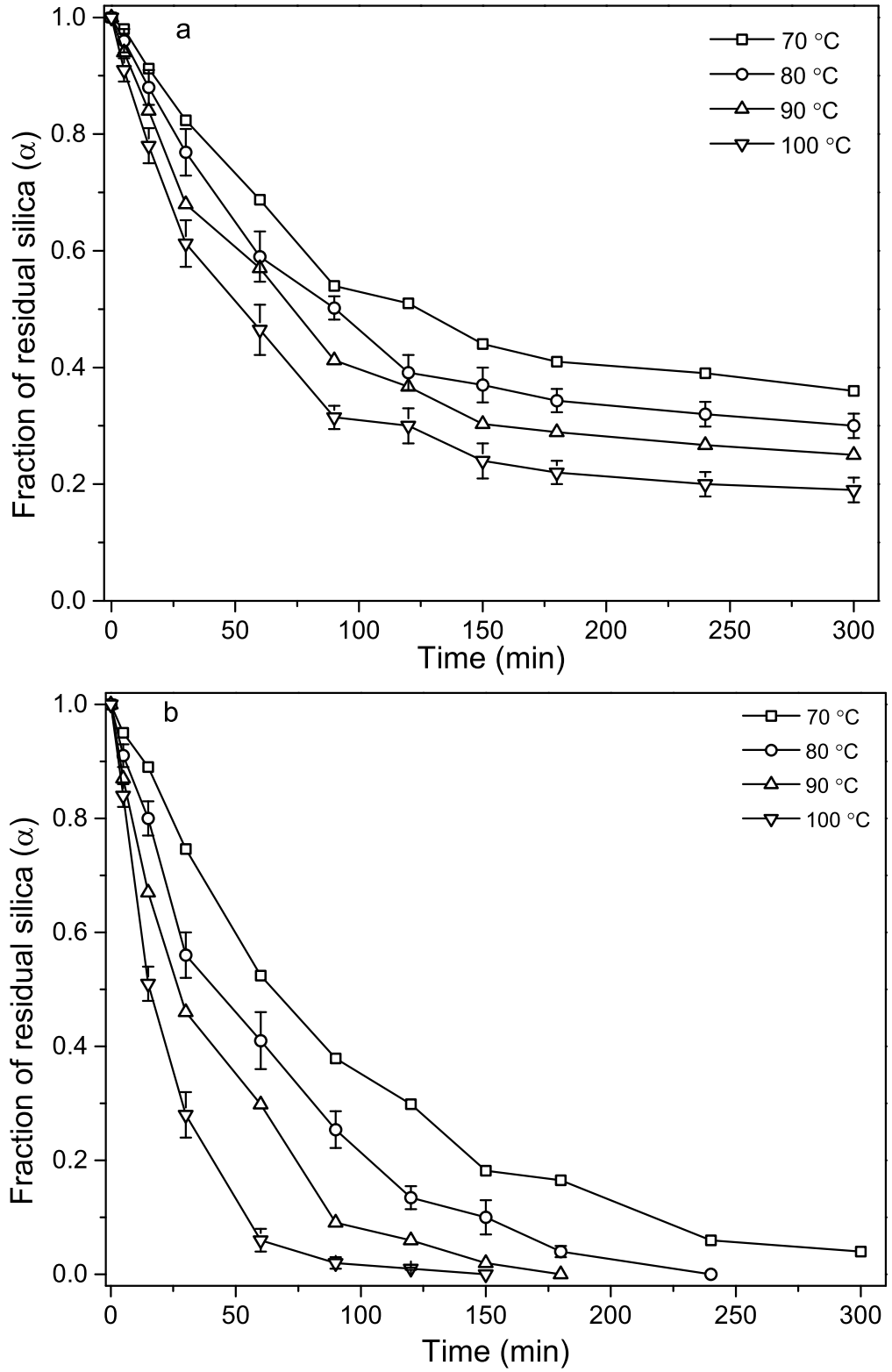

Figure 3.16: Experimental yields of silica remaining in the extracted bamboo chips at alkaline pre-extraction temperatures of 70-100 ^oC (initial NaOH concentration: a = 0.15 mol/L; b = 0.45 mol/L).

240 *min*. These results indicate that alkaline pretreatment of bamboo chips could be a promising method to resolve the associated silica challenges encountered in pulping with bamboo.

To further investigate the mass transfer effects during alkaline treatment of bamboo chips versus bamboo powder, NaOH concentration of the alkaline pre-extraction liquors was measured. Taking the experiments carried out at 100 ^oC as an example, the consumed OH^- was calculated and shown in Fig. 3.17. As shown, the consumed NaOH during alkaline treatment of bamboo powder was generally higher than that of bamboo chips. This could be attributed to the slower diffusion of NaOH from the bulk liquor to the inside of bamboo chips and the degraded products such as sodium acetate from the inside of bamboo chips to the bulk liquor. These results confirmed that mass transfer plays an important role in the diffusion of chemicals into and out of the bamboo chips.

The total xylose content (xylose and xylooligomers) in the hydrolysates obtained from the treatments of bamboo chips and bamboo powder was also determined and shown in Fig. 3.18. As shown in Fig. 3.18, more xylose was present in the bulk liquors in bamboo-powder experiments compared to that of liquors obtained from the treatment of bamboo chips. These results also revealed the importance of accessibility of bamboo components to NaOH and transportation of formed products inside the bamboo chips to the bulk liquor during the alkaline pre-extraction process. Moreover, compared the data shown in Fig. 3.18 to Figs. 3.12 and 3.15, it can be found that with the increase of treatment time from 140 to 180 *min*, the xylan removal from bamboo biomass was increased, whereas the xylan content in the hydrolysates was almost constant or even decreased a little. This might be explained by the fact that some

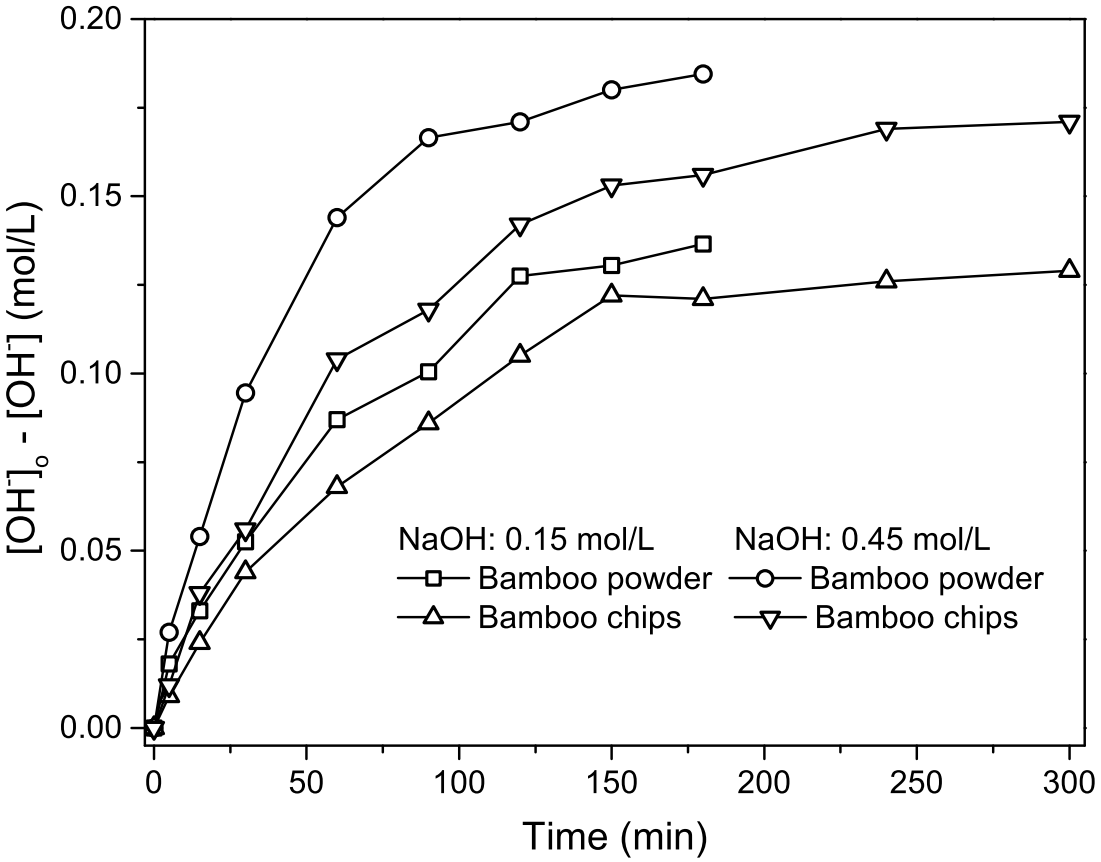

Figure 3.17: The effect of mass transfer on consumed NaOH during alkaline pre-extraction of bamboo (alkaline pre-extraction temperature = 100 ^oC).

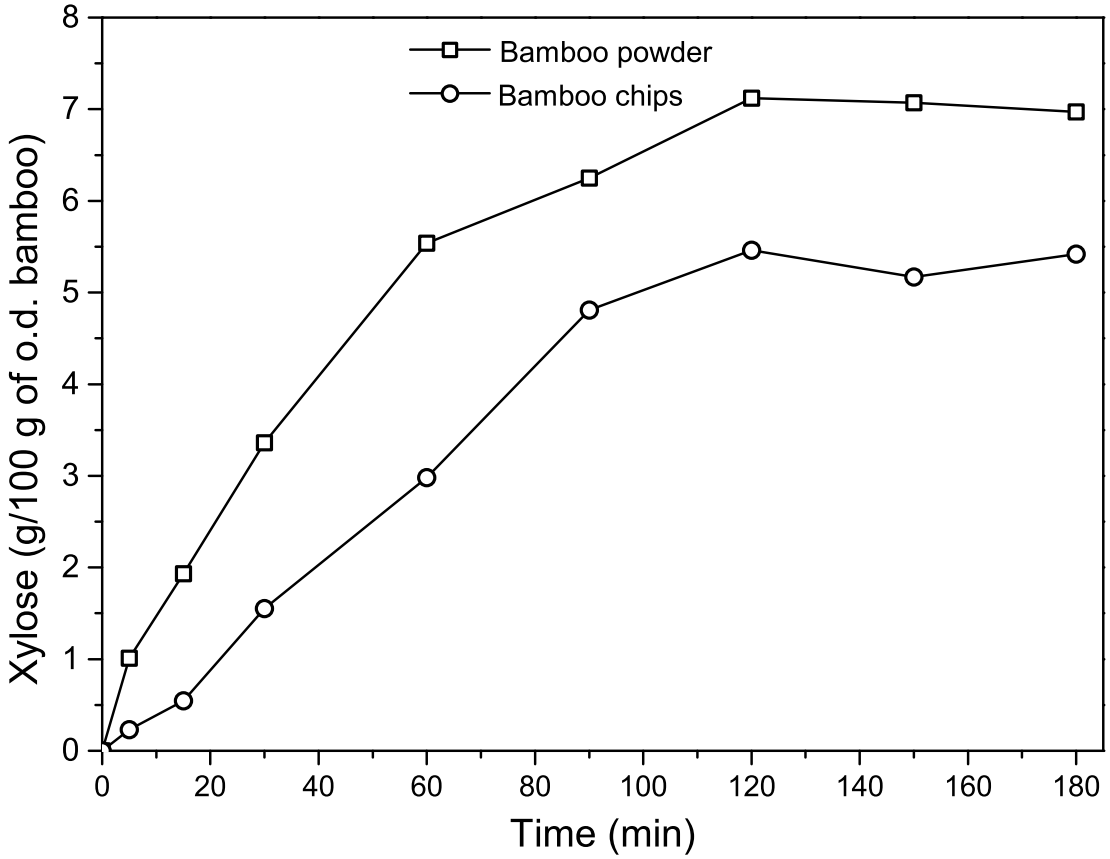

Figure 3.18: The effect of mass transfer on xylose yields during alkaline pre-extraction of bamboo (alkaline pre-extraction was carried out at 100 ^oC with initial NaOH concentration of 0.45 mol/L).

xylose units were degraded to undetected products when increasing the treatment severity.

On the basis of above results and discussion, the reaction mechanism for the alkaline pre-treatment of bamboo chips can be generalized as follows:

1) Transportation of hydroxide ions from the bulk liquor to the exterior surface of chips;

2) Penetration of hydroxide ions to the inside of chips;

3) Alkaline solubilization of silica and xylan inside bamboo chips;

4) Diffusion of dissolved xylooligomers, xylose and silicates to the chip exterior;

5) Transportation of the soluble silicates and xylan degradation products into the bulk liquor.

It is apparent that mass-transfer effects play a significant role in the reaction kinetics of alkaline pre-extraction of silica and hemicellulose from bamboo chips.

3.3.4 Summary

Low temperature alkaline pre-extraction of bamboo chips prior to subsequent pulping processes was demonstrated to be an effective way to selectively extract silica and hemicellulose from bamboo biomass without degrading cellulose and lignin. The comparison of the extraction of silica and xylan between bamboo powder and bamboo chips revealed the importance of mass-transfer effects during the process of alkaline pre-extraction of bamboo chips. Under the studied extraction conditions, almost 100% of silica and up to 50% of hemicellulose in bamboo chips were extracted. Taking account into the consideration for efficient dissolution of silica and hemicellulose, the removal was more efficient at a pre-extraction temperature of 100 ^oC compared to 80 ^oC. Moreover, during alkaline pre-extraction silica and hemicellulose from bamboo chips, the increase of treatment severity led to the degradation of extracted xylan, resulting in the decrease of xylan content detected in the extraction liquor. In addition, based on the comparison of responses of bamboo powder and bamboo chips to the alkaline pre-extraction process, the mechanism of the extraction of the bamboo components has been proposed, mainly including the transportation of chemicals from bulk liquor to the inside of bamboo chips and diffusion of dissolved bamboo

components from the inside of bamboo chips to the bulk liquor.

3.4 Response Surface Experimental Design on Alkaline Pre-extraction of Bamboo

3.4.1 Introduction

In previous sections, we presented the work with pure amorphous silica, bamboo powder and bamboo chips to understand the reaction mechanisms during alkaline pre-extraction of silica and hemicellulose from the bamboo biomass. To investigate the feasibility of industrial application of the proposed technology, it is necessary to expand the study and implement the extraction process at an industrial scale. For the process scale-up and optimization, the establishment of the relationship between responses of bamboo components and treatment conditions is of great importance. To optimize the alkaline pre-extraction conditions, the response surface methodology (RSM), a widely practiced approach for the optimization of various industrially important processes (Chang et al. (2002); Poojary and Mugeraya (2012)), was investigated in this section. In the work reported below, by means of central composite rotatable design (CCRD) and RSM, the optimal pre-extraction process parameters were determined for the extraction of silica and hemicelluloes while preserving cellulose and lignin in the residual solids (maintaining yield of chip and pulp and minimizing effect of lignin co-precipitation). Moreover, a lower liquid to wood ratio (4 L/kg versus 10 L/kg) for alkaline pre-extraction of commercial bamboo chips was investigated in this section to reduce the fresh water consumption.

3.4.2 Materials and Methods

Washed commercial bamboo chips used in this section were the same as that used in Chapter 2. Chemicals were reagent grade and solutions were prepared with purified deionized water.

Response surface methodology (RSM) was assembled for the alkaline pre-extraction of bamboo with the objective of achieving the most hemicellulose and silica extraction and the least loss of cellulose and lignin thus residual hemicellulose and silica in the treated chips and chip yield were considered as the responses. To achieve the goal of this study, a three-factor central composite rotatable design (CCRD) was used in the current work.

To improve the utility of this proposed process, NaOH charge instead of NaOH concentration was investigated in the current work. Based on the concentration of NaOH used in the previous sections conduted on the treatment of bamboo powder and bamboo chips, the range for the NaOH charge was chosen to be 6-18% (based on the o.d. weight of the original chip mass). The three variables i.e. reaction temperature (T), NaOH charge ($[OH^-]_o$) and extraction time (t) were studied at five levels (-1.682, -1, 0, +1, +1.682), where the desired ranges of values of the variables were coded to lie at ± 1 for the factorial points, 0 for centre points and ± 1.682 for the axial points. The experimental domain was defined by previous preliminary experiments, which showed the potential of increasing hemicellulose and silica extraction efficiency while maintaining cellulose and lignin in the residual solids. The ranges of the independent variables and experimental design levels are listed in Table 3.6. According to CCRD, a set of 20 experimental runs was carried out (Cochran and Cox (1968)), shown in

Table 3.6: Experimental range of pre-extraction variables and coded levels according to response surface methodology.

Variable	Symbol	Coded variable level				
		Lowest	Low	Centre	High	Highest
		-1.682	-1	0	+1	+1.682
Temperature (^oC)	T	59.8	70	85	100	110.2
NaOH charge (%)	$[OH^-]_o$	1.91	6	12	18	22.09
Extraction time (min)	t	13	30	55	80	98

Table 3.7. The order of the experiments was randomized. Runs 1-14 were performed in duplicate.

Data were analyzed by multiple regressions through the least-square method with the Design Expert Version 6.0.6 software (Stat-Ease, Inc., Minneapolis, MN, USA). A second-order polynomial equation was used to express the responses as a function of the three independent variables (Equation 3.38).

$$Y = b_0 + \sum_{i=1}^{k} b_i x_i + \sum_{i=1}^{k} b_{ii} x_i^2 + \sum_{i=1}^{k} \sum_{j=i+1}^{k} b_{ij} x_i x_j \qquad k = 3 \tag{3.38}$$

where Y is the predicted response, b_0 is the constant coefficient, b_i, b_{ii} and b_{ij} are the coefficients of linear, quadratic and second-order interaction regression terms, respectively, k is the number of independent variables, x_i and x_j are the coded independent variables (temperature, NaOH charge, and time). The estimation of regression coefficient parameters, three dimensional (3-D) response surface graphs and response optimization were performed using MATLAB Version 8.5.0 software.

The alkaline pre-extraction experiments were carried out in a rotating reactor system (Aurora Products, Savona, BC, Canada) which consists of 4 stainless steel digesters of 2 L each placed in a single rotating frame. The reactors were rotated

at 50 rpm with 60-s clockwise rotations followed by 60-s counter clockwise rotations throughout the reaction process. The maximum rated pressure and temperature of the digesters are 15 bar and 205 ^oC, respectively, which are monitored wirelessly by Honeywell XYR 5000 transducers. In all alkaline pre-extraction experiments, the liquid-to-wood ratio was kept constant at 4 L/kg. For the alkaline pre-extraction run, bamboo chips of 100 g o.d. and the calculated volume of deionized water and NaOH solution (stock concentration of 100 g/L) were mixed and placed in a digester. Subsequently, the reactor was placed in the digester system for alkaline pre-extraction. The temperature ramp-up time was kept constant at 20 min. Before using for experiments, bamboo chips were pre-soaked in deionized water for 72 h to expel air inside bamboo chips, aid the impregnation of NaOH from the bulk liquor to the inside of bamboo chips and ensure a uniform penetration during the alkaline pre-extraction process. Upon completion of a run, the vessel was rapidly cooled in a cold water bath and the pre-extracted chips were recovered from the liquor through filtration. The chips were washed thoroughly with deionized water until the filtrate was neutral. The the wet washed bamboo chips were stored at 4 ^oC for further analysis and kraft cooking. The alkaline pre-extraction liquor (APEL) was collected and stored at 4 ^oC for the chemical composition analysis and further experimentation.

The chemical composition (carbohydrates and lignin) of both solid and liquid fractions was determined according to the NREL standard protocol described in Chapter 2. The ash and silica content were also determined according to the methods described in Chapter 2. The silica content of the APEL was measured by using the silicon molybdenum blue photometric method (Tong et al. (2005)). All experiments were performed at least in triplicate.

3.4.3 Results and Discussion

To extend the application of the proposed process and optimize the NaOH pre-treatment parameters, response surface methodology (RSM) with a central composite rotatable design (CCRD) was employed. The experimental conditions and corresponding responses of the dependent variables (percentages of extracted hemicellulose and silica, chip yield) are listed in Table 3.7. The experimental data were used to calculate the coefficients of the second-order polynomial equation. According to the analysis of variance (ANOVA), the statically significant model terms with p-value less than 0.05 were obtained and used for the response regression and the model expression. The mathematical models were expressed in terms of coded variables. The non-significant model terms were removed.

As discussed in Section 3.2 and data shown in Table 3.7, over 93% of extracted hemicellulose was in the form of xylan. The second-order polynomial functions representing xylan extraction (Y_1), silica extraction (Y_2) and chip yield (Y_3) can be expressed as a function of three operating parameters of alkaline pre-extraction, namely extraction temperature (T), NaOH charge ($[OH^-]_o$) and reaction time (t). The resultant models adequately represented the experimental data as $r^2 > 0.95$.

As shown in Table 3.7, the amount of xylan removal ranged from 8.1 to 39.4% of the initial xylan in the starting material. Equation 3.39 shows the relationship between the percentage of extracted xylan and pre-treatment variables of NaOH charge,

Table 3.7: Experimental design and observed responses of the dependent variables.

Run no.	Independent variables			Dependent variables		
	temperature (^oC)	NaOH (%)	time (min)	Extracted xylan (%)	Extacted silica(%)	Chip yield (%)
1	110.2	12	55	34.6	92.1	86.6
2	59.8	12	55	10.2	42.2	95.6
3	85	1.91	55	8.4	22.3	97.1
4	85	22.09	55	36.5	90.2	89.3
5	85	12	97	21.4	85.6	90.3
6	85	12	13	13.6	45.7	95.7
7	70	18	80	21.5	83.7	91.4
8	70	18	30	20.4	58.7	93.8
9	70	6	30	8.1	28.2	96.6
10	100	18	30	26.1	91.6	90.4
11	70	6	80	8.2	60.9	95.5
12	100	18	80	39.4	99.7	86.3
13	100	6	80	21.3	70.9	91.2
14	100	6	30	12.3	62.3	93.5
15	85	12	55	19.3	78.3	92.1
16	85	12	55	18.3	77.8	91.5
17	85	12	55	19.2	76.9	91.2
18	85	12	55	18.7	78.7	91.4
19	85	12	55	18.2	80.2	91.7
20	85	12	55	18.5	79.5	91.2

temperature and time.

$$Y_1 = 18.20 + 5.93T + 7.74[\mathrm{OH}^-]_o + 2.61t + 1.14T^2 + 1.15{[\mathrm{OH}^-]_o}^2 + 2.76Tt \qquad (r^2 = 96.32\%, \quad {r_{adj.}}^2 = 94.09\%) \tag{3.39}$$

where Y_1 is fraction of extracted xylan (%, based on the starting xylan mass), T, $[\mathrm{OH}^-]_o$ and t are reaction temperature, NaOH charge and reaction time, respectively. Independent variables are standardized.

The studied alkaline pre-extraction variables showed positive effects on the extraction of xylan from bamboo chips. The results of ANOVA for the CCRD are presented in Table 3.8; the tests of F-value and P-value were used to determine the significance of the regression coefficients of each parameter. The larger the value of F and smaller value of P, the more significant of the corresponding coefficient term (Atkinson et al. (1992)), which also means that the larger coefficient the stronger effect of the corresponding term. Accordingly, during the alkaline extraction of hemicellulose from bamboo, the NaOH charge had the strongest effect on the extraction of xylan while reaction time had the weakest effect (Table 3.8).

Fig. 3.19 shows the 3-D surface plots of the effect of the interaction between NaOH charge (%) and reaction temperature (^oC) on the fraction of extracted xylan at the fixed reaction time of 80 min. As shown, up to 50% of original xylan in raw bamboo chips could be extracted during alkaline pre-extraction and that the amount of extracted xylan increased with increasing NaOH charge and reaction temperature (Fig. 3.19). For example, about 6% of the original xylan mass was extracted by treating bamboo chips at 60 ^oC with 12% NaOH charge for 80 min. In contrast, at

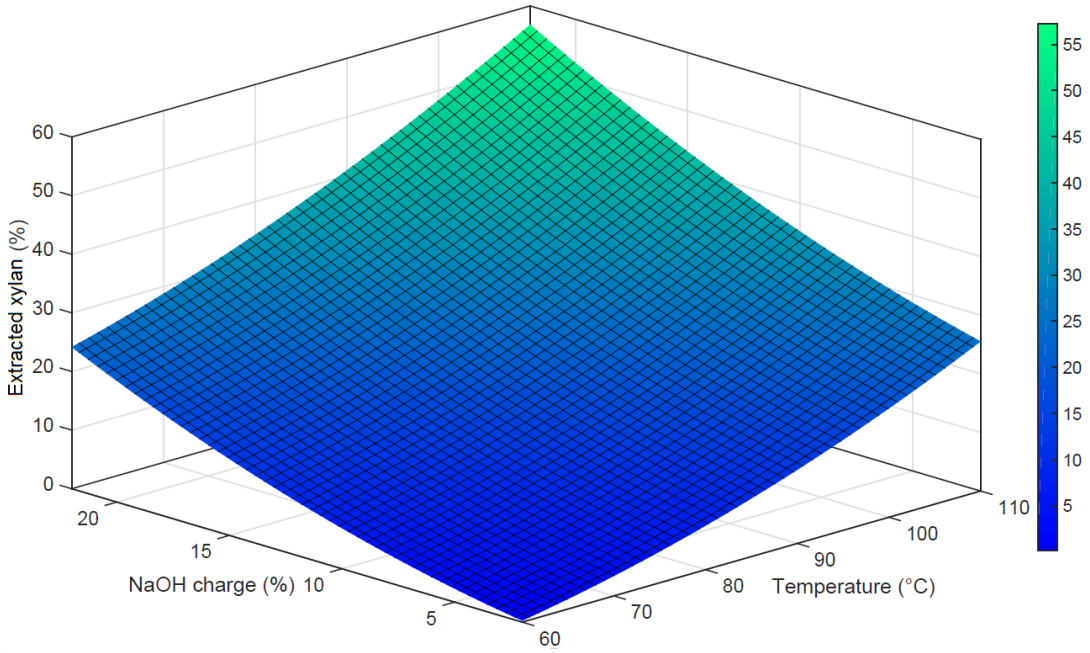

Figure 3.19: Effect of temperature and NaOH charge on the extraction of xylan at a fixed reaction time of 80 *min*.

110 ^oC with the same NaOH charge (12% of o.d. chip mass), about 40% of xylan could be extracted (Fig. 3.19). The maximum xylan extraction predicted by response surface was 59.9% when treating bamboo chips at 110 ^oC with 22.1% NaOH charge for 97 *min*.

During alkaline pre-treatment, the amount of extracted silica is significantly depended on the severity of the pre-extraction process. As shown in Table 3.7, the fraction of extracted silica ranged from 22.3 to 99.7% of the initial silica mass. Based on the experimental data, a quadratic regression model (second-order) was obtained, after exclusion of the non-significant terms according to the analysis of variance. The

equation for the fraction of extracted silica is shown in Equation 3.40.

$$Y_2 = 72.91 + 12.55T + 16.15[\mathrm{OH}^-]_o + 10.24t - 5.27[\mathrm{OH}^-]_o{}^2 - 5.75Tt \qquad (r^2 = 93.97\%, \quad r_{adj.}{}^2 = 91.81\%) \tag{3.40}$$

where Y_2 is fraction of extracted silica (%, based on the starting silica mass), T, $[\mathrm{OH}^-]_o$ and t are reaction temperature, NaOH charge and reaction time, respectively. Independent variables are standardized.

Equations 3.40 revealed that the amount of silica extraction from bamboo chips was positively affected by the all three studied factors, namely extraction temperature, NaOH charge and reaction time. As illustrated in Table 3.8, NaOH charge had the strongest effect on the extraction of during alkaline pre-extraction of bamboo chips followed by extraction temperature and time. This is not in agreement with the literature observation obtained from sodium carbonate (Na_2CO_3) pretreatment of wheat straw (Pekarovic et al. (2005)). One likely reason for the difference is that the bamboo chips used in the present research had been pre-soaked in deionized water for 72 h to expel the air inside the chips. In contrast to the dry wheat straw used by Pekarovic et al. (2005), pre-soaked chips are expected to experience more uniform penetration of NaOH solution and relatively reduce the mass transfer effects. In addition, the range of conditions tested as well as the alkali reagent used (NaOH versus Na_2CO_3) in this study are different from those used by Pekarovic et al. (2005). Based on the industrial aspect, NaOH might be a better choice due to its abundance as white liquor in a typical kraft pulp mill.

Fig. 3.20 shows the 3-D surface plots of the effect of the interaction between NaOH

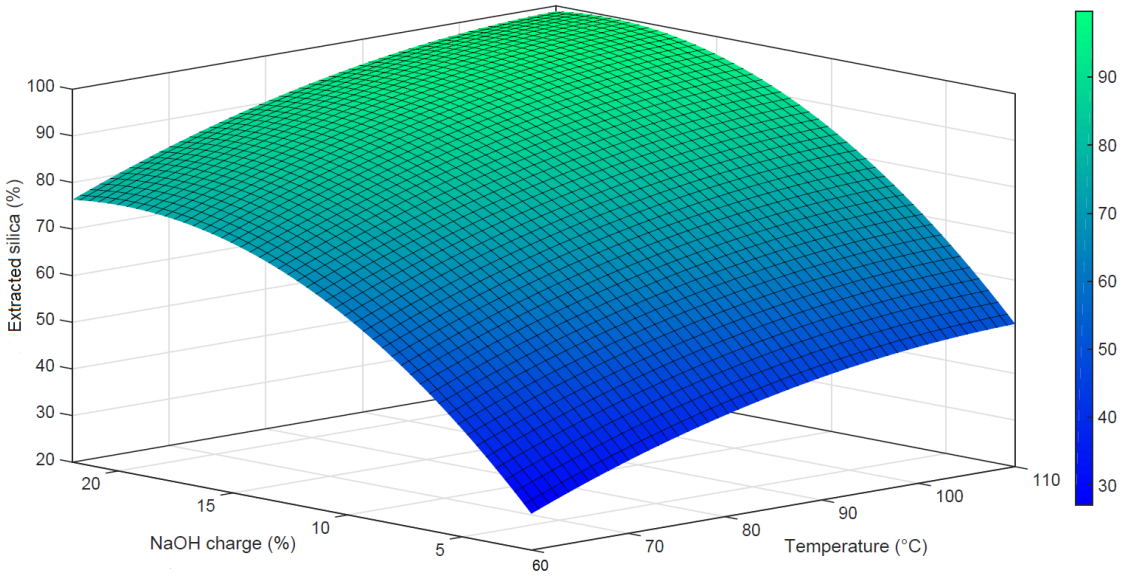

Figure 3.20: Effect of temperature and NaOH charge on the extraction of silica at a fixed reaction time of 80 *min*.

charge and temperature on the extraction of silica at the fixed time of 80 min. The fraction of extracted silica increased with increasing NaOH charge and temperature. For example, treating bamboo chips for 80 min with 6% NaOH charge at 70 ^oC and 100 ^oC, about 61% and 71% of initial silica in bamboo chips could be removed, respectively. In contrast, at 100 ^oC with 18% NaOH charge for 80 *min*, all silica in untreated bamboo chips was removed. The dissolution rate of silica in NaOH solution increased with increasing NaOH concentration and reaction temperature (Fig. 3.20); this is in agreement with previous studies on the dissolution of amorphous silica in NaOH solutions (Niibori et al. (2000)). Moreover, with the increase of treatment temperature, more xylan was extracted, resulting in more pores of the treated chips; this improves the penetration of NaOH into chips and the diffusion out of soluble silicates, thus leading to faster extraction of silica.

Results in Table 3 indicated that the chip yield depended on all three factors,

NaOH loading, extraction temperature and time; the chip yield from the pretreated samples ranged from 84% to 97% of the initial dry chip mass. Based on the experimental data, the coefficients of the second-order response function on the coded levels representing the chip yield was calculated, shown as Equation 3.41.

$$Y_3 = 91.67 - 2.29T - 2.08[\mathrm{OH}^-]_o - 1.38t + 0.57[\mathrm{OH}^-]_o{}^2 \qquad (r^2 = 94.86\%, \quad r_{adj.}{}^2 = 93.48\%) \tag{3.41}$$

where Y_3 is chip yield (%, based on initial chip mass), T, $[\mathrm{OH}^-]_o$ and t are reaction temperature, NaOH charge and reaction time, respectively. Independent variables are standardized.

According to Equation 3.41, the chip yield was inversely affected by increasing temperature, NaOH charge and extraction time. The chip yield loss was mainly affected by NaOH charge and in minor extent by temperature and time (Table 3.8). As shown in Fig. 3.21, increasing the treatment intensity decreased the chip yield. For example, the use of 6% NaOH resulted in chip yield between 95% and 97% at 80 ^oC while the yield decreased to 91-94% at 100 ^oC.

To further assess the effects of alkaline pretreatment on the dissolution of bamboo components, the composition (sugars, lignin and silica) of the solid fraction remaining after pretreatment was determined. Table 3.9 shows the results of extraction in terms of chemical composition of pre-treated chips. As shown in Table 3.9, the glucan content in the treated bamboo chips increased due to the removal of hemicellulose. The increase of cellulose content is favorable for the subsequent treatments designed to produce dissolving grade pulp or fermentable glucan for lignocellulosic

Table 3.8: Values of regression coefficients of the fitted second order polynomials.

Factor	Regression coefficient	F-value	P-value
Percentage of extracted xylan	-	-	-
Model	-	78.73	< 0.0001 (significant)
b_0	18.20	-	< 0.0001
Linear	-	-	-
b_1	5.93	152.3	< 0.0001
b_2	7.74	260.5	< 0.0001
b_3	2.61	29.50	0.0001
Quadratic	-	-	-
b_{11}	1.14	5.97	0.295
b_{22}	1.15	6.16	0.0275
Interaction	-	-	-
b_{13}	2.76	19.39	0.0007
Percentage of extracted silica	-	-	-
Model		43.60	< 0.0001 (significant)
b_0	72.91	-	< 0.0001
Linear	-	-	-
b_1	12.55	59.99	< 0.0001
b_2	16.15	99.34	< 0.0001
b_3	10.24	39.94	< 0.0001
Quadratic	-	-	-
b_{22}	-5.27	11.37	0.0046
Interaction	-	-	-
b_{13}	-5.75	7.37	0.0167
Chip yield	-	-	-
Model		69.14	< 0.0001 (significant)
b_0	91.67	-	< 0.0001
Linear	-	-	-
b_1	-2.29	122.45	< 0.0001
b_2	-2.08	101.35	< 0.0001
b_3	-1.38	44.51	< 0.0001
Quadratic	-	-	-
b_{22}	0.57	8.24	0.0117

Note: the response surface regression and models were expressed in terms of coded variables, without taking into account the statistically non-significant terms.
b_1, b_2 and b_3 are values of the coefficients of temperature, NaOH charge, and time, respectively.

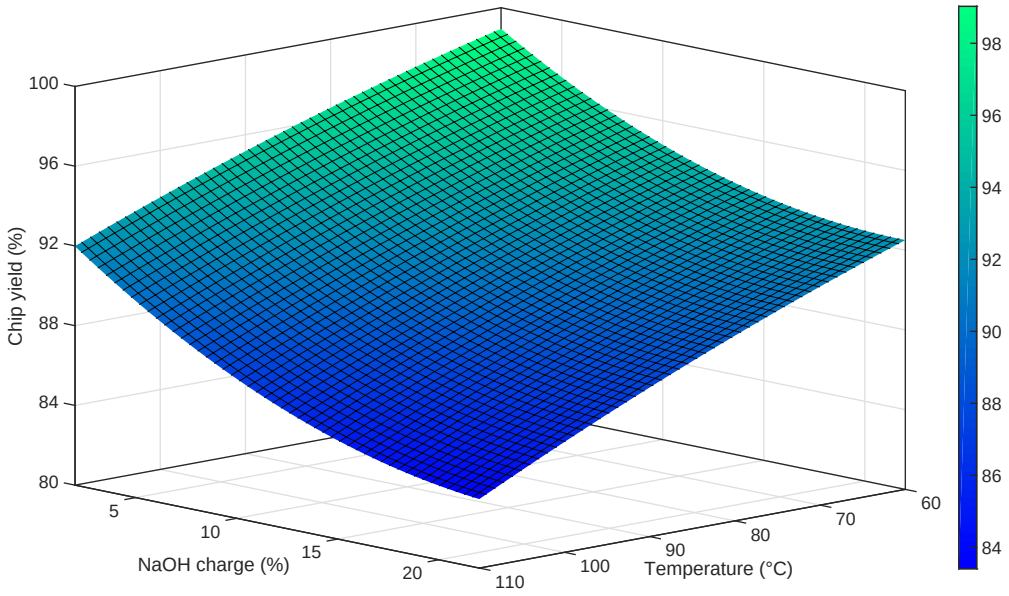

Figure 3.21: Effect of temperature and NaOH charge on chip yield at a fixed reaction time of 80 *min*.

fuels production. However, for the production of regular kraft pulp, the removal of hemicellulose might negatively affect the physical properties of final paper due to the loss of hydrogen bonding (Bai et al. (2012)). These results showed that the treatment time, temperature and NaOH charge used in this study did not significantly degrade the lignin in bamboo chips. These results confirmed the obtained conclusions that alkaline pre-extraction under studied conditions had little effect on the extraction of cellulose and lignin from bamboo chips and alkaline pre-extraction is a promising method for solving the silica problems during bamboo biomass fractionation.

Equations 3.39, 3.40 and 3.41 were used to identify suitable NaOH treatment conditions to the reach the target of extracting more than 97% of silica from bamboo chips while persevering cellulose and lignin in the treated solids. Moreover, the selected conditions should also be able to lower capital costs and heat losses, and reduce the pretreatment time. Using the software (Design Expert Version 6.0.6), the opti-

Table 3.9: Experimental design and observed responses of the dependent variables.

Run	Composition (%)[a]					
no.	Glucose	Galactose	Arabinose	Lignin	Xylose	Silica
1	53.5(0.8)	0.4(0.05)	0.8(0.1)	27.8(0.2)	15.3(0.3)	0.10(0.02)
2	49.8(0.3)	0.6(0.02)	0.7(0.05)	26.0(0.1)	19.1(0.6)	0.68(0.4)
3	49.9(0.05)	0.3(0.1)	0.7(0.07)	25.7(0.2)	19.2(0.4)	0.9(0.05)
4	52.4(0.1)	0.5(0.02)	0.6(0.1)	27.3(0.6)	14.4(0.3)	0.12(0.03)
5	52.1(0.8)	0.6(0.06)	0.6(0.05)	27.0(0.1)	17.7(0.7)	0.15(0.04)
6	50.1(0.4)	0.7(0.05)	0.7(0.07)	25.7(0.4)	18.3(0.3)	0.64(0.04)
7	52.1(0.5)	0.4(0.08)	0.6(0.05)	26.7(0.3)	17.4(0.2)	0.20(0.02)
8	50.8(0.2)	0.8(0.07)	0.8(0.1)	26.1(0.4)	17.2(0.2)	0.49(0.03)
9	49.7(0.4)	0.6(0.1)	0.4(0.06)	25.6(0.2)	19.3(0.8)	0.83(0.02)
10	52.3(0.8)	0.6(0.1)	0.8(0.05)	27.0(0.2)	16.6(0.3)	0.10(0.03)
11	50.4(0.6)	0.4(0.04)	0.6(0.06)	25.8(0.1)	19.5(0.5)	0.46(0.02)
12	53.8(0.2)	0.8(0.05)	0.5(0.1)	27.8(0.2)	14.2(0.4)	0.01(0.01)
13	51.5(0.6)	0.4(0.06)	0.6(0.09)	26.7(0.3)	17.5(0.7)	0.36(0.04)
14	50.9(0.8)	0.3(0.07)	0.7(0.04)	26.2(0.2)	19.0(0.6)	0.45(0.03)
15	51.5	0.9	0.8	26.5	17.8	0.26
16	51.6	0.7	0.5	26.6	18.1	0.27
17	52.1	0.6	0.7	26.8	18.0	0.28
18	52.0	0.7	0.8	26.2	17.7	0.26
19	51.7	0.4	0.6	26.6	18.1	0.24
20	52.1	0.8	0.4	26.1	18.2	0.25

Note: values of range between duplicate measurements are given within bracket.
[a]Composition of the solid fractions resulting from the pre-treatments were expressed as the percentage of dry matter of treated bamboo chips.

Table 3.10: Confirmation runs of the alkaline pre-extraction of bamboo chips according to RSM.

Alkaline pre-treatment	Extracted xylan (%)		Extracted silica (%)		Chip yield (%)	
	Actual	Predicted	Actual	Predicted	Actual	Predicted
18% NaOH, 100 ^oC, 90 min	37.8	39.5	99.8	100	87.3	86.5
17% NaOH, 97 ^oC, 70 min	32.4	35.7	94.8	96.2	89.4	87.7

mized alkaline pre-extraction conditions were determined to be at a temperature of 95-100 ^oC with NaOH charge of 16-18% (based on the o.d. chip mass) for 70-90 min. To verify the model and validate the proposed methodology, pre-treatment experiments were conducted under two different conditions which were using 18% NaOH at 100 ^oC for 90 min and 17% NaOH charge at 97 ^oC for 70 min, respectively. Table 3.10 shows the experimental results on the alkaline pre-extraction of bamboo chips. The actual silica and xylan extraction data were close to the predicted values. For example, treating bamboo chips with 18% NaOH at 100 ^oC for 90 min resulted in 97.6% and 34.3% of initial silica and xylan removal, which were close to predicted values of 99.6% and 36.8%, respectively. The results clearly demonstrated the noteworthy extraction of silica and hemicellulose from bamboo chips.

3.4.4 Summary

The application of response surface methodology (RSM) and central composite rotatable design (CCRD) for modelling the influence of the three operating variables (temperature, NaOH charge and time) on the treatment efficiency (extraction of silica and hemicellulose from bamboo chips) has been discussed. RSM has helped to locate the conditions for best silica removal with minimal loss of cellulose and lignin.

According to model equations and confirmatory experiments, 97% desilication at a chip yield of about 82% was reached by treating bamboo chips at temperatures of 95-100 ^oC with NaOH charge of 16-18% (based on the original o.d. chip mass) for 70-90 min.

3.5 Summary

In this chapter the dissolution of pure amorphous silica in NaOH solution and NaOH treatment of bamboo biomass were investigated.

Under the alkali concentrations studied, the shrinking core model could be used to describe the silica dissolution rate of pure amorphous silica. During alkaline treatment of bamboo biomass, several reactions between bamboo components and NaOH take place in parallel and consuming a significant amount of OH^-. To describe the reactions, toy chemistries, representing the dominant mechanism of alkaline pretreatment, were posed. A toy model that illustrates the change of OH^- concentration during the reaction process was established. The main objective of this part of work is to remove the most silica and hemicellulose from bamboo chips and solve the silica associated challenges during pulping bamboo, so the experimental data on the dissolution of silica and xylan were presented. The test of the utility of the proposed toy model was presented in the published paper.

The consumption of OH^- by other bamboo components resulted in lower silica dissolution rate than that found for pure amorphous silica particles. With the increase of the OH^- concentration ($\geq 0.45\ mol/L$) used for alkaline pretreatment of bamboo powder, the silica removal rate could be described by the classic shrinking core model.

The comparison of the extraction of the extraction of silica and xylan between bamboo powder and bamboo chips revealed the importance of mass-transfer effects during alkaline pre-extraction of bamboo chips. Based on the comparison of responses of bamboo powder and bamboo chips to the alkaline pre-extraction process, the mechanism of the extraction of the bamboo components has been proposed.

The application of response surface methodology (RSM) and central composite rotatable design (CCRD) for modelling the influence of the three operating variables (temperature, NaOH charge and time) on the treatment efficiency (extraction of silica and hemicellulose from bamboo chips) has been discussed. RSM has helped to locate the conditions for best silica removal with minimal loss of cellulose and lignin. According to model equations and confirmatory experiments, 97% desilication at a chip yield of about 82% was reached by treating bamboo chips at temperatures of 95-100 ^oC with NaOH charge of 16-18% (based on the o.d. chip mass) for 70-90 min.

In this chapterïijN̆ the removal of silica and hemicellulose from bamboo biomass was investigated during the alkaline pre-extraction of bamboo powder and bamboo chips. Results demonstrate that alkaline pre-extraction of bamboo prior to pulping and biorefinery processes is an effective way to extract silica and hemicelluloes selectively without degrading cellulose and lignin.

Chapter 4

Feasibility of Using Alkaline Pre-extraction in Kraft Pulping

4.1 Introduction

The kraft process has long been the dominant method for the production of chemical pulp due to its versatility in dealing with different raw materials coupled with high quality of resultant pulp and the efficient recovery of energy and cooking chemicals (Garrote et al. (2003)). Moreover, for bamboo, kraft pulping is generally preferred to soda pulping when preparing chemical pulp or dissolving grade pulp (Rydholm (1965)). Therefore, the technologies used for bamboo delignification are similar to those generally applied to wood pulping. The kraft pulping treatment involves the heating of lignocellulosic materials in an aqueous solution of sodium hydroxide (NaOH) and sodium sulfide (Na_2S) from approximately 70 ^oC to cooking temperature (up to 180 ^oC), followed by 1-2 h cooking period. During this treatment, alkaline delignification reactions break both phenolic and nonphenoplic $\beta-O-4$ ether bonds, and remove the methoxyl groups ($-O-CH_3$), leading to the formation of phenolate ions, which are soluble. Na_2S in the reaction system accelerates the lignin break down, in turn reducing the cellulose degradation caused by NaOH.

To resolve the silica challenges encountered with bamboo pulping, alkaline pre-extraction of silica and hemicellulose from bamboo chips have been extensively studied in Chapter 3. The treated chips , with silica content less than 0.03% (w/w), can be used as the ideal starting material for the production of pulp and paper or even dissolving-grade pulp. Moreover, alkaline pre-extraction has been reported to be able to increase pore volume and surface area of wood chips, which might benefit for the subsequent pulping processes. Thus, it is of great importance to investigate the effect of alkaline pre-extraction on kraft pulping of bamboo.

In addition, the liquor generated during alkaline treatment of bamboo chips can not be directly mixed with black liquor and sent to chemical recovery process. Because if we do so, the silica associated challenges will come back to the kraft pulping process. The alkaline pre-extraction liquor (APEL) obtained from alkaline pretreatment contains a large amount of silica and hemicellulose, which could be a potential sustainable source for various high-value products if recovered. Silica is an essential starting material for the consumer products such as catalysts, thixotropic agents, pharmaceuticals, film substrates, electric and thermal insulators composite filler, etc. (Kalapathy et al. (2002); Liou and Yang (2011)). On the other hand, currently, industrial production of nanosilica is mainly from relative expensive sources of tetraethoxysilane and tetramethoxysilane under high temperature treatment ($> 1300\ ^oC$) (Affandi et al. (2009)). Likewise, hemicellulose can also be used for various applications such as production of ethanol, xylitol, bio-polymeric films, or as papermaking additives (Jun et al. (2012); Huang et al. (2010); Ren et al. (2009); Schild et al. (2010)). Therefore, the recovery of these valuable dissolved materials, silica and hemicellulose, from the APEL in an economical and eco-friendly manner is critical to their downstream processing and

utilization for value-added products.

Among the chemicals used for the precipitation of silica from alkali aqueous media (Minu et al. (2012); Zhang et al. (2013)), carbon dioxide (CO_2), present in the waste flue gas from the pulp mill recovery circle, provides a convenient option. In typical chemical pulp mills, a mixture of combustible materials and inorganic chemicals known as black liquor (spent cooking liquor) is a by-product of fibre extraction from wood. Black liquor is normally burned in the recovery boiler to recover pulping chemicals and energy for the mill operation. The burning of black liquor in the mill recovery cycle and the calcination of lime mud generated in the lime kiln generate a large amount of waste flue gas, containing mainly CO_2 (5-40%) and water vapor with small amounts of sulfur dioxide (SO_2) and nitric oxides (NO_X) (Berglin and Berntsson (1998); Hektor and Berntsson (2007)), which can be used to precipitate silica from the APEL. Moreover, the utilization of waste gas can, to some extent, alleviate environmental problems by reducing pulp mill greenhouse gas emissions. Thus, the APEL treatment process can also be regarded as a CO_2-capture system. Moreover, different from the sodium-based salts formed by applying other acids like sulfuric acid, nitric acid or hydrochloric acid in silica precipitation, the sodium carbonate (Na_2CO_3) formed when using CO_2 can be easily recovered as sodium hydroxide (NaOH) by the reaction with low-price calcium oxide (CaO), which is called the causticizing reaction. Moreover, the generated calcium carbonate ($CaCO_3$) can be recovered as CaO again by the calcining process in the lime kiln. Causticizing and calcining are standard chemical recovery practices in commercial kraft or soda pulping. Compared to the black liquor obtained from alkaline pulping of high silica content non-woody materials such as cereal straw, bamboo or switchgrass (Schild et al. (2010)), the lignin

content of the APEL obtained from bamboo was very low (see Chapter 3). Thus, lignin co-precipitation, which normally occurs during the desilication of black liquor with CO_2 treatment (Kopfmann and Hudeczek (1988); Schild et al. (2010); Minu et al. (2012); Zhang et al. (2013)), will be significantly less and as a result, pure silica can be separated and the calorific value of the black liquor obtained from subsequent kraft pulping will be preserved.

In this chapter, a novel and green concept is proposed for the production of kraft pulp, pure amorphous silica particles and polymeric hemicellulose from bamboo chips. In the proposed scheme, alkaline pretreatment was initially carried out to remove the most of silica from bamboo chips. The treated chips were served as raw materials for the production of pulp and paper and the liquid phase was sequentially treated with carbon dioxide (CO_2) and ethanol for the recovery of dissolved silica and hemicellulose.

4.2 Materials and Methods

4.2.1 Raw Material

Bamboo chips were the same as that used in Chapter 2. Alkaline treated chips were obtained from the experimental runs carried out in Chapter 3. The three pretreatment runs were those using 18% NaOH (based on o.d. weight of chips) at 100 ^oC for 1 and 5 h and 18% NaOH at 80 ^oC for 3 h. All chemicals used in this chapter were analytical grade and purchased from Fisher Scientific, Canada.

Alkaline pre-extraction liquor (APEL) was generated from the sodium hydroxide

(NaOH) pretreatment of bamboo chips with alkali charge of 12% (w/w) (based on oven dried chips) and the liquid-to-wood ratio of 8 L/kg in a 5 L flask for 3 h at 90 ^oC heated using a laboratory-scale water bath (see Chapter 3). Gases of CO_2 and nitrogen (N_2) with 99.99% purity were purchased from Praxair Technology Inc., Canada in cylinders. Distilled and deionized water was applied for all treatment processes.

4.2.2 Kraft Pulping

Pulping of pre-extracted and untreated (without alkaline pre-extraction) bamboo chips by the kraft process was conducted in four 300 mL stainless steel reactors in an oil bath under conditions covering the range of practical interest. For all cooks, the temperature was raised to 165 ^oC in 85 min and held at 165 ^oC for 75 min. The liquid-to-wood ratio and sulfidity were fixed at 4 L/kg and 25% (percentage of Na_2S, expressed as Na_2O), respectively. The effective alkali (EA) (expressed as Na_2O) was varied in the range of 13-19% (based on oven dried wood mass). For each kraft cook, 45 g o.d. extracted or non-extracted bamboo chips and the calculated volume of cooking chemicals and deionized water were placed in the reactor and mixed for 10 min. Afterwards, the cooking process was carried out according to the conditions being investigated. Upon completion of a cook, the reactor was rapidly cooled and kraft pulp was recovered using vacuum filtration. The kraft pulp was thoroughly washed with deionized water until the pH of the filtrate reached neutral. Then, the pulp was disintegrated, screened, and filtered to measure total yield, screened yield, and rejects of the kraft cooking process. All experiments were performed in triplicate.

4.2.3 Evaluation of Pulps

The ash content of pulp was determined according to TAPPI T211 om-02. Silica content of the pulp was measured according to the methods shown in Chapter 3. The kappa number of screened pulps was determined according to TAPPI T236 om-99. The fines content of the pulps was measured with a Fibre Quality Analyzer (Op Test Equipment Inc., ON, Canada) based on TAPPI T271 om-07. The pre-extracted and untreated bamboo pulps were beaten in a laboratory disc refiner (PFI mill) at different revolutions according to TAPPI T248 sp-00. The freeness (drainability) of the pulps was determined according to TAPPI T227 om-99 (Canadian Standard Method). Standard handsheets of about 60 g/m^2 were made by TAPPI T 205 sp-02. The handsheets were tested for tensile and tear strength properties using TAPPI T 220 sp-01.

4.2.4 Preparation of Silica Particles from the APEL

The mechanisms for the liquor neutralization and silica precipitation with carbon dioxide (CO_2) are shown in Equations 4.1 and 4.2. A schematic diagram of the experimental apparatus used in this work is illustrated in Figure 4.1. The apparatus was constructed to measure the effects of CO_2 treatment time and temperature on the silica precipitation from the APEL and analyze the compositions of all coexisting gases via an online gas chromatograph. Glass reactors with the ratio of length to diameter of 6 were used (No. 7 apparatus in Fig. 4.1). The composition of residual gas was analyzed on a CX-3400 gas chromatograph (GC) (Varian Canada Inc., Missinssauga, Ontario) equipped with a thermal conductivity detector (TCD) and flame ionization

detector along with a CP-PoraPLOT U capillary column. Ultra high purity Helium (He) was used as carrier gas. The gas sample was collected with a stainless steel sampling valve (Agilent Technologies, Inc., Model 8134). The sampling valve was flushed out three times with He before collecting a sample for analysis.

$$2\,NaOH + CO_2 \longrightarrow Na_2CO_3 + H_2O \tag{4.1}$$

$$Na_2SiO_3 + 2\,CO_2 + 2\,H_2O \longrightarrow H_2SiO_3\downarrow + 2\,NaHCO_3 \tag{4.2}$$

Two separate studies were conducted in this work. In the first study, a series of CO_2 treatment experiments were carried out over various temperatures (20-100 ^oC) and times (5-120 min). The temperature of the single experiment was maintained in an electrically heated water bath. For a silica precipitation run, 200 mL APEL was added into the reactor before placing in the water bath for 15 min to reach the desired temperature. Then, the CO_2 was introduced into the bottom of the reactor at the flow rate of 0.1 L/min. Upon completion of an experimental run, the reactor was taken out from the water bath and let for precipitation for 24 h. The precipitate was washed several times with deionized water and carefully collected. The collected precipitate was dried at 120 ^oC in the oven for 24 h. The moisture free samples were used for the fourier transform infrared spectroscopy (FTIR) analysis. Then, the dry sample was incinerated in a muffle furnace at 700 ^oC for 4 h to completely remove any adsorbed organics.

In the second study, the mixture gas of CO_2 and nitrogen (N_2) was used to simulate for the waste flue gas under conditions (such as temperature) optimized by the first study. The flow rates of CO_2 and N_2 were 0.1 L/min and 0.2 L/min, respectively. The

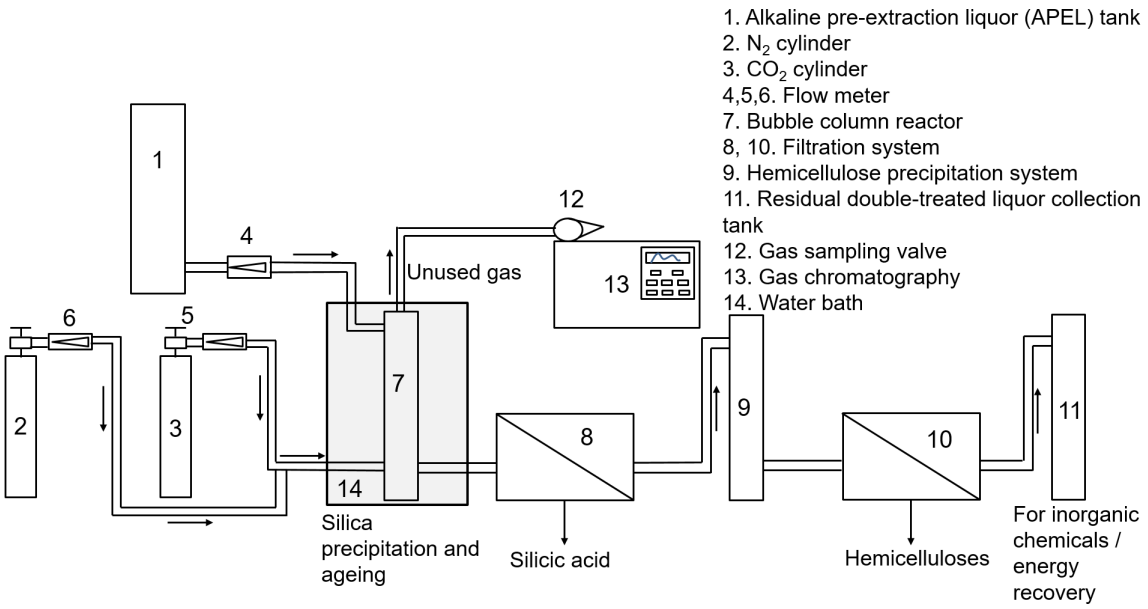

Figure 4.1: A schematic of experimental set-up for recovering silica and hemicellulose and reducing CO_2 emissions.

treatment time was set to 5-120 *min* at the fixed temperature. After each treatment, gas samples (300 μL) were taken for analysis with the Gas Chromatography (GC). The precipitate was collected as previously described.

4.2.5 Isolation of Hemicellulose and Preparation of Hemicellulose-based Polymeric Film

The separation of hemicellulose from the CO_2-treated APEL was achieved by ethanol precipitation and filtration. In the precipitation process, 95% ethanol was slowly added to the filtrate obtained from the silica isolation with a volumetric ratio of 3 while stirring. The stirring was stopped after another 5 *min* after final addition. The mixture was kept at 20 ^oC for 24 h to allow the formed precipitate to settle. Then, the hemicellulose were recovered by centrifugation (3000 *rpm*, 10 *min*) and washed

with 95% ethanol until the supernatant became colorless. Finally, the obtained hemicellulose particles were vacuum dried at 45 ^oC for 36 h.

The hemicellulose-based polymeric films were made with adding 30% plasticizer (glycerol) without adding any other agents according to Mikkonen and Tenkanen (2012). Briefly, the precipitated hemicellulose were dissolved in deionized water at 85 ^oC. Two hemicellulose concentrations, 10 and 20 g/L, were used for the testing of mechanical properties including tensile strength and elongation at break, water vapour transfer rate (WVTR), and water vapour and oxygen permeability, respectively. After cooling for 5 min and adding glycerol, the solutions were sonicated for 5 min, cast into Teflon-coated Petri dishes, and dried in a constant temperature (23 $\pm$ 0.5 ^oC) and humidity (50%) (CTH) room for 7 days. The films were conditioned in the CTH room before analysis, with exception of the samples for the measurements of water sorption which were stored in vacuum desiccators.

4.2.6 Analytical Methods

The residual alkali concentration in the black liquor obtained from kraft pulping was determined by the titration with hydrochloric acid (HCl) according to TAPPI T 625 cm-85.

For the determination of the chemical composition of the APEL, the liquor was neutralized using dilute sulfuric acid. Then the samples were autoclaved with 4% (w/w) H_2SO_4 for 60 min. After hydrolysis, the compositional analysis was following the NREL standard protocols used in previous chapter (see Chapter 2). Total solid content of the APEL was determined by vacuum drying at 45 ^oC for 48 h. Silica

content of liquors was measured by using the silicon molybdenum blue photometric method described in Chapter 3 (Tong et al. (2005)). Lignin content ofthe black liquors was determined gravimetrically by acid precipita-tion and centrifugation (Rocha et al. (2012)).

Mineral composition of the silica powders obtained after incineration at 700 ^oC was determined by atomic emission measurements using an ICP spectrometer (iCAP 6000 Series, Thermo Scientific, MA, USA) with nitric acid (HNO_3) to prepare testing solutions. Fourier transform infrared spectroscopy experiments of silica particles and hemicellulose were carried out on a Cary 630 FTIR Spectrometer (Agilent Technologies, ON, Canada) using the ATR model. The absorption spectra were recorded in the absorption band mode in the range of 4000 to 500 cm^{-1}. The number-average molecular weight (Mn) and weight-average molecular weight (Mw) of hemicellulose were determined by size exclusion chromatography (SEC) with a DAWNEOS-Optilab rEX (Wyatt Technology Inc., USA) equipped with a high performance liquid chromatography (HPLC) pump (Waters Corp., USA) and two columns, TSK-GELG-4000 PWx1 (7.8×300 mm) and TSK-GEL G-2500 PWx1 (7.8×300 mm). The eluent phase used was 0.02 mol/L potassium dihydrogen phosphate (KH_2PO_4) containing 0.2 N NaCl. The flow rate was 0.5 mL/min, and the operating temperature was 35 ^oC. The solution was filtered with 0.45 μm membrane and injected in the SEC system for analysis, the glucan was used calibration standards. The PDI (polydispersity index) is the ratio of weight-average molecular weight (Mw) to number-average molecular weight (Mn).

The tensile strength and elongation at break of the conditioned films were determined according to ASTM D882-12 (2005). Water vapor transfer rate (WVTR),

water vapor permeability (WVP) and oxygen transmission were measured according to ASTM E96/E96M-10, ASTM E96/E96M-05 and ASTM D3985-81 standards, respectively.

4.3 Results and Discussion

4.3.1 Kraft Pulping

Chips from three representative alkaline pre-treatment runs with residual silica content less than 0.04% (w/w) were selected for subsequent kraft pulping. To improve the efficiency when applied in a mill process, higher NaOH charge and shorter reaction times were used for the pre-extraction. These conditions have the potential to extract higher levels of hemicellulose and silica with less cellulose degradation (see previous discussion in Chapter 3).

To evaluate the effect of alkaline pretreatment on kraft pulping of bamboo chips, effective alkali (EA) charge was chosen as the variable while reaction temperature and time were kept constant. In the kraft cooking process, four levels of effective alkali (EA) charges were studied to investigate the effectiveness of alkaline pre-extraction on the kraft pulping of bamboo. To compare the kraft pulping process of extracted bamboo chips and original chips on a uniform basis, the alkali charged to the treated chips was adjusted according to the analysis of the residual alkali in the extract liquor.

Table 4.1 shows the effect of alkaline pre-extraction on the kraft pulping of bamboo chips. It should be noted that the pulping yield was expressed as the overall pulp yield (measured based on the initial o.d. mass of bamboo chips). As shown in

Table 4.1, at all EA charges, kraft pulps from alkaline pre-treated chips had lower kappa numbers (lower residual lignin content in the kraft pulp) than the non pre-extracted bamboo chips, showing that the alkaline pre-treatment had a positive effect on delignification during kraft cooking. This might be due to the fact that the removal of hemicellulose/lignin during alkaline pre-extraction process resulted in chips having a more open structure thus improving the accessibility of the cooking chemicals to lignin in chips and improving the rate of diffusion of degraded lignin into the black liquor. For example, a kappa number of 16.0 could be achieved by pulping extracted chips at 100 ^oC for 1 h with 17% EA while 19% EA was needed when pulping with control chips (without pre-treatment) under the same conditions. Increasing the pre-treatment severity (longer time and higher temperature) also decreased the kappa number of pulp obtained under the same kraft cooking conditions (results of chips treated at 100 ^oC for 1 and 5 h, respectively (Table 4.1). Compared to the normal kappa number (30-50) of brownstock in a modern kraft pulp mill (Salmela et al. (2008); Mân Vu et al. (2004)), lower kappa numbers (lower lignin contents) of pulps obtained from alkaline pretreated chips were achieved in this study; this translates into lower demand for bleaching chemicals and, hence lower bleaching costs.

Table 4.1: Effect of alkaline pre-extraction and effective alkali charge on kraft pulping of bamboo.

Pre-extracted bamboo chips	EA (%)	Rejects[a] (%)	Total yield[a] (%)	Kappa number	Residual silica in pulp[a] (%)	Silica in BL[a] (%)	CSF (mL)	Fines[b] (%)	Hemicellulose[b] (%)
Non-extracted	13	2.3 ±0.2	55.1 ±1.4	30.1 ±0.5	0.19 ±0.03	0.91 ±0.03	549 ±10	17.4	25.5
	15	1.8 ±0.4	53.9 ±1.2	22.6 ±0.2	0.16 ±0.01	0.95 ±0.04	538 ±8	18.6	23.8
	17	1.5 ±0.5	53.6 ±1.7	18.8±0.6	0.14±0.02	0.95 ±0.03	544 ±12	19.1	20.4
	19	1.3 ±0.3	53.1±1.2	15.9±0.5	0.13±0.03	0.97±0.04	531±7	19.8	15.41
80 ^oC 3 h	13	0.5 ±0.2	54.3 ±1.8	27.2 ±0.6	≈ 0.01	≈ 0.01	629 ±12	14.2	20.11
	15	0.4 ±0.3	53.1 ±1.2	20.7 ±0.7	≈ 0.01	≈ 0.01	624 ±9	14.4	16.85
	17	0.2 ±0.1	52.2 ±1.5	16.5 ±0.4	ND	≈ 0.04	608 ±13	14.4	13.77
	19	≈ 0.01	51.0 ±0.8	13.9 ±0.2	ND	≈ 0.02	618 ±11	14.7	11.68
100 ^oC 1 h	13	0.3 ±0.1	52.3 ±2.3	27.6 ±1.2	≈ 0.01	≈ 0.01	635 ±8	13.8	19.38
	15	≈ 0.1	52.7 ±1.3	19.8 ±0.9	ND	0.04 ±0.02	624 ±8	14.0	16.76
	17	≈ 0.1	52.1 ±1.5	16.4 ±0.3	ND	≈ 0.02	619 ±12	14.4	13.55
	19	ND	51.4 ±1.2	12.9 ±0.8	ND	0.04 ±0.01	620 ±11	14.6	11.25
100 ^oC 5 h	13	≈ 0.1	52.2 ±1.6	22.4 ±1.0	ND	ND	649 ±5	13.1	15.22
	15	ND	51.5 ±1.9	16.1 ±0.7	ND	ND	640 ±16	13.6	14.66
	17	ND	50.9 ±1.0	13.8 ±0.6	ND	ND	620 ±9	14.0	12.36
	19	ND	50.3 ±1.0	11.1 ±0.4	ND	ND	612 ±12	14.2	10.17

[a] Calculations were based on original oven dried chip mass. [b] Calculations were based on oven dried pulp mass.
EA-effective alkali. ND-not detected. BL-black liquor. CSF-Canadian standard freeness.

The total pulp yield of extracted chips was generally slightly lower than that of the control under the same kraft cooking conditions (Table 4.1). It should be noted that pulps from extracted chips had lower kappa numbers (lower lignin content), which accounted for 0.3-0.6% of the pulp yield. In addition, a lower rejects content in the pulp could be obtained with alkaline pre-extracted chips (below 0.5%) compared to the 1.3-1.5% of the controls; this could be related to the fact that extracted chips have a more open structure enabling better penetration of cooking chemicals resulting in a more even cook. The screened pulp yield obtained from the extracted chips was similar to that of the control or even higher. Total pulp yield decreased with increasing EA charge for both the pre-treated chips and control. Similar results have been obtained by kraft pulping of alkaline pre-extracted aspen chips (Jun et al. (2012)).

The initial kraft pulp (brownstock), drainage resistance is an important parameter as it strongly affects the downstream operations such as pulp washing. In this study, the drainage resistance of the brownstock was determined as Canadian Standard Freeness (CSF). As shown in Table 4.1, the CSF of pre-extracted pulps were in the range of 600-700 mL whereas the freeness of the non-extracted pulps ranged from 520-560 mL. Additionally, the measured amount of fines, determined as fibrous materials with sizes between 0.07 and 0.2 mm, was lower in pre-extracted pulps than in control pulps (Table 4.1); these results were in agreement with studies on kraft pulping of hemicellulose extracted sugar maple (Duarte et al. (2011)). This might be attributed to the pulping process was not strong enough to degrade fibres themselves (Duarte et al. (2011)). Therefore, the higher CSF values of extracted pulps were in accordance with the decrease in the fines content. Higher CSF means faster rates of water drainage during brownstock washing, which improves the mill efficiency.

The most significant observation was the very low residual silica content in kraft pulp from pre-extracted chips. As can be seen in Table 4.1, the residual silica content of the pulp from pre-extracted chips was below 0.02% while it was 0.15-0.19% (based on original o.d. chip mass) in the control. One reason for the high residual silica content of the pulp from non-extracted chips might be that the silicates dissolved during pulping adhere onto the fibre surface and are not removed during subsequent pulp washing. High silica contents in kraft pulp make it unsuitable for use in high grade products such as ashless filter paper or facial tissue. In addition to the challenges of silica in the kraft pulp, high silica content in black liquor also causes problems in the chemical recovery process such as scaling of evaporators, decrease in causticizing efficiency, and the generation of large amount of solid waste (calcium silicate mixed with calcium carbonate). Moreover, silica in the black liquor is difficult to remove because of the high lignin content. Therefore, alkaline pre-extraction is a promising approach to solve the silica problems when pulping bamboo.

4.3.2 Pulp Physical Properties

It is important to assess the impact of the extraction process on the physical properties of resulting pulps. As indicated in Fig. 4.2 the initial freeness of the control pulp was much lower than the initial freeness of the pulps from chip pre-extracted with 19% EA. The rate of freeness drop with PFI refining was similar for all the pulps. These results indicate that pulps from alkaline pre-extracted chips need more refining energy to attain the same level of freeness as the control. This agrees well with the generalized experience that pulps with low content of hemicellulose and fines are

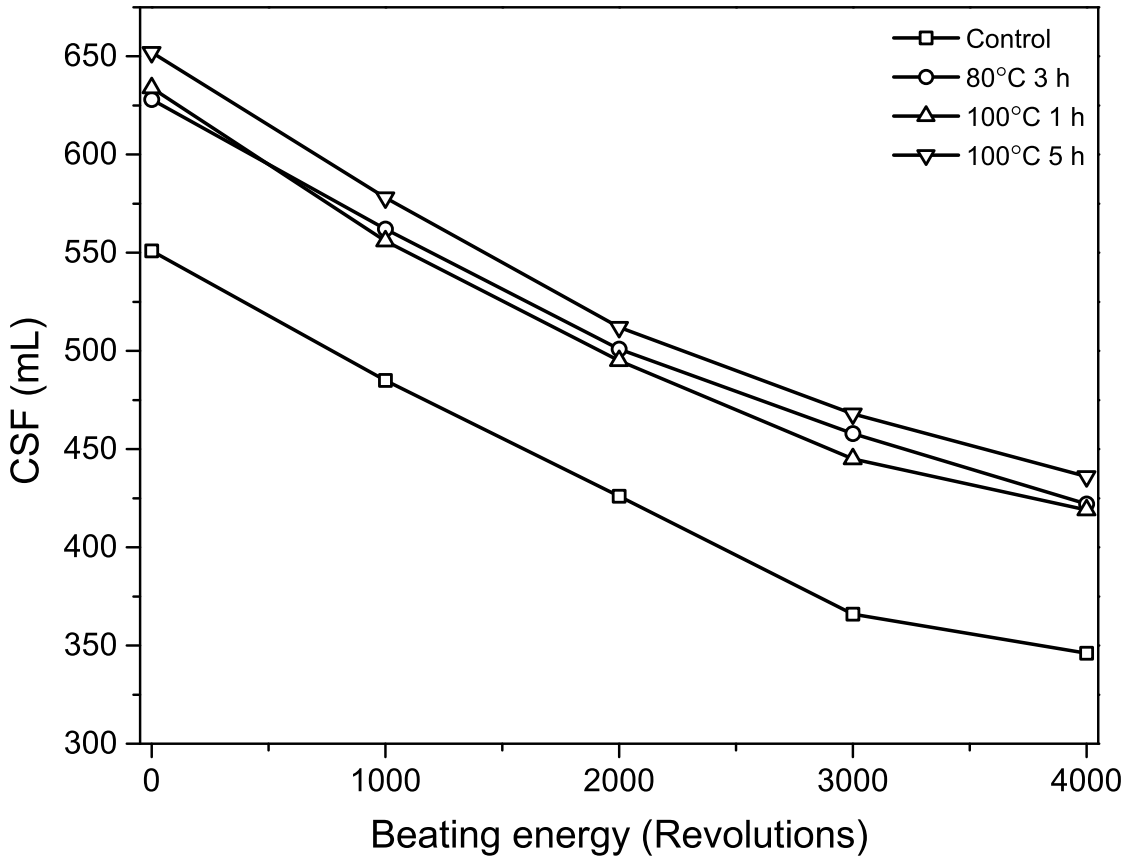

Figure 4.2: Plot of pulp freeness (CSF) versus PFI mill revolution for pulps obtained from kraft pulping of extracted and non-extracted chips with 19% EA.

difficult to beat to a target freeness due to the small degree of internal fibrillation with increased refining (Walton et al. (2010)). Similar refining results were also obtained in kraft pulping with extracted and non-extracted chips with 15%, 17% and 19% EA (data not shown).

The strength properties of all pulps were determined at the CSF of 425 mL. Plots of tensile and tear indices against EA charge of handsheets of pulps from pre-extracted chips and the control pulp are shown Figs. 4.3 and 4.4, respectively. Tensile strength index of pulps from alkaline pretreated bamboo chips initially increased with increasing EA charge, thereafter it decreased. For the control samples, the tensile

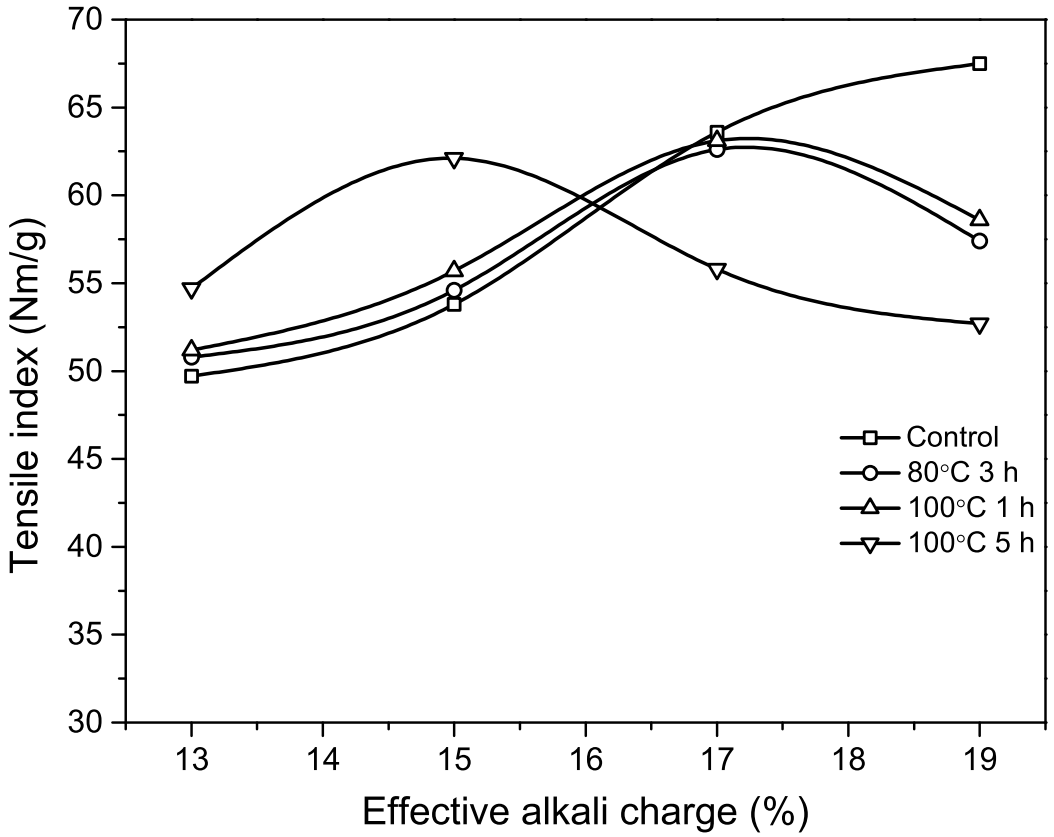

Figure 4.3: Effect of pre-extraction and effective alkali charge on the tensile index of pulp.

index increased with increasing EA charge. These results confirmed the result that the delignification rate of pre-extracted chips was faster than the control. With the higher removal of lignin from treated chips at lower EA charge, more bonding could be formed among cellulosic fibres than in the case of the control, resulting in the improvement of physical properties of handsheets. However, with continually increasing the EA charge, compared to the control pulps, the handsheet strength of pulps from extracted bamboo chips decreased significantly. One likely reason is the lower hemicellulose content in extracted pulps, resulting in fewer bonding.

It can be seen in Fig. 4.3 that the tensile strength index of pulps from chips extracted using milder pre-treatment conditions (80 ^oC for 3 h and 100 ^oC for 1 h)

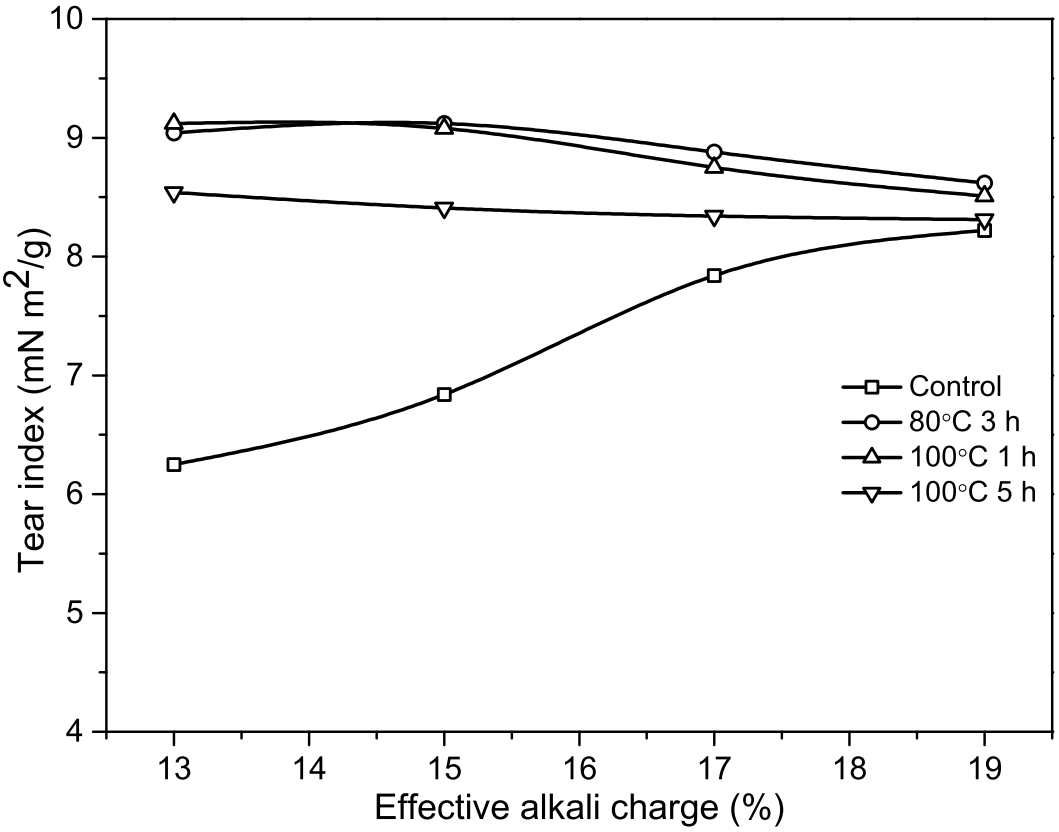

Figure 4.4: Effect of pre-extraction and effective alkali charge on the tensile index of pulp.

decreased at EA charges higher than 17%. This decrease began at 15% EA in the pulps from chips extracted at high severity (100 ^oC for 5 h). This is probably due to the loss of different amounts of hemicellulose during the alkaline pre-extraction processes. With the increase in the intensity of alkaline pre-extraction, more hemicellulose were removed, resulting in higher cellulose/hemicellulose ratio, which will form larger macrofibrils during handsheet making (Molin and Teder (2002), Walton et al. (2010)), resulting in lower bonding. In addition, at the highest tensile index of handsheets, hemicellulose contents of the pulps were 15.41%, 11.68%, 11.25% and 10.17% (based on o.d. pulp mass) for non-treated chips and chips pre-treated under conditions of 80 ^oC for 3 h, 100 ^oC for 1 h, and 100 ^oC for 5 h, respectively. Thus, it confirmed the assumption that hemicellulose content plays an important role in the strength properties of paper.

Fig. 4.4 shows that the tear index of extracted pulp was better than that of non-extracted pulp. The overall improvement of tear strength with alkaline pre-extraction can be explained by the removal of lignin and hemicellulose making the resultant kraft pulps to contain more cellulose per gram handsheet. On the other hand, the removal of fines might also improve the tear index of the extracted pulps.

Results of the kraft pulping with extracted and non-extracted chips show that the alkaline pre-extraction is suitable for the production of papermaking fibre. Moreover, it also might be an alternative approach for the production of dissolving grade pulps (high purity cellulose) from bamboo. Moreover, the pre-extraction process removes hemicellulose and silica from the black liquor cycle which will improve the efficiency of the chemical recovery process for the recovery of energy and inorganic chemicals (NaOH and Na_2S). The hemicellulose and silica removed during the process can

potentially be converted into other value-added products.

4.3.3 APEL Properties

Based on our previous study on alkaline pretreatment of bamboo chips to extract the maximum silica and hemicellulose while minimizing the degradation of cellulose and lignin (Chapter 3), the APEL was produced from the alkaline extraction with a NaOH charge of 10-14% (based on o.d. chip mass) at 90 ^oC for 3 h with a liquid-to-wood ratio of 8 L/kg in the laboratory. Table 4.2 shows the chemical composition and other properties of the generated APELs.

The concentration of silica, released as soluble sodium silicate (Na_2SiO_3), was 1.45, 1.73 and 1.70 g/L in the APELs obtained from 10, 12 and 14% NaOH charges, respectively. Based on the silica concentration in the APEL, the liquid-to-wood ratio (8 L/kg) used for the extraction and the moisture content of treated chips (60-65%), it was calculated that up to 99% of silica in raw chips was removed with 12-14% NaOH, whereas about 86% of silica was removed with 10% NaOH charge (based on o.d. chip mass). This was further confirmed by the measurement of the silica content of extracted chips, which was 0.17% (w/w) in the case of 10% NaOH charge and less than 0.02% (w/w) with 12% and 14% NaOH charge.

The maximum concentration of lignin (mainly monomeric and oligomeric lignols) of the liquors was 1.99 g/L; this means that only about 5.1% of initial lignin was removed during alkaline pre-extraction under the studied conditions. The low lignin concentration is favorable for the silica precipitation from the APEL. The extracted glucan in the liquors ranged from 1.24-1.46 g/L with increasing NaOH charge from

10-14% (based on o.d. chip mass), corresponding to 1.7-2.0% of the initial glucan. In the liquors, xylan had a concentration of 8.78-9.97 g/L depending on NaOH charge, corresponding to about 30% of xylan being removed during alkaline pretreatment. Concentrations of galactan and arabinan in the APELs were 0.2-0.5 g/L, respectively, while acetic acid concentration was about 2.75 g/L. According to the measurements, the sum of biomass yield and dissolved materials in the APELs were calculated to be 98.5% for the treatments under the three NaOH charges (10-14% w/w). This 1.5% biomass loss might be due to other undetermined dissolved inorganics and degradation products. The pH of generated APELs were 12.97, 13.12 and 13.28 for 10%, 12% and 14% NaOH charges, respectively.

Based on the above experimental data, utilization of 12% NaOH charge (on o.d. chip mass) not only had the potential of removing all silica from bamboo chips but also could reduce the chemical consumption compared to that of 14% NaOH charge. Consequently, the APEL obtained from the pretreatment with 12% NaOH charge (based on o.d. chip mass) was selected and subjected for the recovery of silica and hemicellulose.

4.3.4 Isolation of Silica from APEL with Carbon Dioxide

During CO_2 treatment of the APEL, soluble sodium silicates (Na_2SiO_3) are converted to the insoluble colloid silicic acid (H_2SiO_3), which can be removed from the liquor (see Equation 4.2). In this work, silica was recovered from the APEL by lowering its pH with CO_2 at different temperatures (20-100 ^oC). Fig. 4.5 shows the effect of temperature and pH on the removal of silica from the APEL. Evidently, the temperature

Table 4.2: Chemical composition of alkaline pre-extraction liquor (APEL).

Component	NaOH charge		
	10	12	14
Biomass yield (%)	88.8	87.5	86.6
Solid content (%)	3.26	3.31	3.32
Lignin (g/L)	1.42	1.74	1.99
Glucan (g/L)	1.24	1.29	1.46
Xylan (g/L)	8.78	9.26	9.97
Galactan (g/L)	0.21	0.22	0.34
Arabinan (g/L)	0.32	0.41	0.45
Silica (g/L)	1.45	1.73	1.70
Sodium acetate (g/L)	2.76	2.77	2.74
pH	12.97	13.12	13.28

Values are expressed as averages of the three replicate measurements.

had a minor effect on the amount of silica precipitated from the APEL. At the five studied temperatures, the percentage of removed silica varied 93-97% at a final liquor pH of about 9.0. The amount of silica removed was increased slightly by increasing the temperature from 20 to 60 ^oC. Increasing in temperature to 100 ^oC led to a small reduction in silica removal. The maximum silica removal was achieved at 60-80 ^oC. Moreover, compared to low temperature (20-60 ^oC), higher temperature (80-100 ^oC) required more CO_2 to reach the same final pH. For example, it required about 120 min to decrease the pH of the APEL to 9.0 at 100 ^oC at a 0.1 L/min CO_2 flow rate; in contrast, at 20 ^oC with the same flow rate, pH 9.0 was reached in about 25 min. This is due to the decreasing solubility of CO_2 with increasing temperature of the solution, which means that the utilization of flue gas would be less efficient at higher temperatures. Therefore, it can be concluded that the optimum temperature for the precipitation and recovery of silica from the APEL was around 60 ^oC. Additionally, since the temperature of the obtained APEL after pre-treatment (conducted at 90 ^oC) was around 65 ^oC, the proposed process would not require extra heat in the

precipitation step.

In contrast to temperature, the liquor pH plays a much more important role in silicic acid precipitation from the APEL. During the bubbling process, the pH of the APEL gradually decreased over time towards a plateau at all studied temperatures. As shown in Fig. 4.5, in the pH range of 13.12 to 11.0, only about 4.8-8.7% of silica was precipitated from the APEL at all studied temperatures. However, when the pH of the liquor was decreased from 11.0 to 9.0 by bubbling CO_2 for a longer time (25-120 min), a sharp increase in the amount of precipitated silicic acid occurred; up to 93-97% of raw silica in the APEL was removed at the five treatment temperatures. For example, at 60 ^oC, about 96% of silica was removed from the APEL by lowering the pH to 9.0. With continuous bubbling of CO_2 into the liquor, more carbonic acid is formed, and the pH drops as the acid concentration increases resulting in the rapid formation of the insoluble silicic acid at pH 11.0 to 9.0. About 2-5% of silica still remained dissolved in the APEL even when the pH was decreased to 8.2. This can be attributed to the solubility of silica even at low pH values, which means not all silica can be precipitated by lowering the pH of the solution (Hegde and Rao (2006); Liu et al. (2008)). In addition, it should be noted that it was very difficult to reduce the pH of the APEL below 8.0 even at the lowest temperature (20 ^oC) tested in this study, which might be due to the bicarbonate/carbonate buffering system formed in the APEL. In contrast, lowering the pH to 8.2 was much easier to achieve. Accordingly, the pH of silica precipitation from the APEL should be limited to about 8.2 in order to maintain mill efficiency.

The APEL after silica removal can be used as a raw feedstock for the recovery of hemicellulose to produce ethanol, xylitol or polymeric films; so it is of great impor-

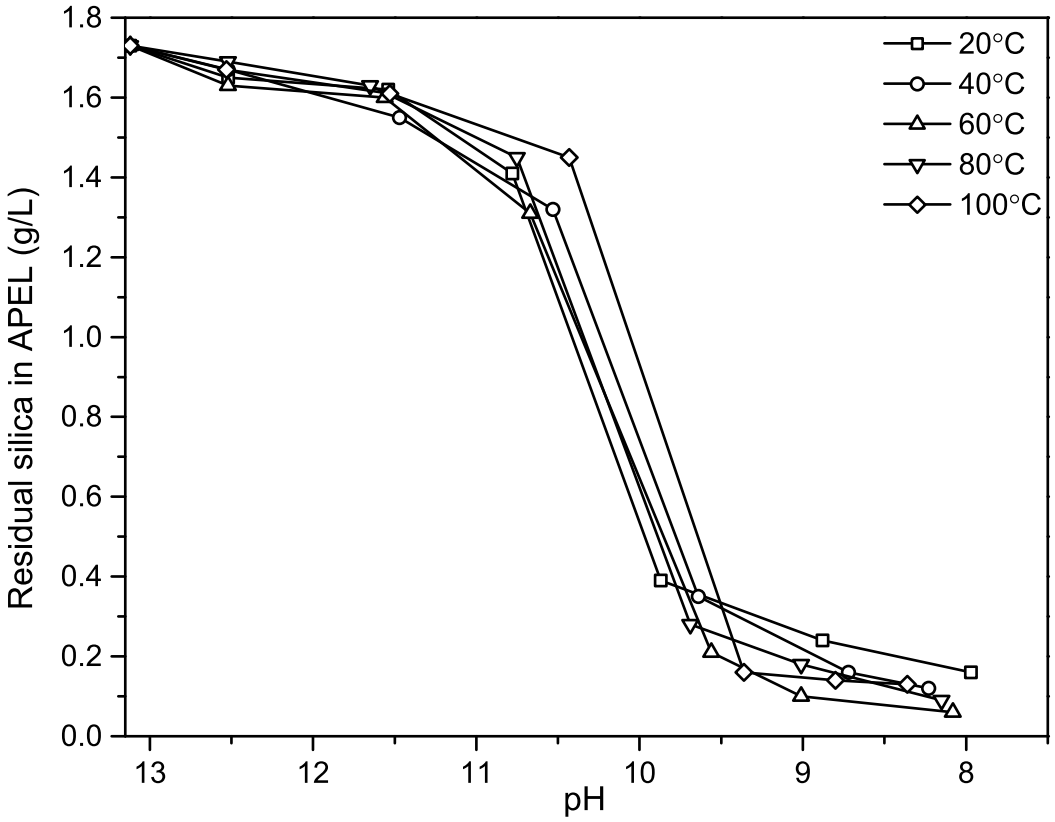

Figure 4.5: Effect of temperature and pH on the precipitation of silica from the APEL.

tance to minimize the loss of hemicellulose during the CO_2 treatment stage. Analysis of the chemical composition of APEL recovered after maximum silica removal at 60 ^oC showed that only about 4% of hemicellulose was removed during the silica removal. The likely reasons for hemicellulose loss include the potential co-precipitation of hemicellulose with silica as well as wash-off during the silica separation process. It can be concluded that the precipitation and filtration of silica from the APEL does not significantly influence the hemicellulose concentration in the supernatant, and will not have a large negative effect on subsequent hemicellulose recovery.

4.3.5 Capture of CO_2 from the CO_2/N_2 Mixture

With the fundamental information obtained from the silica precipitation with CO_2 only, an attempt for developing the utilization of flue gas for recovering silica was initiated. Thus, in this study, a mixture gas of CO_2 (0.1 L/min) and N_2 (0.2 L/min) was used to simulate for the flue gas from the chemical recovery circle of the kraft pulp mills (Fan et al. (2009)). During the treatment process, the unused gas was released from the reactor to make the pressure in the reactor constant at 1 atm. The released gas phase composition was analyzed during the silica precipitation at different times, the CO_2 composition is given in Table 4.3. The CO_2 concentration in the gas phase was found to gradually increase with increasing treatment time. This is because initially more CO_2 was dissolved in the liquor and consumed by the reactions with chemicals such as NaOH and Na_2SiO_3 in the APEL; with prolonged treatment, the chemical reactions were completed and the content of CO_2 in the APEL reached saturation.

Table 4.3: Gas phase CO_2 measurements during silica precipitation.

Time (min)	CO_2 (%) ($\pm$ 0.3)
0	33.33
10	20.34
20	20.78
30	21.43
40	22.53
50	23.59
60	25.25
70	26.43
80	27.42
90	28.19
100	28.73
110	29.15
120	29.52

Based on the compositional analysis of the residual gas phase, the actual adsorption or consumption of CO_2 for a period of 5-120 min was calculated. As shown in Fig. 4.6, the adsorption/uptake of CO_2 by the APEL initially increased with increasing time, thereafter it reached a plateau. At 60 and 120 min, the pH of the treated APEL was determined to be 8.16 and 8.08, respectively. These results confirmed that the maximum consumption of CO_2 was completed at 60 min and it was very difficult to reduce the pH of the APEL below 8.0 with CO_2. As illustrated in Fig. 4.5, during the process of reducing the pH of APEL from 13.12 to 8.16, 1.94 L CO_2 (at a density of 1.842 g/L) was consumed per 200 mL APEL. Thus, the adsorption of CO_2 is calculated to be 7.15 g_{CO_2}/L_{APEL} (based on the 12% NaOH charge used in this study). Moreover, since the real flue gas might contain small amounts of other acidic compounds such as SO_2, NO_X or H_2S (Douskova et al. (2009)), which will also be removed by the APEL, resulting in a relatively clean gas for emissions.

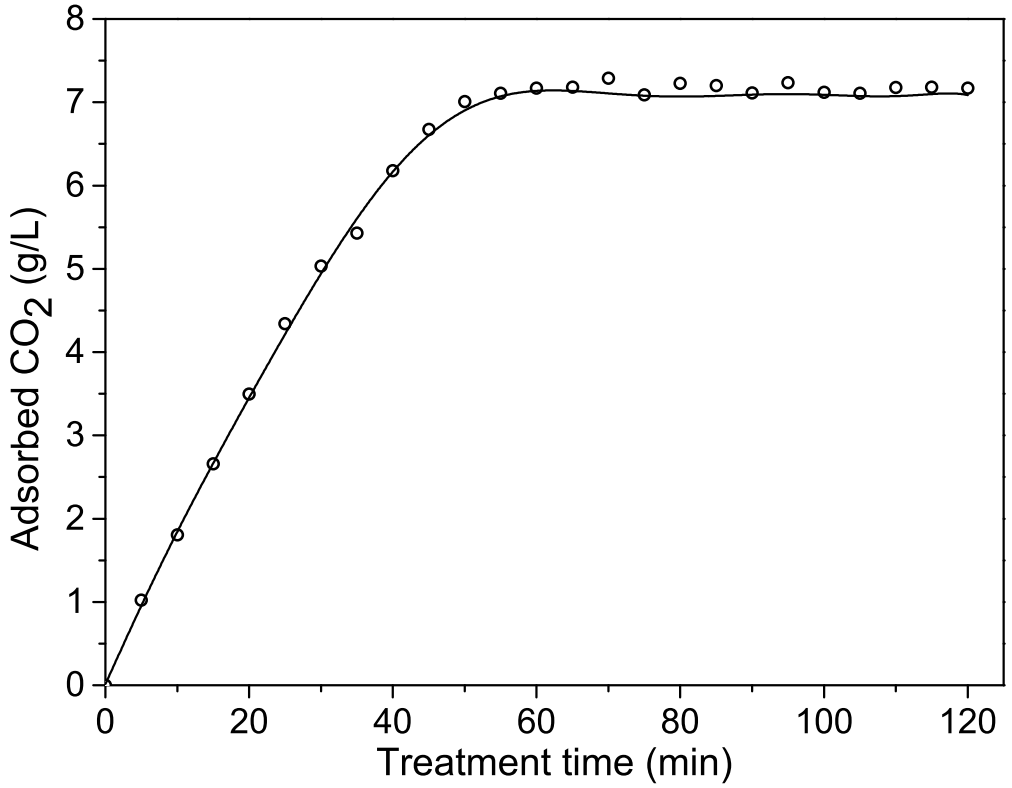

Figure 4.6: CO_2 adsorption measurement curve for the precipitation of silica from the APEL at 60 ^oC.

Table 4.4: Mineral composition of silica powder prepared from the APEL.

Element	Weight percentage (%)
Calcium (Ca)	0.12
Manganese (Mn)	0.0026
Iron(Fe)	0.0071
Aluminum (Al)	Not detected
Copper (Cu)	0.0097
Magnesium (Mg)	0.0075
Potassium (K)	0.0057
Sodium (Na)	0.0034
Sum	0.156

4.3.6 Compositional and FTIR Analysis of Silica Powders

To remove organics (lignin and sugars) and prepare highly purified silica powder, oven dried silica samples were burnt at 700 ^oC for 4 h. The weight percentages of the mineral ingredients present in the silica powders after burning were measured using an iCP spectrometer (Table 4.4). As can be seen in Table 4.4, the impurities contained in the silica powders were calcium, manganese, iron, copper, magnesium, potassium and sodium; among which the concentration of calcium was the highest (0.12% w/w) while the total impurities accounted for about 0.16% (w/w). These results showed that the produced powders contained more than 99.8% (w/w) of silica, confirming the hypothesis that high purity silica could be produced from the APEL of bamboo. Such high purity of the precipitated porous silica particles makes it an excellent starting material for various high-value products such as pharmaceuticals that require silica purity higher than 99.7% (Morpurgo et al. (2010)).

Fig. 4.7 shows the FTIR spectra of the silica powders before (a) and after (b) high temperature (700 ^oC) burning. As shown in Fig. 4.7a, the two absorption peaks at 3408 cm^{-1} and 1596 cm^{-1} are principally attributed to stretching of -OH groups

and bending modes of absorbed water in precepitated silica particles, respectively (Kačuráková et al. (1998)). The predominant absorption band at 1074 cm^{-1} can be assigned to Si-O-Si asymmetric stretching and, absorbance peaks at 794 cm^{-1} is due to the symmetric Si-O-Si bond (An et al. (2010); Knauss and Wolery (1988)). Peaks of Fig. 4.7a (before high temperature burning) confirmed that very little hemicellulose co-precipitated during the silicic acid precipitation process. Comparison of the FTIR spectra 4.7b (after burning at 700 ^oC) and 4.7a shows the disappearance of the two absorption peaks at 3408 cm^{-1} and 1596 cm^{-1} upon burning, indicating the complete removal of organics and water producing high purity silica powders. Other absorbance bands at 1084 cm^{-1} and 792 cm^{-1} (Fig. 4.7b) are also assigned to Si-O-Si asymmetric stretching and symmetric Si-O-Si bond, respectively (Hegde and Rao (2006)). The shift in the 1074 cm^{-1} peak in Fig. 4.7a to 1084 cm^{-1} in Fig. 4.7b is likely due to the elimination of the hydrogen bond (O-H) and the weakening of Si-O-Si after high temperature treatment. The IR bands of silica powder investigated in this study were similar to those reported in other investigations (Barik et al. (2008); Kalapathy et al. (2002)). Also, the absence of peaks at around 1510 cm^{-1} and 2930 cm^{-1} in the FTIR analysis confirmed that lignin did not co-precipitate with silica during APEL processing (Liu et al. (2008)). Therefore, alkaline pre-extraction effectively decouples desilication from the major delignification reactions of kraft pulping. This is a significant benefit in kraft pulping because, with a pre-extraction step, silica does not fractionate into the black liquor during the kraft cook. Scaling and other problems that occur during kraft chemical recovery are hence eliminated. Moreover, if necessary, cleaner lignin fractions with lower ash, can be recovered from black liquor.

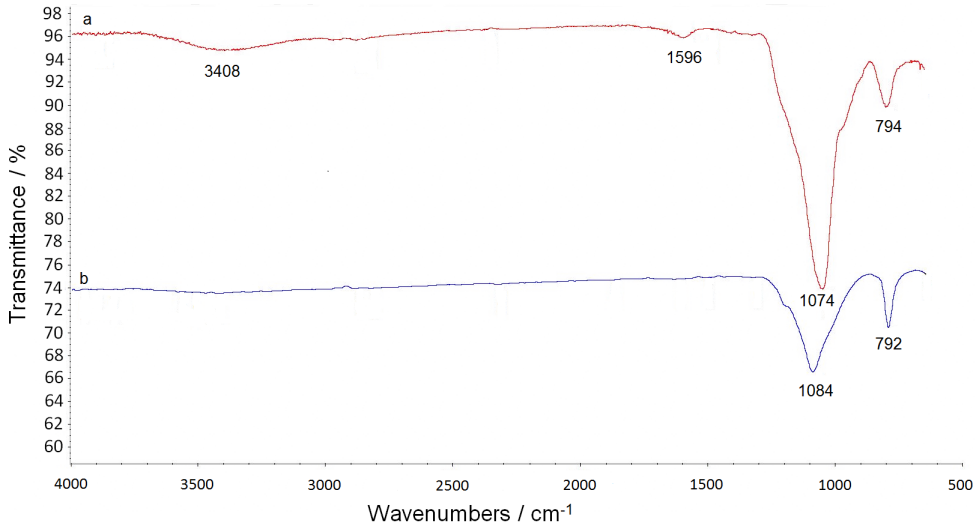

Figure 4.7: Fourier transform infrared (FTIR) spectra of silica produced from the APEL of bamboo (a: before burning; b: after burning at 700 ^oC).

4.3.7 Precipitation, Characterization and Utilization of Hemicellulose from the Treated APEL

The hemicellulose recovery was conducted on the APEL after silica removal at optimum conditions (CO_2 treatment at 60 ^oC to pH 8.6). Chemical composition analysis of the isolated hemicellulose showed that the total sugar content was 92.2%, in which xylan, galactan, arabinan and glucan contents were 78.1%, 2.1%, 1.8%, and 10.2%, respectively. The measured lignin and ash contents were 2.7% and 1.1%, respectively. The uronic acid content was determined to be 4.0%, which was in good accordance with reports that about 4-5% of uronic acid appeared as 4-O-methyl-D-glucuronic acid residues in bamboo feedstocks (Billa et al. (1996)). In the literature, similar composition results have been reported for alkaline extracted hemicellulose from hardwood and sugar cane bagasse (Peng et al. (2009); Jun et al. (2012)). Due to the co-precipitation of lignin and possibly extractives, the isolated hemicellulose had a

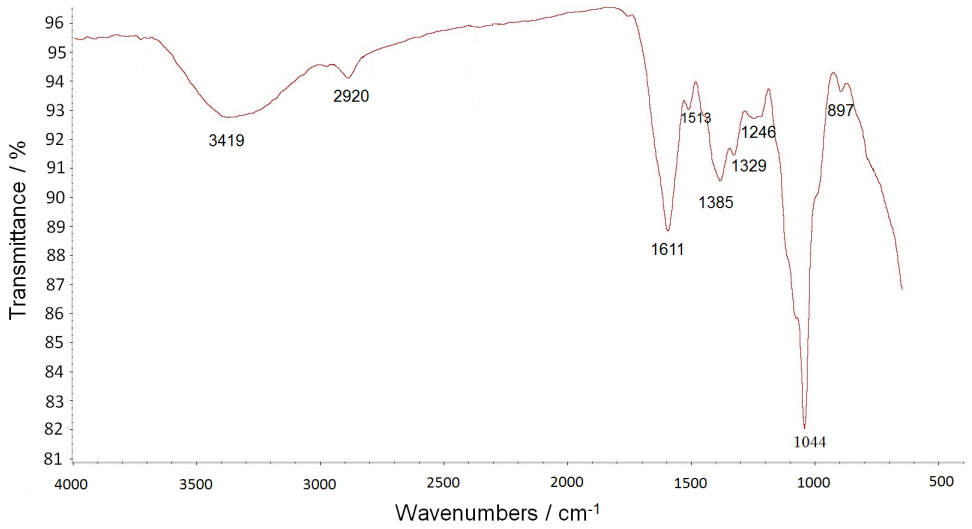

Figure 4.8: Fourier transform infrared (FTIR) spectra of hemicellulose produced from the APEL.

brightness of 32.6% ISO. After hemicellulose precipitation, the residual liquor can be sent to the traditional kraft chemical recovery process to recover inorganics such as sodium hydroxide for alkaline pre-extraction or kraft cooking.

Fig. 4.8 shows the FTIR spectra of the isolated hemicellulosic fraction. The strong broad band at 3419 cm^{-1} is attributed to the stretching of O-H bond. The absorbance at 2920 cm^{-1} was due to the C-H stretching vibration. The absorbance at 1611 cm^{-1} can be assigned to absorbed water in hemicellulose (Wen et al. (2011)). The prominent absorption peak of 1044 cm^{-1} is due to C-O stretching in C-O-C linkages. The absorption bands of 1385, 1329, and 1246 cm^{-1} are characteristic of hemicellulose obtained by alkali extraction (Xu et al. (2007)). The absorbance at 897 cm^{-1} can be assigned to $\beta - glycosidic$ linkages between the sugar units (Liu et al. (2011)). The small absorption peak of 1513 cm^{-1} is characterized by aromatic skeleton vibrations belonging to lignin (Billa et al. (1996)).

To further characterize the isolated hemicellulose, size exclusion chromatography

(SEC) was used to determine the average molecular weight and the polydispersity index (PDI). The measured weight-average (Mw), number-average (Mn) molecular weights and the PDI were 26,770, 18,920 g/mol and 1.41 respectively. The small PDI value indicates that the obtained hemicellulose have a good chemical and structural homogeneity, which is favorable for downstream applications such as production of hemicellulose-based bio-polymeric films or other applications.

The obtained hemicellulose were used to prepare biopolymeric films by the addition of 30% glycerol as the plasticizer. The tensile strength, elongation at break, WVTR and WVP were determined to be 30 MPa, 3.0%, 310 $g/(m^2 \cdot d)$, and 0.8 $gmm/(m^2 \cdot d \cdot kPa)$, respectively. At 50% relative humidity (RH), the oxygen permeability of the films formed with hemicellulose was 0.23 $cm^3 \cdot m/(m^2 \cdot d \cdot kPa)$, which was substantially lower compared to the films formed with amylose and ethylene vinyl alcohol at the same pH (Wen et al. (2011); Xu et al. (2007)). These results showed that the hemicellulose recovered from APEL could be used as a good alternative, sustainable resource for the production of high-value added films (Liu et al. (2011); Stading et al. (1998)). As the property standards vary depending on end-use, polymeric film produced from bamboo xylan (obtained in this study) needs to be further investigated to increase the tensile strength and the brightness.

4.3.8 Proposed Modification to Kraft Pulping Process and Mass Balance

Based on our findings, shown in Chapters 3 and 4, we propose a process for the integration of low temperature alkaline pre-extraction of silica and hemicellulose from

bamboo chips into a commercial kraft pulping as illustrated in Fig. 4.9. In a typical kraft pulp mill, alkali is readily abundant as kraft white liquor, so the integration of this pre-extraction stage could be achieved without major capital investment of extensive process changes. In the proposed process scheme, washed bamboo chips are treated with alkali solution under atmospheric conditions prior to kraft pulping. The treated chips with very low silica content are processed through kraft pulping or pre-hydrolysis kraft pulping to produce high-grade kraft pulp or dissolving pulp. The extraction liquor (APEL) is treated for the recovery of dissolved materials including silica and hemicellulose, which is critical to maximize revenue to the kraft pulp mill through the production of value added products. To precipitate silica from the APEL, CO_2, a waste gas readily available as flue gas in pulp mills, was used to convert the soluble silicates into insoluble silicic acid, which is isolated via filtering. Then, the filtered samples were dried and burnt at 700 ^oC to remove any residual organics and produce silica particles. The obtained amorphous silica particles can be easily pulverized to nanosilica for various applications (Liou (2004)). The separation of the maximum amounts of silica from the APEL significantly improves the recovery of residual alkali and lime mud in the chemical recovery cycle of a typical kraft pulping process. Ethanol was then added to the CO_2 treated APEL to precipitate the hemicellulose. The recovered hemicellulose can be used as the starting material for bio-polymeric films production, biofuels fermentation or other applications. It is expected that the alkaline pre-extraction will lower the alkali and other chemicals charges required during subsequent kraft pulping and bleaching stages (Helmerius et al. (2010)). Moreover, kraft white liquor, generated during the chemical recovery circuit in the kraft pulp mill, can be readily used as the alkali solution for silica and

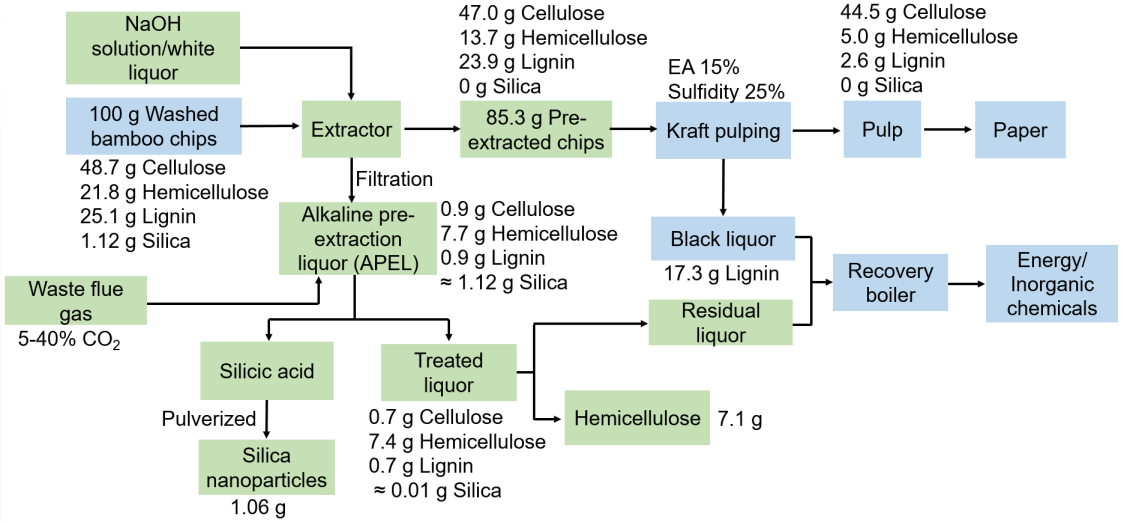

Figure 4.9: Proposed process of kraft pulping with extraction and recovery units of silica and hemicellulose from bamboo chips.

hemicellulose pre-extraction (Jun et al. (2012)). After the sequential steps of silica and hemicellulose recovery, the double-treated APEL can be mixed with black liquor from kraft pulping and sent to the traditional chemical recovery circuit to recover energy and inorganic chemicals for mill operations.

Taking the 3 h pre-extraction at 100 ^oC with 18% NaOH as an example, the mass balance of the main components of bamboo around the whole system from pre-treatment to kraft cooking can be determined (Fig. 4.9). Mass balance of each fraction is expressed in terms of dried material mass. With regards to the pre-treatment stage, the sum of recovered organics (cellulose, hemicellulose, lignin) and inorganic (silica) in both biomass residual and APEL corresponded to 97.4% of those in the raw bamboo chips. The 2.6% material loss is due to the degradation of lignin and/or hemicellulose into unidentified products. The analysis of the APEL showed that about 35% of hemicellulose (mainly xylan) and 99% of silica contained in raw bamboo chips were extracted, showing a good revenue source for the mill and a novel way for solving

the silica problems.

The generated APEL was subjected to CO_2 treatment to recover silica particles; about 1.06 g silica (after combustion at 700 ^oC) was produced. The CO_2 treated liquor was used for the hemicellulose recovery, in which the precipitated hemicellulose was determined to be 7.1 g. Based on 100 g o.d. mass of chips entering the pre-extraction process, the mass of obtained silica (1.06 g) and hemicellulose (7.1 g) corresponded to 95.5% and 92.2% of the two components in the APEL, respectively. The losses of silica and hemicellulose during the recovery process might be due to the solubility of silica even at low pH and hemicellulose separation during CO_2 treatment process, respectively.

The pretreated bamboo chips (without washing) were subjected to kraft cooking, performed at 15% EA charge and 25% sulfidity. Based on 100 g o.d. mass of chips entering the pre-extraction-kraft pulping process, the mass of obtained pulp was determined to be 52.5 g, in which masses of cellulose, hemicellulose, and lignin were 44.1 g, 4.9 g, and 2.7 g, respectively. The recovered masses of cellulose and hemicelluloes in the brownstock corresponded to 94.7% and 36.5% of the two components in the pre-treated chips, respectively, showing reasonable agreement with previous studies (Pinto et al. (2005); Mân Vu et al. (2004)). The losses of cellulose and hemicellulose during delignification might be due to peeling reactions and alkaline degradation, respectively (Rocha et al. (2012)). For the material balance of lignin during kraft pulping, as shown, the total amount of precipitated lignin in the black liquor and lignin in the final pulp was 19.9 g, which was equivalent to 82.8% of the lignin in pre-treated chips. The 17.2% loss of lignin in raw chips during kraft cooking might be due to water washing of the kraft pulp and incomplete lignin precipitation during black

liquor acidification. Finally, with regards to the main components (cellulose, hemicellulose, and lignin), the overall recovery of the proposed system from pre-extraction to kraft pulping and byproducts recovery showed a good mass balance of 80.2%.

Moreover, one important aspect of the proposed scheme is the adsorption of CO_2 in a cost-effective way, which transfers the industrial waste (flue gas) to a valuable starting material; this has the potential for lowering capital and operating costs and reducing pulp mill greenhouse gas emissions. In using silica-rich biomasses for biorefineries, this proposed process has several advantages, for example, it creates a silica-free substrate with high digestibility. During the subsequent processing of alkaline extracted chips, lower chemical or enzyme charge could be expected (Kumar et al. (2009); Jun et al. (2012); Huang et al. (2008)). Additionally, a relatively clean lignin fraction could be obtained from the spent liquor after cooking or enzymatic hydrolysis of silica- and extractive-free bamboo chips.

For a biomass-to-pulp plant that has a capacity of 600 tons bleached kraft pulp per day, about 1500 o.d. tons of bamboo chips are required. With the studied bamboo, about 16.8 $tons/day$ of silica is processed into the pulping scheme, which causes serious problems in chemical recovery circuit and quality of final pulp. With the proposed technology, alkaline pretreatment of bamboo chips carried out with a liquid-to-wood ratio of 8 L/kg at 90 ^oC and 12% NaOH charge (based on o.d. chip mass) for 3 h, about 9500 m^3/day APEL will be generated. To precipitate the dissolved silica in the APEL, about 67.9 $tons/day$ of CO_2 is required, which will might improve the handling of acidic compounds in the mill waste gas. Moreover, the separation of the maximum amounts of silica from the APEL significantly improves the recovery of residual alkali and lime mud in the chemical recovery cycle of a typical kraft pulp-

ing process. The extraction of silica prior to pulping also increases the evaporation efficiency by lowering the viscosity of black liquor obtained from kraft pulping and eliminating the scale buildup in the evaporators (Cardoso et al. (2009)). In addition, the reduction of silica content of the lime mud generated during the causticizing stage of kraft chemical recovery makes the lime mud recyclable, necessitating disposal of large amount of solid waste which is detrimental to the environment (Pekarovic et al. (2005)). In addition, hemicellulosic sugars in the APEL can be separated by ultrafiltration or nanofiltration (Ahsan et al. (2014)), which greatly reduces the amount of ethanol required.

One of the most advantageous aspects of our proposed approach is that the method decouples silica from organics-rich black liquor enabling silica recovery without substantial loss of lignin and hemicellulose. Moreover, the proposed approach may work for a bioethanol plant as well with using high-silica biomasses as raw material.

4.4 Process Engineering

4.4.1 Process Description

To evaluate the feasibility of the proposed process in an industrial mill application, a mass balance of each operation stage was calculated. Taking into account the existing equipment and the pulping process of the typical kraft pulp mill (Chongqing Lee & Man mill, China as an example), a process combination was designed to resolve the silica problems and recover byproducts, shown in Fig. 4.10.

In the proposed process, before kraft cooking, bamboo chips are pre-treated with

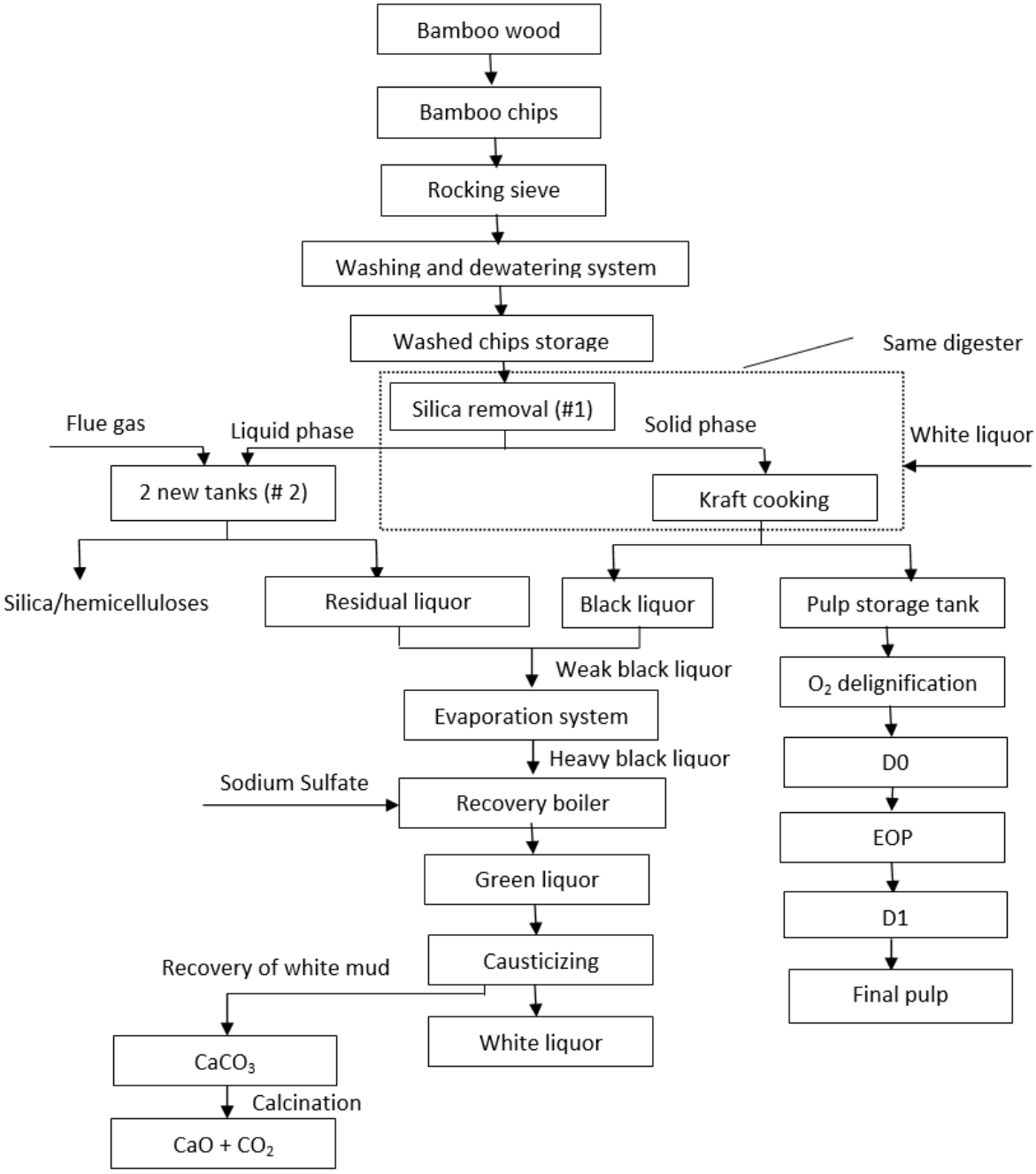

Figure 4.10: Combination of the new stages in a typical kraft bamboo pulp mill.

a NaOH solution (white liquor) in the digester, which converts insoluble silica into soluble sodium silicate. The solution of dissolved sodium silicate is separated from the bamboo chips by displacement with fresh white liquor. Then carbon dioxide (flue gas) is added into the pre-extraction liquor (APEL) to lower the pH and convert sodium silicate into insoluble silicic acid, which can be precipitated and removed from the liquor. After this, the resulting liquor is mixed with black liquor from Kraft cooking to be sent to the chemical recovery process. Because the silica in the mixed liquor has been removed, current problems encountered during chemical recovery processes, including scaling of evaporators, low evaporation efficiency, and the inability to recycle lime mud, are substantially resolved.

Table 4.5: Mass balance of the pulp line.

Program	Liquid phase (L)		Solid phase		
	input	output	input	rejects	dissolved material
Chips	470	-	530	-	-
Screening system	-	16.45	-	18.55	-
Chip washing system (5 L/kg)	2650	2638.52	511.45	7.67	-
Silica/hemicellulose extraction (8 L/kg)	3565.21	3316.78	503.78	5.04	70.53
Kraft cooking (4.4 L/kg)	1241.80	607.32	428.21	-	-
Washing of brown stock	3637.25	2566.29		8.35	141.52
O_2 delignification stage	8082.83	8323.13	269.99	2.70	27.0
D0 stage	3641.69	3653.08	242.99	1.21	1.21
EOP stage	3608.40	3631.29	240.56	1.20	1.68
D1 stage	3565.05	3576.24	237.67	0.71	0.48
Overall	30458.23	28329.10	236.48	293.52	
Final pulp storage	$L_{in} - L_{out} = 2129.13$		$Q_{in} - Q_{out} = 236.48$		
Real pulp consistency in the storage tank	$236.48/(2129.13 + 236.48) = 10\%$				

4.4.2 Mass Balance of Pulp Line and Chemical Recovery Process

According to the calculations of the mass balance of each operation step (Appendix A3), a summary of the pulping process with the silica and hemicellulose extraction stage was made, shown in Table 4.5. The APEL obtained from the silica/hemicellulose stage is 3312.35 L, which will consume about 23.7 kg CO_2 for the recovery of silica from the APEL. Moreover, according to the calculation for illustrating an industrial process, a cost estimate on the proposed stages, alkaline pretreatment and recovery of dissolved biomass, can be made.

Table 4.6 shows the mass balance of the chemical recovery process. Due to the lack of data with stages of recovery boiler, causticizing system and calcination, mass

Table 4.6: Mass balance of the chemical recovery process.

Program	Input		Output	
	liquid (L)	solid (kg)	liquid (L)	solids weight (kg)
Silica recovery	3450.89	75.57	3379.79	71.1
Hemicellulose recovery	3379.79	64.44	3043.09	336.7
Evaporation	5575.98	170.52	284.2	-
Recovered silica	$71.1 \times 10\% = 7.11\ kg$			
Recovered hemicellulose	$336.7 \times 10\% = 33.67\ kg$			

balance of this part was not made.

This proposed modification to the typical kraft pulping process not only solves the silica problems in the kraft pulping of bamboo, but also provides a kraft pulp mill a green pathway to manufacture high-value products from the pre-extracted and precipitated silica and hemicellulose. This proposed process has several advantages, for example, it increases the revenue to the kraft pulp mill by recovering silica and hemicellulose for various consumer products. It also converts waste industrial flue gas containing CO_2 to a valuable starting material for silica precipitation. Moreover, the extraction of silica prior to pulping increases the evaporation efficiency by lowering the viscosity of black liquor obtained from kraft pulping and eliminating the scale buildup of evaporators. In addition, the reduction of silica content of the lime mud generated during the causticizing stage of chemical recovery circuit of kraft pulping process makes the lime mud recyclable, as opposed to its disposal as a solid waste. Another significant aspect of the process is the ease in which it can be implemented in existing kraft-based pulping mills.

4.5 Summary

Alkaline pre-extraction of the bamboo chips improved the delignification during kraft pulping even at lower effective alkali charges. Pulp from pre-extracted bamboo chips showed similar screened yield to that of non-extracted chips while initial drainage resistance (CSF) improved slightly. The tensile strength index of the pulp actually benefited from the alkaline pre-treatment at low EA charges. The tear strength index of the kraft pulp was improved by the alkaline pre-extraction. Silica was not detected in the kraft pulp and black liquor obtained with pre-extracted bamboo chips indicating that the process provides a solution to silica problems encountered in bamboo pulping.

All the silica and a part of the hemicellulose in bamboo chips were fractionated into an alkaline pre-extraction liquor (APEL) during alkali pre-treatment of bamboo chips. To recover the dissolved silica and hemicellulose from the APEL, a sequential route involving carbon dioxide (CO_2) precipitation and ethanol treatment was developed. Up to 97% of silica dissolved in the APEL was recovered by treating the APEL at 60 ^oC with CO_2 (flue gas could be used in pulp mills) to a final pH of 8.2. The CO_2 adsorption capacity of the APEL was determined to be 7.15 g_{CO_2}/L_{APEL}. The precipitated silica nanoparticles had a purity of 99.8%, indicating that the isolated silica can be used as the starting material for various high-value products. The hemicellulose isolated from the CO_2-treated APEL had a uniform molecular weight distribution, showing their potential for downstream conversion into high-value bio-products. Moreover, polymeric film fabricated from the isolated hemicellulose showed good properties such as high tensile strength and elongation at break and, relatively low WVTR, WVR and oxygen permeability.

Through this study, an environmentally friendly way to produce pure silica nanoparticles and polymeric hemicellulose from bamboo has been developed. In addition, the removal of silica prior to biomass processing in pulp mills or biorefineries solves the problems created by silica in the recovery cycle of kraft pulping. The proposed use of pulp mill waste gas containing carbon dioxide would recycle pulp mill greenhouse gas emissions and contribute to reduce global warming.

A mass balance of the proposed alkaline pretreatament-kraft pulping process was performed. The silica extracted during pretreatment can be recovered from the APEL by lowering the pH prior to pulping the raw material. Moreover, CO_2 present in the waste flue gas can be used to lower the pH of the APEL avoiding increased CO_2 emissions from the lime kiln. In addition, the removal of silica also makes the generated lime mud recyclable during the subsequent calcination process producing good quality CaO that can be used in causticizing thus avoiding solid waste disposal issues and the necessity of purchasing fresh lime. Both the utilization of flue gas and the recovery of CaO improve the sustainability of the conventional pulping process and make the bamboo pulping process more environmentally friendly.

Chapter 5

Summary of Thesis and Recommendations for Future Research

5.1 Summary of Contributions

In this thesis, a series of experimental and numerical studies were conducted to study hemicellulose hydrolysis during acidic pre-hydrolysis and the removal of silica and hemicellulose during alkaline pretreatment. The effect of alkaline pretreatment on subsequent kraft pulping was also investigated by evaluating the resultant pulp properties. To investigate if additional value could be obtained from the pulping process (a biorefinery concept) the feasibility of recovering dissolved silica and hemicellulosic sugars in the alkaline pre-extraction liquor was carried out. To further confirm this feasibility, a statistical mass balance of the whole proposed process was performed. Specifically, the conclusions of this thesis are:

1. The evolution of proton concentration was examined during the auto- and dilute-acid hydrolysis of bamboo chips. A "toy model" was successfully proposed that described the reaction. The toy model predicts the existence of a

steady state solution, which is dictated by the equilibrium constants, and the initial added acid and acetyl group levels. The model qualitatively follows the trend given by experiment. The model was tested at room temperature to examine the changes in pH when ash neutralization is the dominant mechanism. Under these conditions, the pH remains essentially constant both at low initial pH and under autohydrolysis conditions. When the hydrolysis reaction proceeded at elevated temperatures, the pH initially increased, then decreased at longer times due to the difference in the rates of the neutralization and deacetylation reactions. With our toy model we propose a chemical reaction pathway that satisfactorily describes experimentally determined proton concentration under both autohydrolytic and dilute acid hydrolysis conditions. This accurate modeling of the proton concentration should significantly improve the existing kinetic models of hemicellulose hydrolysis and facilitate more efficient process optimization and scale-up.

2. Alkaline pretreatment with NaOH was demonstrated to be an effective way to selectively extract silica and hemicellulose from bamboo biomass without degrading cellulose and lignin.

   (a) The dissolution of pure amorphous silica with different particle sizes in NaOH solution was experimentally studied in the lab. Results showed that surface area was the controlling parameter of the reaction rate between silica and NaOH. The standard shrinking core model could be used to describe the silica dissolution rate in the alkali solution under the NaOH concentrations studied in this work.

(b) Large deviations were obtained when using the shrinking core to describe the removal of silica from bamboo powder at low NaOH concentration ($<$ 0.45 mol/L).

(c) During alkaline pretreatment of bamboo biomass, several reactions, such as degradation of xylan, dissolution of silica and neutralization of acetyl and uronic acid groups, occur in parallel. Due to the consumption of OH^- by several bamboo chemical components, the dissolution rate of silica in bamboo powder was lower than that of pure amorphous silica particles.

(d) The extraction of xylan and silica from bamboo powder increased with the increase of the treatment severity such as higher temperature, higher NaOH charge and longer reaction time. All silica and up to 55% of xylan could be extracted by treating bamboo powder with initial NaOH concentration of 0.45 mol/L at 100 ^oC for 180 min.

(e) To understand the effect of chip size on the extraction rates of silica and xylan from bamboo biomass, alkaline pretreatment of bamboo chips was carried out under the same conditions used for bamboo powder. Results demonstrated that mass-transfer effects play an important role in the pre-extraction of both silica and xylan from bamboo chips. A 5-step extraction mechanism was proposed based on the experimental results.

(f) The response surface methodology (RSM) and central composite rotatable design (CCRD) were used to determine the most significant variables for maximum removal of silica and hemicellulose while maintaining cellulose and lignin content. Polynomial equations describing extraction of xylan

and silica, and chip yield were obtained as a function of the treatment variables of temperature, NaOH charge and time. According to the equations and confirmatory experiments, 97% desilication could be reached by treating bamboo chips for 70 -90 min at temperatures of 95-100 ^oC with NaOH charges of 16-18% (based on the o.d. chip mass). Under these conditions up to 40% of the xylan could be extracted.

(g) All silica and up to 45% of hemicellulose were removed from bamboo chips under the studied conditions. The alkaline pretreatment of bamboo chips provides a novel way to resolve the silica issue encountered when pulping with bamboo.

3. Alkaline pre-extraction of the bamboo chips improved delignification during subsequent kraft pulping even at lower effective alkali (EA) charge. Pulp from pre-extracted bamboo chips showed similar screened pulp yield to that of non-extracted chips while initial pulp freeness (CSF) improved slightly. The tensile strength index of the pulp actually benefited from the alkaline pre-treatment at low EA charges. The tear strength index of the kraft pulp was improved by the alkaline pre-extraction. Silica was not detected in the kraft pulp and black liquor obtained using pre-extracted bamboo chips, indicating that the process provides a solution to silica problems encountered in bamboo pulping.

4. Recovery of dissolved silica and hemicellulose from the spent liquor is of great importance in converting the kraft pulp mill into a biorefinery unit.

(a) To recover the dissolved silica and hemicellulose from the alkaline pre-extraction liquor (APEL), a sequential route involving carbon dioxide

(CO_2) and ethanol precipitation was developed. Up to 97% of silica dissolved in the APEL was recovered by treating the APEL at 60 ^oC with CO_2 to a final pH of 8.2. The CO_2 adsorption capacity of the APEL was determined to be 7.15 g_{CO_2}/L_{APEL} with the 12% NaOH charge used for pretreatment of bamboo chips. The precipitated silica had a purity of 99.8%, indicating it can be an excellent starting material for various high-value products. For a typical bamboo-to-pulp mill with a capacity of 600-700 tons pulp per day, about 67.9 tons/day CO_2 is required and 16.8 tons/day silica is generated.

(b) The hemicellulose isolated from the CO_2-treated APEL had a uniform molecular weight distribution, showing their potential for downstream conversion into high-value bio-products. Moreover, polymeric film fabricated from the isolated hemicellulose showed good properties such as high tensile strength and elongation at break and, relatively low WVTR, WVP and oxygen permeability.

5. According to our findings, we proposed a scheme that integrates alkaline extraction and the recovery of silica and hemicellulose from bamboo into a commercial kraft pulping process. In the proposed process, extracted bamboo chips serve as the starting material for a kraft-based pulping processes to produce conventional kraft pulp, while the extraction liquor is used for the recovery of dissolved materials such as silica and hemicellulose. Moreover, the pre-extraction of silica from bamboo chips also makes the generated lime mud ($CaCO_3$) from causticizing recyclable in the lime kiln, avoiding disposal of large amounts of solid

waste and the requirement for purchase of fresh lime.

6. A statistical mass balance for the proposed process was also presented. Results demonstrated the feasibility of the proposed process for the production of kraft pulp and the resolution of silica challenges.

5.2 Recommendations for Future Work

The results of this thesis provide a strong foundation for future work. The focus of the future work could be in several areas, these are:

1. Further development of the kinetic model for the hydrolysis of xylan during auto- and dilute-acid hydrolysis of bamboo chips.

2. Establishing the mathematical model to describe the reactions during alkaline pretreatment of bamboo powder and bamboo chips.

3. To develop a more efficient and costly-effective way to recover hemicellulose from the silica-free alkaline pre-extraction liquor (APEL).

4. An optimization study can be conducted to produce high grade dissolving pulp by integrating silica pre-extraction into the pulping process.

5. Reactor design. Design a liquor tank for the recovery and separation of silicic acid from the alkaline pre-extraction liquor (APEL) with flue gas treatment.

6. A techno-economical analysis is generally required to assess the feasibility of the proposed process for the utilization of bamboo in biorefineries.

References

Affandi, S., Setyawan, H., Winardi, S., Purwanto, A., and Balgis, R. (2009). A facile method for production of high-purity silica xerogels from bagasse ash. *Adv. Powder Technol.*, 20(5):468–472.

Agbor, V. B., Cicek, N., Sparling, R., Berlin, A., and Levin, D. B. (2011). Biomass pretreatment: fundamentals toward application. *Biotechnol. Adv.*, 29(6):675–685.

Aguilar, R., Ramırez, J., Garrote, G., and Vázquez, M. (2002). Kinetic study of the acid hydrolysis of sugar cane bagasse. *J. Food Eng.*, 55(4):309–318.

Ahsan, L., Jahan, M. S., and Ni, Y. (2014). Recovering/concentrating of hemicellulosic sugars and acetic acid by nanofiltration and reverse osmosis from prehydrolysis liquor of kraft based hardwood dissolving pulp process. *Bioresour. Technol.*, 155:111–115.

Alexander, G. B., Heston, W., and Iler, R. K. (1954). The solubility of amorphous silica in water. *J. Physical Chem.*, 58(6):453–455.

Altaner, C. and Jarvis, M. (2008). Modelling polymer interactions of the 'molecular velcro' type in wood under mechanical stress. *J. Theoretical Biology*, 253(3):434–445.

Alvarez-Vasco, C. and Zhang, X. (2013). Alkaline hydrogen peroxide pretreatment of softwood: hemicellulose degradation pathways. *Bioresour. Technol.*, 150:321–327.

Amada, S. (1995). Hierarchical functionally gradient structures of bamboo, barley, and corn. *Mrs Bulletin*, 20(01):35–36.

An, D., Guo, Y., Zhu, Y., and Wang, Z. (2010). A green route to preparation of silica powders with rice husk ash and waste gas. *Chem. Eng. J.*, 162(2):509–514.

Anatskii, F. and Ratinov, V. (1969). Mechanism and kinetics of reaction between active silicon and alkali-metal hydroxides. *Doklady Akademi Nauk Sssr*, 186(6):1341.

Arato, C., Pye, E. K., and Gjennestad, G. (2005). The lignol approach to biorefining of woody biomass to produce ethanol and chemicals. *App. Biochem. Biotechnol.*, 123(1-3):871–882.

Atkinson, A., Donev, A., and Tobias, R. (1992). Optimum experimental designs. *Oxford University Press, New York, NY*.

Avdeef, A., Comer, J. E., and Thomson, S. J. (1993). ph-metric log p. 3. glass electrode calibration in methanol-water, applied to pka determination of water-insoluble substances. *Analytical Chem.*, 65(1):42–49.

Bai, L., Hu, H., and Xu, J. (2012). Influences of configuration and molecular weight of hemicelluloses on their paper-strengthening effects. *Carbohydr. Polym.*, 88(4):1258–1263.

Barik, T., Sahu, B., and Swain, V. (2008). NanosilicaâĂŤfrom medicine to pest control. *Parasitology Res.*, 103(2):253–258.

Benkhedda, K., Infante, H. G., Ivanova, E., and Adams, F. C. (2000). Trace metal analysis of natural waters and biological samples by axial inductively coupled plasma time of flight mass spectrometry (icp-tofms) with flow injection on-line adsorption preconcentration using a knotted reactor. *J. Analy. Atomic Spectrometry*, 15(10):1349–1356.

Bennett, D. M. and Sangster, A. (1981). The distribution of silicon in the adventitious roots of the bamboo sasa palmata. *Canadian J. Botany*, 59(9):1680–1684.

Berglin, N. and Berntsson, T. (1998). Chp in the pulp industry using black liquor gasification: thermodynamic analysis. *App. Thermal Eng.*, 18(11):947–961.

Bergna, H. E. and Roberts, W. O. (2005). *Colloidal silica: fundamentals and applications*, volume 131. CRC Press.

Billa, E., Tollier, M.-T., and Monties, B. (1996). Characterisation of the monomeric composition ofin situwheat straw lignins by alkaline nitrobenzene oxidation: Effect of temperature and reaction time. *J. Sci. Food Agricul.*, 72(2):250–256.

Blumberg, A. A. (1959). Differential thermal analysis and heterogeneous kinetics the reaction of vitreous silica with hydrofluoric acid. *J. Physical Chem.*, 63(7):1129–1132.

Borrega, M., Nieminen, K., and Sixta, H. (2011). Effects of hot water extraction in a batch reactor on the delignification of birch wood. *BioResources*, 6(2):1890–1903.

Borrega, M., Tolonen, L. K., Bardot, F., Testova, L., and Sixta, H. (2013). Potential

of hot water extraction of birch wood to produce high-purity dissolving pulp after alkaline pulping. *Bioresour. Technol.*, 135:665–671.

Brennan, M. A. and Wyman, C. E. (2004). Initial evaluation of simple mass transfer models to describe hemicellulose hydrolysis in corn stover. *App. Biochem. Biotechnol.*, 115(1-3):965–976.

Brückner, R. (1970). Properties and structure of vitreous silica i. *J. Non-crystalline Solids*, 5(2):123–175.

Cahela, D. R., Lee, Y., and Chambers, R. (1983). Modeling of percolation process in hemicellulose hydrolysis. *Biotechnol. Bioeng.*, 25(1):3–17.

Cardoso, M., de Oliveira, É. D., and Passos, M. L. (2009). Chemical composition and physical properties of black liquors and their effects on liquor recovery operation in brazilian pulp mills. *Fuel*, 88(4):756–763.

Carrasco, F. and Roy, C. (1992). Kinetic study of dilute-acid prehydrolysis of xylan-containing biomass. *Wood Sci. Technol.*, 26(3):189–208.

Chand, N., Jain, D., and Nigrawal, A. (2006). Investigation on gradient dielectric characteristics of bamboo (dentroclamus strictus). *J. App. Poly. Sci.*, 102(1):380–386.

Chandra, R. P., Arantes, V., and Saddler, J. (2015). Steam pretreatment of agricultural residues facilitates hemicellulose recovery while enhancing enzyme accessibility to cellulose. *Bioresour. Technol.*, 185:302–307.

Chandra, R. P., Chu, Q., Hu, J., Zhong, N., Lin, M., Lee, J.-S., and Saddler, J. (2016). The influence of lignin on steam pretreatment and mechanical pulping of poplar to achieve high sugar recovery and ease of enzymatic hydrolysis. *Bioresour. Technol.*, 199:135–141.

Chang, Y.-N., Huang, J.-C., Lee, C.-C., Shih, L., and Tzeng, Y.-M. (2002). Use of response surface methodology to optimize culture medium for production of lovastatin by monascus ruber. *Enzyme Microbial Technol.*, 30(7):889–894.

Chen, C.-T. A. and Marshall, W. L. (1982). Amorphous silica solubilities iv. behavior in pure water and aqueous sodium chloride, sodium sulfate, magnesium chloride, and magnesium sulfate solutions up to 350 ^oC. *Geochimica et Cosmochimica Acta*, 46(2):279–287.

Chundawat, S. P., Venkatesh, B., and Dale, B. E. (2007). Effect of particle size based separation of milled corn stover on afex pretreatment and enzymatic digestibility. *Biotechnol. Bioeng.*, 96(2):219–231.

Cochran, W. and Cox, G. (1968). Experimental designs, john wiley, new york.

Collin, B., Doelsch, E., Keller, C., Panfili, F., and Meunier, J.-D. (2012). Distribution and variability of silicon, copper and zinc in different bamboo species. *Plant Soil*, 351(1-2):377–387.

Conner, A. H. and Lorenz, L. F. (1986). Kinetic modeling of hardwood prehydrolysis. part iii. water and dilute acetic acid prehydrolysis of southern red oak. *Wood Fiber Sci.*, 18(2):248–263.

Cosgrove, D. C. et al. (2012). Comparative structure and biomechanics of plant primary and secondary cell walls. *Frontiers Plant Sci.*, 3:1–6.

Cox, G. B. (1993). The influence of silica structure on reversed-phase retention. *J. Chromatography A*, 656(1):353–367.

Dammström, S., Salmén, L., and Gatenholm, P. (2008). On the interactions between cellulose and xylan, a biomimetic simulation of the hardwood cell wall. *BioResources*, 4(1):3–14.

De Lopez, S., Tissot, M., and Delmas, M. (1996). Integrated cereal straw valorization by an alkaline pre-extraction of hemicellulose prior to soda-anthraquinone pulping. case study of barley straw. *Biomass Bioenergy*, 10(4):201–211.

Dence, C. W. (1992). The determination of lignin. In *:Methods in Lignin Chemistry*, pages 33–61. Springer.

Ding, T., Zhou, J., Wan, D., Chen, Z., Wang, C., and Zhang, F. (2008). Silicon isotope fractionation in bamboo and its significance to the biogeochemical cycle of silicon. *Geochimica et Cosmochimica Acta*, 72(5):1381–1395.

Douskova, I., Doucha, J., Livansky, K., Machat, J., Novak, P., Umysova, D., Zachleder, V., and Vitova, M. (2009). Simultaneous flue gas bioremediation and reduction of microalgal biomass production costs. *App. Microbiology Biotechnol.*, 82(1):179–185.

Duarte, G. V., Ramarao, B. V., Amidon, T. E., and Ferreira, P. T. (2011). Effect of

hot water extraction on hardwood kraft pulp fibers (acer saccharum, sugar maple). *Ind. Eng. Chem. Res.*, 50(17):9949–9959.

East, C. P., Fellows, C. M., and Doherty, W. O. (2013). Aspects of the kinetics and solubility of silica and calcium oxalate composites in sugar solutions. *J. Food Eng.*, 117(3):291–298.

Engström, A.-C., Ek, M., and Henriksson, G. (2006). Improved accessibility and reactivity of dissolving pulp for the viscose process: pretreatment with monocomponent endoglucanase. *Biomacromolecules*, 7(6):2027–2031.

Esteghlalian, A., Hashimoto, A. G., Fenske, J. J., and Penner, M. H. (1997). Modeling and optimization of the dilute-sulfuric-acid pretreatment of corn stover, poplar and switchgrass. *Bioresour. Technol.*, 59(2):129–136.

Fan, S., Li, S., Wang, J., Lang, X., and Wang, Y. (2009). Efficient capture of co_2 from simulated flue gas by formation of tbab or tbaf semiclathrate hydrates. *Energy Fuels*, 23(8):4202–4208.

Farrell, E. P., Führer, E., Ryan, D., Andersson, F., Hüttl, R., and Piussi, P. (2000). European forest ecosystems: building the future on the legacy of the past. *Forest Ecology Management*, 132(1):5–20.

Fauteux, F., Rémus-Borel, W., Menzies, J. G., and Bélanger, R. R. (2005). Silicon and plant disease resistance against pathogenic fungi. *FEMS Microbiol. Lett.*, 249(1):1–6.

Fengel, D. and Wegener, G. (1983). *Wood: chemistry, ultrastructure, reactions*. Walter de Gruyter, New York, USA.

Fleming, B. and Crerar, D. (1982). Silicic acid ionization and calculation of silica solubility at elevated temperature and ph application to geothermal fluid processing and reinjection. *Geothermics*, 11(1):15–29.

García-Aparicio, M., Parawira, W., Van Rensburg, E., Diedericks, D., Galbe, M., Rosslander, C., Zacchi, G., and Görgens, J. (2011). Evaluation of steam-treated giant bamboo for production of fermentable sugars. *Biotechnol. Progress*, 27(3):641–649.

Garrote, G., DomıÌĄnguez, H., and Parajó, J. C. (2001). Generation of xylose solutions from eucalyptus globulus wood by autohydrolysis–posthydrolysis processes: posthydrolysis kinetics. *Bioresour. Technol.*, 79(2):155–164.

Garrote, G., Eugenio, M. E., Díaz, M. J., Ariza, J., and López, F. (2003). Hydrothermal and pulp processing of Eucalyptus. *BioresouR. Technol.*, 88(1):61–68.

Gáspár, M., Kálmán, G., and Réczey, K. (2007). Corn fiber as a raw material for hemicellulose and ethanol production. *Process Biochem.*, 42(7):1135–1139.

González-Muñoz, M., Alvarez, R., Santos, V., and Parajó, J. (2012). Production of hemicellulosic sugars from pinus pinaster wood by sequential steps of aqueous extraction and acid hydrolysis. *Wood Sci. Technol.*, 46(1-3):271–285.

Gossett, J. M., Stuckey, D. C., Owen, W. F., and McCarty, P. L. (1982). Heat treatment and anaerobic digestion of refuse. *J. Environ. Eng. Div.*, 108:437–454.

Gratani, L., Crescente, M. F., Varone, L., Fabrini, G., and Digiulio, E. (2008). Growth pattern and photosynthetic activity of different bamboo species growing in the botanical garden of rome. *Flora-Morphology, Distribution, Functional Ecology Plants*, 203(1):77–84.

Greenberg, S. and Price, E. (1957). The solubility of silica in solutions of electrolytes. *J. Physical Chem.*, 61(11):1539–1541.

Grénman, H., EraÌĺnen, K., Krogell, J., WillfoÌĺr, S., Salmi, T., and Murzin, D. Y. (2011). Kinetics of aqueous extraction of hemicelluloses from spruce in an intensified reactor system. *Ind. Eng. Chem. Res.*, 50(7):3818–3828.

Gunnarsson, I. and Arnórsson, S. (2000). Amorphous silica solubility and the thermodynamic properties of H_4SiO_4 in the range of 0 to 350 ^oc at p sat. *Geochimica et Cosmochimica Acta*, 64(13):2295–2307.

Gütsch, J. S., Nousiainen, T., and Sixta, H. (2012). Comparative evaluation of autohydrolysis and acid-catalyzed hydrolysis of eucalyptus globulus wood. *Bioresour. Technol.*, 109:77–85.

Hallac, B. B. and Ragauskas, A. J. (2011). Analyzing cellulose degree of polymerization and its relevancy to cellulosic ethanol. *Biofuels, Bioprod. Biorefining*, 5(2):215–225.

Hamzeh, Y., Ashori, A., Khorasani, Z., Abdulkhani, A., and Abyaz, A. (2013). Pre-extraction of hemicelluloses from bagasse fibers: Effects of dry-strength additives on paper properties. *Ind. Crops Prod.*, 43:365–371.

He, Y. and Yue, Y. (2008). A review of the effective component and applications of extracts from bamboo leaves. *Biomass Chem. Eng.*, 3:31–37.

Hegde, N. D. and Rao, A. V. (2006). Organic modification of teos based silica aerogels using hexadecyltrimethoxysilane as a hydrophobic reagent. *App. Surface Sci.*, 253(3):1566–1572.

Hektor, E. and Berntsson, T. (2007). Future co_2 removal from pulp mills–process integration consequences. *Energy Conv. Management*, 48(11):3025–3033.

Helmerius, J., von Walter, J. V., Rova, U., Berglund, K. A., and Hodge, D. B. (2010). Impact of hemicellulose pre-extraction for bioconversion on birch kraft pulp properties. *Bioresour. Technol.*, 101(15):5996–6005.

Hong, B., Xue, G., Guo, X., and Weng, L. (2013). Kinetic study of oxalic acid pretreatment of moso bamboo for textile fiber. *Cellulose*, 20(2):645–653.

Hosseini, S. A. and Shah, N. (2009). Multiscale modelling of hydrothermal biomass pretreatment for chip size optimization. *Bioresour. Technol.*, 100(9):2621–2628.

Huang, F. and Ragauskas, A. (2013). Extraction of hemicellulose from loblolly pine woodchips and subsequent kraft pulping. *Ind. Eng. Chem. Res.*, 52(4):1743–1749.

Huang, H.-J., Ramaswamy, S., Al-Dajani, W. W., and Tschirner, U. (2010). Process modeling and analysis of pulp mill-based integrated biorefinery with hemicellulose pre-extraction for ethanol production: A comparative study. *Bioresour. Technol.*, 101(2):624–631.

Huang, H.-J., Ramaswamy, S., Tschirner, U., and Ramarao, B. (2008). A review of separation technologies in current and future biorefineries. *Separa. Purification Technol.*, 62(1):1–21.

Iler, R. K. (1979). *The chemistry of silica: solubility, polymerization, colloid and surface pro perties, and biochemistry.* Wiley.

Jahan, M. S., Lee, Z. Z., and Jin, Y. (2006). Organic acid pulping of rice straw. i: cooking. *Turkish J. Agricul. Forestry*, 30(3):231–239.

Jin, Y., Jameel, H., Chang, H.-m., and Phillips, R. (2010). Green liquor pretreatment of mixed hardwood for ethanol production in a repurposed kraft pulp mill. *J. Wood Chem. Technol.*, 30(1):86–104.

Jun, A., Tschirner, U. W., and Tauer, Z. (2012). Hemicellulose extraction from aspen chips prior to kraft pulping utilizing kraft white liquor. *Biomass Bioenergy*, 37:229–236.

Kačuráková, M., Belton, P. S., Wilson, R. H., Hirsch, J., and Ebringerová, A. (1998). Hydration properties of xylan-type structures: an ftir study of xylooligosaccharides. *J. Sci. Food Agricul.*, 77(1):38–44.

Kadla, J., Kubo, S., Venditti, R., Gilbert, R., Compere, A., and Griffith, W. (2002). Lignin-based carbon fibers for composite fiber applications. *Carbon*, 40(15):2913–2920.

Käkölä, J. and Alén, R. (2006). A fast method for determining low-molecular-mass

aliphatic carboxylic acids by high-performance liquid chromatography–atmospheric pressure chemical ionization mass spectrometry. *J. Sep. Sci.*, 29(13):1996–2003.

Kalapathy, U., Proctor, A., and Shultz, J. (2002). An improved method for production of silica from rice hull ash. *Bioresour. Technol.*, 85(3):285–289.

Kim, S. B. and Lee, Y. (2002). Diffusion of sulfuric acid within lignocellulosic biomass particles and its impact on dilute-acid pretreatment. *Bioresour. Technol.*, 83(2):165–171.

Klapiszewski, Ł., Bartczak, P., Wysokowski, M., Jankowska, M., Kabat, K., and Jesionowski, T. (2015). Silica conjugated with kraft lignin and its use as a novel âĂŸgreenâĂŹsorbent for hazardous metal ions removal. *Chem. Eng. J.*, 260:684–693.

Knauss, K. G. and Wolery, T. J. (1988). The dissolution kinetics of quartz as a function of ph and time at 70 c. *Geochimica et Cosmochimica Acta*, 52(1):43–53.

Kobayashi, T. and Sakai, Y. (1956). Hydrolysis rate of pentosan of hardwood in dilute sulfuric acid. *J. Agricul. Chem. Society of Japan*, 20(1):1–7.

Kopfmann, K. and Hudeczek, W. (1988). Desilication of black liquor: pilot plant tests. *Tappi J.*, 71(10):139–147.

Krzesińska, M., Zachariasz, J., and Lachowski, A. (2009). Development of monolithic eco-composites from carbonized blocks of solid iron bamboo (dendrocalamus strictus) by impregnation with furfuryl alcohol. *Bioresour. Technol.*, 100(3):1274–1278.

Kumar, R., Mago, G., Balan, V., and Wyman, C. E. (2009). Physical and chemical characterizations of corn stover and poplar solids resulting from leading pretreatment technologies. *Bioresour. Technol.*, 100(17):3948–3962.

Larsson, S., Palmqvist, E., Hahn-Hägerdal, B., Tengborg, C., Stenberg, K., Zacchi, G., and Nilvebrant, N.-O. (1999). The generation of fermentation inhibitors during dilute acid hydrolysis of softwood. *Enzyme Microbial Technol.*, 24(3):151–159.

Le, D. M., Sørensen, H. R., Knudsen, N. O., and Meyer, A. S. (2015). Implications of silica on biorefineries–interactions with organic material and mineral elements in grasses. *Biofuels, Bioproducts Biorefining*, 9(1):109–121.

Leenakul, W. and Tippayawong, N. (2010). Dilute acid pretreatment of bamboo for fermentable sugar production. *J. Sustain. Energy Environment*, 1:117–120.

Lehto, J. and Alén, R. (2013). Alkaline Pre-treatment of Hardwood Chips Prior to Delignification. *J. Wood Chem. Technol.*, 33(2):77–91.

Lehto, J. and Alén, R. (2015). Alkaline pre-treatment of softwood chips prior to delignification. *J. Wood Chem. Technol.*, 35(2):146–155.

Li, X. (2004). *Physical, chemical, and mechanical properties of bamboo and its utilization potential for fiberboard manufacturing*. PhD thesis, Beijing Forestry University.

Li, X., Shupe, T., Peter, G., Hse, C., and Eberhardt, T. (2007). Chemical changes with maturation of the bamboo species phyllostachys pubescens. *J. Tropical Forest Sci.*, pages 6–12.

Li, Z., Jiang, Z., Fei, B., Cai, Z., and Pan, X. (2014). Comparison of bamboo green, timber and yellow in sulfite, sulfuric acid and sodium hydroxide pretreatments for enzymatic saccharification. *Bioresour. Technol.*, 151:91–99.

Li, Z., Jiang, Z., Fei, B., Pan, X., Cai, Z., Yu, Y., et al. (2012). Ethanol organosolv pretreatment of bamboo for efficient enzymatic saccharification. *BioResources*, 7(3):3452–3462.

Lier, J. v., Bruyn, P. d., and Overbeek, J. T. G. (1960). The solubility of quartz. *J. Physical Chem.*, 64(11):1675–1682.

Liese, W. (1987). Research on bamboo. *Wood Sci. Technol.*, 21:189–209.

Liese, W. (1992). The structure of bamboo in relation to its properties and utilization. In *Zhu, S., Li, W., Zhang, X. Wang, Z. ed., Bamboo and its use. Proceedings of the International symposium on Industrial Use of Bamboo, Beijing, China*, pages 7–11.

Liou, T.-H. (2004). Preparation and characterization of nano-structured silica from rice husk. *Materials Sci. Eng.: A*, 364(1):313–323.

Liou, T.-H. and Yang, C.-C. (2011). Synthesis and surface characteristics of nanosilica produced from alkali-extracted rice husk ash. *Materials Sci. Eng.: B*, 176(7):521–529.

Littlewood, J., Wang, L., Turnbull, C., and Murphy, R. J. (2013). Techno-economic potential of bioethanol from bamboo in china. *Biotechnol. Biofuels*, 6(1):1.

Liu, H., Hu, H., Jahan, M. S., and Ni, Y. (2013). Furfural formation from the pre-hydrolysis liquor of a hardwood kraft-based dissolving pulp production process. *Bioresour. Technol.*, 131:315–320.

Liu, Q., Wang, S., Zheng, Y., Luo, Z., and Cen, K. (2008). Mechanism study of wood lignin pyrolysis by using tg–ftir analysis. *J. Analy. App. Pyrolysis*, 82(1):170–177.

Liu, X., Lu, M., Ai, N., Yu, F., and Ji, J. (2012). Kinetic model analysis of dilute sulfuric acid-catalyzed hemicellulose hydrolysis in sweet sorghum bagasse for xylose production. *Ind. Crops Prod.*, 38:81–86.

Liu, Z., Ni, Y., Fatehi, P., and Saeed, A. (2011). Isolation and cationization of hemicelluloses from pre-hydrolysis liquor of kraft-based dissolving pulp production process. *Biomass Bioenergy*, 35(5):1789–1796.

Lloyd, T. A. and Wyman, C. E. (2004). Predicted effects of mineral neutralization and bisulfate formation on hydrogen ion concentration for dilute sulfuric acid pre-treatment. In *Proceedings of the Twenty-Fifth Symposium on Biotechnology for Fuels and Chemicals Held May 4–7, 2003, in Breckenridge, CO*, pages 1013–1022. Springer.

Lloyd, T. A. and Wyman, C. E. (2005). Combined sugar yields for dilute sulfuric acid pretreatment of corn stover followed by enzymatic hydrolysis of the remaining solids. *Bioresour. technol.*, 96(18):1967–1977.

Luo, X., Ma, X., Hu, H., Li, C., Cao, S., Huang, L., and Chen, L. (2013). Kinetic study of pentosan solubility during heating and reacting processes of steam treatment of green bamboo. *Bioresour. Technol.*, 130:769–776.

Lux, A., Luxová, M., Abe, J., Morita, S., and Inanaga, S. (2003). *Silicification of bamboo (Phyllostachys heterocycla Mitf.) root and leaf*. Springer.

Ma, J. F. and Yamaji, N. (2006). Silicon uptake and accumulation in higher plants. *Trends Plant Sci.*, 11(8):392–397.

Ma, X., Huang, L., Chen, Y., and Chen, L. (2011). Preparation of bamboo dissolving pulp for textile production; part 1. study on prehydrolysis of green bamboo for producing dissolving pulp. *BioResources*, 6(2):1428–1439.

Machmud, M. N., Fadi, F., Fuadi, Z., and Kokarkin, C. (2013). Alternative fiber sources from gracilaria sp and eucheuma cottonii for papermaking. *Inter. J. Sci. Eng.*, 6(1):1–10.

Malester, I. A., Green, M., and Shelef, G. (1992). Kinetics of dilute acid hydrolysis of cellulose originating from municipal solid wastes. *Ind. Eng. Chem. Res.*, 31(8):1998–2003.

Maloney, M. T., Chapman, T. W., and Baker, A. J. (1985). Dilute acid hydrolysis of paper birch: Kinetics studies of xylan and acetyl-group hydrolysis. *Biotechnol. Bioeng.*, 27(3):355–361.

Mân Vu, T. H., Pakkanen, H., and Alén, R. (2004). Delignification of bamboo (Bambusa procera acher). *Ind. Crops Prod.*, 19(1):49–57.

Mao, H., Genco, J., Yoon, S.-H., van Heiningen, A., and Pendse, H. (2008). Technical economic evaluation of a hardwood biorefinery using the "near-neutral" hemicellulose pre-extraction process. *J. Biobased Materials Bioenergy*, 2(2):177–185.

Mgaidi, A., Jendoubi, F., Oulahna, D., El Maaoui, M., and Dodds, J. (2004). Kinetics of the dissolution of sand into alkaline solutions: application of a modified shrinking core model. *Hydrometallurgy*, 71(3):435–446.

Mikkonen, K. S. and Tenkanen, M. (2012). Sustainable food-packaging materials based on future biorefinery products: Xylans and mannans. *Trends Food Sci. Technol.*, 28(2):90–102.

Minu, K., Jiby, K. K., and Kishore, V. V. N. (2012). Isolation and purification of lignin and silica from the black liquor generated during the production of bioethanol from rice straw. *Biomass Bioenergy*, 39:210–217.

Mittal, A., Chatterjee, S. G., Scott, G. M., and Amidon, T. E. (2009). Modeling xylan solubilization during autohydrolysis of sugar maple wood meal: Reaction kinetics. *Holzforschung*, 63(3):307–314.

Molin, U. and Teder, A. (2002). Importance of cellulose/hemicellulose-ratio for pulp strength. *Nordic Pulp Paper Res. J.*, 17(1):14–19.

Morinelly, J. E., Jensen, J. R., Browne, M., Co, T. B., and Shonnard, D. R. (2009). Kinetic characterization of xylose monomer and oligomer concentrations during dilute acid pretreatment of lignocellulosic biomass from forests and switchgrass. *Ind. Eng. Chem. Res.*, 48(22):9877–9884.

Morpurgo, M., Teoli, D., Pignatto, M., Attrezzi, M., Spadaro, F., and Realdon, N. (2010). The effect of na_2co_3, naf and nh_4oh on the stability and release behavior of sol–gel derived silica xerogels embedded with bioactive compounds. *Acta Biomaterialia*, 6(6):2246–2253.

Mosier, N., Wyman, C., Dale, B., Elander, R., Lee, Y., Holtzapple, M., and Ladisch, M. (2005). Features of promising technologies for pretreatment of lignocellulosic biomass. *Bioresour. Technol.*, 96(6):673–686.

Motomura, H., Fujii, T., and Suzuki, M. (2000). Distribution of silicified cells in the leaf blades of pleioblastus chino (franchet et savatier) makino (bambusoideae). *Annals Botany*, 85(6):751–757.

Motomura, H., Fujii, T., and Suzuki, M. (2006). Silica deposition in abaxial epidermis before the opening of leaf blades of pleioblastus chino (poaceae, bambusoideae). *Annals Botany*, 97(4):513–519.

Motomura, H., Mita, N., and Suzuki, M. (2002). Silica accumulation in long-lived leaves of sasa veitchii (carrière) rehder (poaceae–bambusoideae). *Annals Botany*, 90(1):149–152.

Negro, C., Blanco, M., Lopez-Mateos, F., DeJong, A., LaCalle, G., Van Erkel, J., and Schmal, D. (2001). Free acids and chemicals recovery from stainless steel pickling baths. *Separa. Sci. Technol.*, 36(7):1543–1556.

Neupane, S., Adhikari, S., Wang, Z., Ragauskas, A., and Pu, Y. (2015). Effect of torrefaction on biomass structure and hydrocarbon production from fast pyrolysis. *Green Chem.*, 17(4):2406–2417.

Niibori, Y., Kunita, M., Tochiyama, O., and Chida, T. (2000). Dissolution Rates of Amorphous Silica in Highly Alkaline Solution. *J. Nuclear Sci. Technol.*, 37(4):349–357.

Öhgren, K., Bura, R., Saddler, J., and Zacchi, G. (2007). Effect of hemicellulose and lignin removal on enzymatic hydrolysis of steam pretreated corn stover. *BioresouR. Technol.*, 98(13):2503–2510.

Okubo, K., Fujii, T., and Yamamoto, Y. (2004). Development of bamboo-based polymer composites and their mechanical properties. *Composites Part A: App. Sci. Manufacturing*, 35(3):377–383.

Okunev, A., Shaurman, S., Danilyuk, A., Aristov, Y. I., Bergeret, G., and Renouprez, A. (1999). Kinetics of the sio 2 aerogel dissolution in aqueous naoh solutions: experiment and model. *J. Non-crystalline Solids*, 260(1):21–30.

Pan, X.-J., Sano, Y., and Ito, T. (1999). Atmospheric acetic acid pulping of rice straw ii: behavior of ash and silica in rice straw during atmospheric acetic acid pulping and bleaching. *Holzforschung*, 53(1):49–55.

Pauly, M., Albersheim, P., Darvill, A., and York, W. S. (1999). Molecular domains of the cellulose/xyloglucan network in the cell walls of higher plants. *Plant J.*, 20(6):629–639.

Pavlostathis, S. G. and Gossett, J. M. (1985). Alkaline treatment of wheat straw for increasing anaerobic biodegradability. *Biotechnol. Bioeng.*, 27(3):334–344.

Pekarovic, J., Pekarovicova, A., Joyce, T. W., et al. (2005). Desilication of agricultural residues-the first step prior to pulping. *Appita J.*, 58(2):130–134.

Peng, F., Ren, J.-L., Xu, F., Bian, J., Peng, P., and Sun, R.-C. (2009). Fractional

study of alkali-soluble hemicelluloses obtained by graded ethanol precipitation from sugar cane bagasse. *J. Agricul. Food Chem.*, 58(3):1768–1776.

Perrin, D. D., Dempsey, B., and Serjeant, E. P. (1981). *pKa prediction for organic acids and bases*, volume 1. Springer.

Pinto, P., Evtuguin, D., and Neto, C. P. (2005). Structure of hardwood glucuronoxylans: modifications and impact on pulp retention during wood kraft pulping. *Carbohydrate Poly.*, 60(4):489–497.

Piperno, D. R. (2014). *Phytolyth analysis: an archaeological and geological perspective*. Elsevier.

Poojary, H. and Mugeraya, G. (2012). Laccase production by phellinus noxius hp f17: Optimization of submerged culture conditions by response surface methodology. *Res. Biotechnol.*, 3(1):9–20.

Prychid, C. J., Rudall, P. J., and Gregory, M. (2003). Systematics and biology of silica bodies in monocotyledons. *Botanical Review*, 69(4):377–440.

Pu, Y., Treasure, T., Gonzalez, R., Venditti, R. A., and Jameel, H. (2013). Autohydrolysis pretreatment of mixed softwood to produce value prior to combustion. *BioEnergy Res.*, 6(3):1094–1103.

Pye, E. K. (2008). Industrial lignin production and applications. *Biorefineries-Industrial processes and products: Status quo and future directions*, pages 165–200.

Raven, J. A. (1983). The transport and function of silicon in plants. *Biological Reviews*, 58(2):179–207.

Ren, J., Peng, F., and Sun, R. (2009). The effect of hemicellulosic derivatives on the strength properties of old corrugated container pulp fibres. *J. Biobased Materials Bioenergy*, 3(1):62–68.

Richmond, K. E. and Sussman, M. (2003). Got silicon? the non-essential beneficial plant nutrient. *Current Opinion Plant Biology*, 6(3):268–272.

Rissanen, J. V., Grénman, H., WillfoÌĺr, S., Murzin, D. Y., and Salmi, T. (2014a). Spruce hemicellulose for chemicals using aqueous extraction: kinetics, mass transfer, and modeling. *Ind. Eng. Chem. Res.*, 53(15):6341–6350.

Rissanen, J. V., Grénman, H., Xu, C., Willför, S., Murzin, D. Y., and Salmi, T. (2014b). Obtaining spruce hemicelluloses of desired molar mass by using pressurized hot water extraction. *ChemSusChem*, 7(10):2947–2953.

Rocha, G. J., Martín, C., da Silva, V. F., Gómez, E. O., and Gonçalves, A. R. (2012). Mass balance of pilot-scale pretreatment of sugarcane bagasse by steam explosion followed by alkaline delignification. *Bioresour. Technol.*, 111:447–452.

Rogalinski, T., Ingram, T., and Brunner, G. (2008). Hydrolysis of lignocellulosic biomass in water under elevated temperatures and pressures. *J. Supercritical Fluids*, 47(1):54–63.

Rousset, P., Aguiar, C., Labbé, N., and Commandré, J.-M. (2011). Enhancing the combustible properties of bamboo by torrefaction. *Bioresour. Technol.*, 102(17):8225–8231.

Rydholm, S. A. (1965). Pulping processes. *Interscience publishers, Wiley, New York, USA*, pages pp. 676–687.

Saake, B. and Lehnen, R. (2007). Lignin. *in: Ullmann's Encyclopedia of Industrial Chemistry*.

Saeman, J. F. (1945). Kinetics of wood saccharification-hydrolysis of cellulose and decomposition of sugars in dilute acid at high temperature. *Ind. Eng. Chem. Res.*, 37(1):43–52.

Saka, S. (2004). The raw materials of ca 2.1 wood as natural raw materials for cellulose acetate production. In *Macromolecular Symposia*, volume 208, pages 7–28. Wiley Online Library.

Salmela, M., Alén, R., and Vu, M. T. H. (2008). Description of kraft cooking and oxygenâĂŞalkali delignification of bamboo by pulp and dissolving material analysis. *Ind. Crops Prod.*, 28(1):47–55.

Sanchez, O. J. and Cardona, C. A. (2008). Trends in biotechnological production of fuel ethanol from different feedstocks. *Bioresour. Technol.*, 99(13):5270–5295.

Sangster, A. and Parry, D. (1981). *Ultrastructure of silica deposits in higher plants*. Springer.

Sathitsuksanoh, N., Zhu, Z., Ho, T.-J., Bai, M.-D., and Zhang, Y.-H. P. (2010). Bamboo saccharification through cellulose solvent-based biomass pretreatment followed by enzymatic hydrolysis at ultra-low cellulase loadings. *Bioresour. Technol.*, 101(13):4926–4929.

Scheller, H. V. and Ulvskov, P. (2010). Hemicelluloses. *Plant Biology*, 61(1):263.

Schild, G., Sixta, H., and Testova, L. (2010). Multifunctional alkaline pulping. delignification and hemicellulose extraction. *Cellulose Chem. Technol.*, 44(1):35–45.

Scurlock, J., Dayton, D., and Hames, B. (2000). Bamboo: an overlooked biomass resource? *Biomass Bioenergy*, 19(2000):229–244.

Sella Kapu, N. and Trajano, H. L. (2014). Review of hemicellulose hydrolysis in softwoods and bamboo. *Biofuels, Bioprod. Biorefining*, 8(6):857–870.

Shen, J. and Wyman, C. E. (2011). A novel mechanism and kinetic model to explain enhanced xylose yields from dilute sulfuric acid compared to hydrothermal pretreatment of corn stover. *Bioresour. Technol.*, 102(19):9111–9120.

Shi, H., Fatehi, P., Xiao, H., and Ni, Y. (2011). A combined acidification/PEO flocculation process to improve the lignin removal from the pre-hydrolysis liquor of kraft-based dissolving pulp production process. *BioresouR. Technol.*, 102(8):5177–5182.

Sierka, M. and Sauer, J. (1997). Structure and reactivity of silica and zeolite catalysts by a combined quantum mechanics [ndash] shell-model potential approach based on dft. *Faraday Discussions*, 106:41–62.

Sixta, H. (2006). Handbook of pulp, vol. 1, wiley-vch, weinheim.

Sluiter, A., Hames, B., Ruiz, R., Scarlata, C., Sluiter, J., Templeton, D., and Crocker, D. (2012). Determination of structural carbohydrates and lignin in biomass. *Laboratory Analytical Procedure*, 1617.

Song, Z., Liu, H., Li, B., and Yang, X. (2013). The production of phytolith-occluded carbon in china's forests: implications to biogeochemical carbon sequestration. *Global Change Biology*, 19(9):2907–2915.

Spencer, R. R. and Akin, D. E. (1980). Rumen microbial degradation of potassium hydroxide-treated coastal bermudagrass leaf blades examined by electron microscopy. *J. Animal Sci.*, 51(5):1189–1196.

SriBala, G. and Vinu, R. (2014). Unified kinetic model for cellulose deconstruction via acid hydrolysis. *Ind. Eng. Chem. Res.*, 53(21):8714–8725.

Stading, M., Hermansson, A.-M., Gatenholm, P., et al. (1998). Structure, mechanical and barrier properties of amylose and amylopectin films. *Carbohydr. Poly.*, 36(2):217–224.

Sterling, C. (1967). Crystalline silica in plants. *American J. Botany*, pages 840–844.

Sun, R., Lawther, J. M., and Banks, W. (1995). Influence of alkaline pre-treatments on the cell wall components of wheat straw. *Ind. Crops Prod.*, 4(2):127–145.

Talvitie, N. (1951). Determination of quartz in presence of silicates using phosphoric acid. *Analy. Chem.*, 23(4):623–626.

Thornton, S., Radke, C., et al. (1988). Dissolution and condensation kinetics of silica in alkaline solution. *SPE Reservoir Eng.*, 3(02):743–752.

Tillman, L., Lee, Y., and Torget, R. (1990). Effect of transient acid diffusion on pretreatment/hydrolysis of hardwood hemicellulose. *App. Biochem. Biotechnol.*, 24(1):103–113.

Tong, G.-l., Lu, Q., Wang, Y., and Zhou, C. (2005). Spectrophotometeric determination of silicon in rice straw and black liquor after rice straw alkaline pulping by silicomolybdate blue. *China Pulp Paper Ind.*, 26:64–66.

Torelli, N. and Čufar, K. (1995). Mexican tropical hardwoods. comparative study of ash and silica content. *Holz als Roh-und werkstoff*, 53(1):61–62.

Torssell, K. B. (1997). *Natural product chemistry: a mechanistic, biosynthetic and ecological approach. 2, Apotekarsocieteten, Stockholm.*

Trajano, H. L. and Wyman, C. E. (2013). *Fundamentals of biomass pretreatment at low pH.* Wiley Online Library, NJ, USA.

Tsuji, H., Isono, Z., and Ono, K. (1965). Studies on dissolving bamboo pulp. *Univ. Osaka Prefecture, Ser. B, Agric. Biology*, 16:89–104.

van Heiningen, A. (2006). Converting a kraft pulp mill into an integrated forest biorefinery. *Pulp Paper Can.*, 107(6):38–43.

Vena, P. F., Brienzo, M., del Prado García-Aparicio, M., Görgens, J. F., and Rypstra, T. (2013). Hemicelluloses extraction from giant bamboo (bambusa balcooa roxburgh) prior to kraft or soda-aq pulping and its effect on pulp physical properties. *Holzforschung*, 67(8):863–870.

Visuri, J. A., Song, T., Kuitunen, S., and Alopaeus, V. (2012). Model for degradation of galactoglucomannan in hot water extraction conditions. *Ind. Eng. Chem. Res.*, 51(31):10338–10344.

Walton, S. L., Hutto, D., Genco, J. M., Van Walsum, G. P., and van Heiningen, A. R. P. (2010). Pre-extraction of hemicelluloses from hardwood chips using an alkaline wood pulping solution followed by kraft pulping of the extracted wood chips. *Ind. Eng. Chem. Res.*, 49:12638–12645.

Wang, H., Loganathan, D., and Linhardt, R. J. (1991). Determination of the pka of glucuronic acid and the carboxy groups of heparin by 13c-nuclear-magnetic-resonance spectroscopy. *Biochemical J.*, 278(3):689–695.

Wen, J.-L., Xiao, L.-P., Sun, Y.-C., Sun, S.-N., Xu, F., Sun, R.-C., and Zhang, X.-L. (2011). Comparative study of alkali-soluble hemicelluloses isolated from bamboo (bambusa rigida). *Carbohydrate Res.*, 346(1):111–120.

Wirth, G. and Gieskes, J. (1979). The initial kinetics of the dissolution of vitreous silica in aqueous media. *J. Colloid Interface Sci.*, 68(3):492–500.

Wyman, C. E., Decker, S. R., Himmel, M. E., Brady, J. W., Skopec, C. E., and Viikari, L. (2005). Hydrolysis of cellulose and hemicellulose. *Polysaccharides: Structural Diversity Functional Versatility*, 1:1023–1062.

Xu, F., Sun, J., Geng, Z., Liu, C., Ren, J., Sun, R., Fowler, P., and Baird, M. (2007). Comparative study of water-soluble and alkali-soluble hemicelluloses from perennial ryegrass leaves (lolium peree). *Carbohydrate Poly.*, 67(1):56–65.

Xu, Z. and Huang, F. (2014). Pretreatment methods for bioethanol production. *App. Biochem. Biotechnol*, 174(1):43–62.

Yamashita, Y., Shono, M., Sasaki, C., and Nakamura, Y. (2010). Alkaline perox-

ide pretreatment for efficient enzymatic saccharification of bamboo. *Carbohydrate Poly.*, 79(4):914–920.

Yan, L., Zhang, L., and Yang, B. (2014). Enhancement of total sugar and lignin yields through dissolution of poplar wood by hot water and dilute acid flowthrough pretreatment. *Biotechnol. Biofuels*, 7(1):1.

Yoon, S.-H. and van Heiningen, A. (2008). Kraft pulping and papermaking properties of hot-water pre-extracted loblolly pine in an integrated forest products biorefinery. *Tappi J*, 7(7):22–27.

Yoon, S.-H. and van Heiningen, A. (2010). Green liquor extraction of hemicelluloses from southern pine in an integrated forest biorefinery. *J. Ind. Eng. Chem.*, 16(1):74–80.

Zaitsev, A., Shelkova, N., and Mogutnov, B. (2000). Thermodynamics of na2o-sio2 melts. *Inorganic Materials*, 36(6):529–543.

Zhang, X., Zhao, Z., Ran, G., Liu, Y., Liu, S., Zhou, B., and Wang, Z. (2013). Synthesis of lignin-modified silica nanoparticles from black liquor of rice straw pulping. *Powder Technol.*, 246:664–668.

Zhang, Y.-H. P. and Lynd, L. R. (2004). Toward an aggregated understanding of enzymatic hydrolysis of cellulose: noncomplexed cellulase systems. *Biotechnol. Bioeng.*, 88(7):797–824.

Zhao, X., Zhang, L., and Liu, D. (2012). Biomass recalcitrance. part i: the chemical

compositions and physical structures affecting the enzymatic hydrolysis of lignocellulose. *Biofuels, Bioprod. Biorefining*, 6(4):465–482.

Zhao, Y., Wang, Y., Zhu, J., Ragauskas, A., and Deng, Y. (2008). Enhanced enzymatic hydrolysis of spruce by alkaline pretreatment at low temperature. *Biotechnol. Bioeng.*, 99(6):1320–1328.

Appendices

A1 Bamboo Raw Material Characterization

Even though bamboo belongs to the grass family, having a woody stem it is structurally quite different from other lignocellulosic materials such as softwoods, hardwoods and cereal straws. Bamboo stem is composed of three parts: epidermal (outmost cell layer of the stem), mid-cortex (the region between epidermal and inner cortex), and inner cortex (the portion encircling the hollow center of the culm). Due to the unique location in the bamboo stem and their functions, these three regions differ substantially in chemical composition including extractives, ash and silica content (Chand et al. (2006)). These differences will affect the bamboo feedstock processing methods in kraft-based pulping and biorefinery applications. It is thought that it may be beneficial to remove one or two regions of the bamboo stem (bamboo epidermal or inner cortex) before pulping. However, the removal of bamboo parts as waste will reduce the useful biomass fraction and cause environmental problems (Li (2004)). Accordingly, before optimizing the pulping processes, the chemical composition and silica mass distribution in the bamboo stem needs to be quantified.

Fresh bamboo trees (1-5 years old) of *Neosinocalamus affinis* Keng were collected in September, 2012 from a natural forest in Sichuan Province, China. Each bamboo

stem was evenly cut into three parts along the length of the bamboo stem: top-middle-bottom. All samples were washed thoroughly with deionized water to remove the dust and other impurities such as sand and soil from the surface of bamboo chips. This washing operation was performed 10 times and then samples were dried for 48 h at room temperature. Subsequently, the samples were cut into small strips with a razor blade and ground using a Wiley Mill. The sample powder that passed through a 40-mesh sieve yet retained on a 60-mesh sieve was collected in glass jars for further use.

For the analysis of chemical composition in different layers along the radial direction, the stems were separated mannually with a plane block (Lee Valley Tools Ltd. Canada) to three layers: epidermal layer ($\approx 0.1\ mm$), mid-cortex ($\approx 3\ mm$) and inner cortex ($\approx 0.2\ mm$). The three fractions of bamboo samples were ground, screened and stored as previously described.

The organic components (carbohydrates and lignin) and inorganics (ash) composition was measured according to the analytical methods (NREL standard protocol) described in Chapter 2.

Fig. A.1 shows the ash and silica contents in different parts of the bamboo stem of different ages. Results showed that the ash content of one year old bamboo was significantly higher than that of three and five year old bamboo. It has been suggested in the literature that the higher ash content observed in younger bamboo could be a result of the larger mass fraction of epidermal tissue present in younger plants (Li et al. (2007)). Analysis of ash along the length of the bamboo stem showed that the ash content was the highest at the top part, an observation also reported by Li (2004) and Rousset et al. (2011). The results indicate that a substantial portion of

the ash in bamboo consists of silica. As shown in Fig. A.1b, the silica content in the five year old bamboo stem was higher than that of one and three year old, and the effect of age was more pronounced in the top regions of the stem. This is in agreement with previous studies that reported increasing silica content with bamboo aging (Motomura et al. (2002)). Moreover, silica level in the bamboo stem decreased gradually from the apical to basal portions of the stem (Fig. A.1b). This observation is similar to the findings by Collin et al. (2012). Analysis of silica distribution in the bamboo stem illustrated that the silica content of bamboo increases with increasing age. With consideration of biomass generated by each unit plantation area, bamboo trees with age $>$ 3 years old should be harvested for pulp and biorefinery applications.

To study whether some parts of the bamboo stem should be removed before processing, take five year old bamboo as an example, the composition of different fractions along the length (top, middle, bottom) of the bamboo stem and layers (epidermal, mid-cortex, inner cortex) across the cross section of the original bamboo stem was determined, shown in Table A1. The composition of each component analyzed (glucan, xylan, galactan, arabinan, lignin, extractives, ash, silica), is expressed as the average mass percentage of this component in the oven dry solids, determined at least three tests. With regards to the composition along the length of the bamboo stem, the cellulose and lignin content of the three fractions along the length of the stem (top, middle, bottom) were similar at around 46.5% and 23.5%, respectively, while the hemicellulose (mainly xylan) content of the bamboo at the top of the stem (24.8%) was the highest, followed by that in the middle (23.4%). Hemicellulose content was the lowest at the bottom of the stem (21.4%). Arabinan and galactan content in all

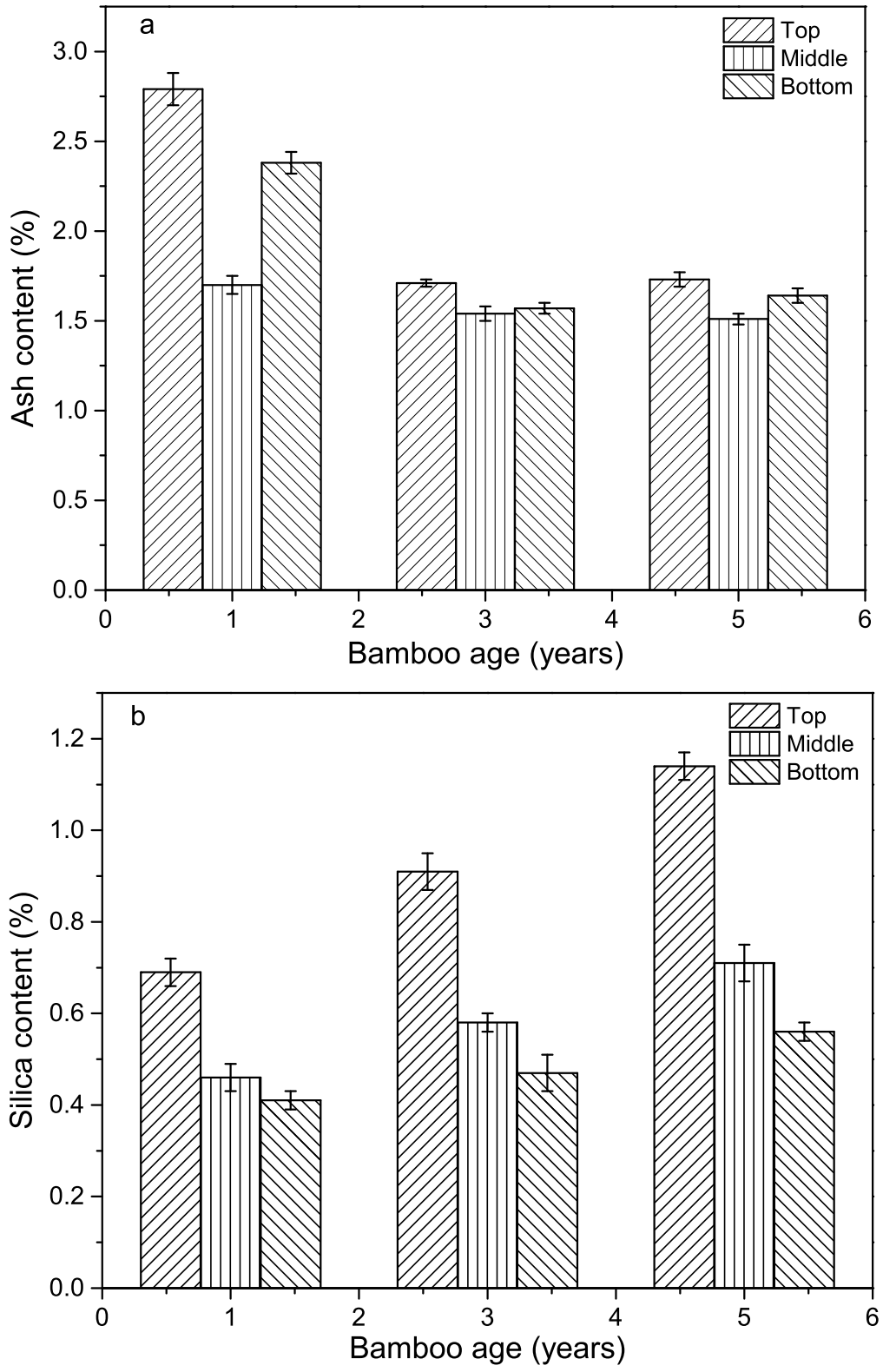

Figure A.1: Ash and silica content in different height locations of the bamboo stem (a: ash content, b: silica content). The measurements were triplicated.

three parts were less than 1% while mannan was undetectable by the HPLC methodology used. The main difference in chemical composition among the three parts along the stem was found in the silica content. At the top of the stem the silica content was 0.91% which decreased by almost 50% to a value of 0.47% at the bottom of the stem. This is in agreement with previous studies that reported decreasing silica levels from the apical to basal portions of the stem (Collin et al. (2012)). The most important observation was that the ratio of silica mass in the three parts was about 1:1:1 due to the difference in the weight fraction of bamboo biomass in each region.

The chemical composition and silica mass distribution of different layers (epidermal, mid-cortex, inner cortex) along the radial direction of the stem are shown in Table A1. It was found that the glucan content of the bamboo mid-cortex (49.4%) was much higher than that of the epidermal layer (44.3%) and the inner cortex (43.3%). Lignin content was found to be highest in the bamboo epidermal portion (28.5%), followed by the inner cortex (24.1%) and mid-cortex (23.2%). The hemicellulose (xylan, arabinan and galactan) content in the epidermal region, mid-cortex, and inner cortex were comparable at 22.3%, 23.5% and 24.4%, respectively. The highest extractives content was in the bamboo inner cortex (8.4%), followed by the mid-cortex (5.2%) and the epidermal layer (4.8%). The ash and silica contents of the bamboo epidermal part were higher than those of the bamboo mid-cortex and inner cortex. The difference in silica content (1.3%) was especially high with that in the epidermal region being about seven-times higher than in the mid-cortex or the bamboo inner cortex. However, the majority of silica mass in the bamboo was located in bamboo mid-cortex (63%) because this region accounts for about 88% of the biomass while the epidermal portion and the inner cortex account for only 6% each. According to the composition

analysis results, the removal of bamboo epidermal layer or inner cortex does not result in a significant decrease of silica amount input into the pulping processes; in contrast, it would increase the capital cost and cause environmental problems by the increasing industrial wastes. Moreover, compared with bamboo mid-cortex, bamboo epidermal part and inner cortex have comparable concentrations of hemicellulose, which can be pre-extracted for bioconversion. Consequently, rather than removing biomass of epidermal region and inner cortex the whole bamboo stem should be used as the raw material in pulping or biorefinery processes.

Table A.1: Chemical composition of 5 year old original bamboo stem (*Neosinocalamus Affinis* Keng).

Conponent	Length direction			Cross section		
	Top	Middle	Bottom	Epidermal	Mid-cortex	Inner cortex
Glucan (%)	46.57±1.52	46.71±1.85	46.89±1.94	44.32±1.56	49.44±2.12	43.35±1.85
Xylan(%)	24.82±1.02	23.43±0.87	21.41±0.98	21.53±1.12	22.61±1.26	23.37±1.55
Galactan (%)	0.58±0.12	0.44±0.25	0.35±0.14	0.18±0.04	0.20±0.04	0.20±0.02
Arabinan (%)	0.63±0.05	0.52±0.11	0.41±0.13	0.62±0.13	0.77±0.14	0.91±0.14
Lignin (%)	23.14±0.21	23.75±0.32	23.56±0.20	28.52±0.22	23.21±0.31	24.08±0.26
Extractives (%)	5.64±0.72	4.12±0.64	3.83±0.81	4.78±0.44	5.24±0.36	8.41±0.29
Ash (%)	1.35±0.10	1.31±0.12	1.28±0.13	2.12±0.08	0.93±0.04	1.26±0.04
Silica (%)	0.91±0.05	0.60±0.02	0.47±0.04	1.32±0.03	0.17±0.02	0.20±0.05
Silica mass fraction	0.36	0.34	0.30	0.32	0.63	0.05

A2 Chip Washing

According to the results of bamboo stem characterization, bamboo chips were prepared from 3 to 7 year old bamboo trees. Due to the commonly practiced methods of harvest and open-pile chip storage, a substantial amount of soil can be detected on the surface and structural pores of bamboo chips. As soil comprises 50-70% of silica by mass, the removal of soil is necessary to minimize silica input into the bamboo processing system. Indeed, the impact of chip cleanliness is underscored by the observation that fresh bamboo chips prepared in the laboratory contained 1.1% (w/w) silica while chips provided by a functional mill measured 1.56% (w/w). Therefore, we examined the feasibility of chip screening and washing with water to remove soil and silica. In the past, several researchers have used screening and washing to remove the soil or other impurities on the surface of bamboo and other non-wood raw materials (De Lopez et al. (1996)). However, the authors did not describe the washing process in detail, especially the important process parameters and their impact on the efficiency of washing. Moreover, to our knowledge, pilot-scale studies on the impact of bamboo washing have not been documented. In the present study, two types of washing methods, continuous washing and batch washing, were investigated (Fig. A.2). The chips used originated from approximately three-year old bamboo and were provided by a mill operated by Lee & Man Paper Manufacturing Ltd., China. Deionized water and recycled white water from pulp line were used in the lab-scale and pilot-scale studies, respectively.

Fig. A.2a shows the effects of washing time and temperature of lab-scale continuous washing on the residual silica content of bamboo chips. At both 17 ^oC and 35

^oC the residual silica content of chips decreased rapidly in the first 10 *min* and then leveled off. The rate of silica removal increased with increasing temperature; a 10 *min* wash at 17 ^oC and 35 ^oC reduced the silica content of the chips by about 25% and 28%, respectively. Silica is reported to be soluble in water, albeit to a minute extent, even at 25 ^oC. Although the solubility is low, the solubility is reported to increase with increasing temperature (Chen and Marshall (1982)). Higher temperature can be expected to increase the kinetic energy of silica molecules. These factors may play a role in the observed increase in silica removal at 35 ^oC compared to 17 ^oC. Prolonged washing beyond 10 *min* (up to 180 *min*) did not result in any further silica removal. It suggests that the fraction of silica loosely entrapped in the material is removed by deionized water washing for a short time. Moreover, during the continuous washing process, the silica content fluctuated, suggesting that silica and silica contained soil in the wash water can be regained by the chips. Bamboo stem has cells with large lumens and it is possible that a portion of the removed silica in the wash water is re-trapped in these pores.

To test whether more silica could be removed by changing wash water at intervals, a series of experiments were carried out by replacing the wash water with fresh water at 10 *min* intervals. As shown in Fig. A.2b, the residual silica content decreased rapidly in the first 10 min and only very little silica was removed thereafter with prolonged washing. The degree of silica removal in 10 *min* was almost identical to continuous washing without changes of wash water, about 25% and 28% at 17 ^oC and 35 ^oC, respectively. This indicates that it is difficult to remove more than 25-28% silica just by washing with water, even with extended washing and wash water changes. Fig. A.2b also shows that the silica regaining process did not occur when

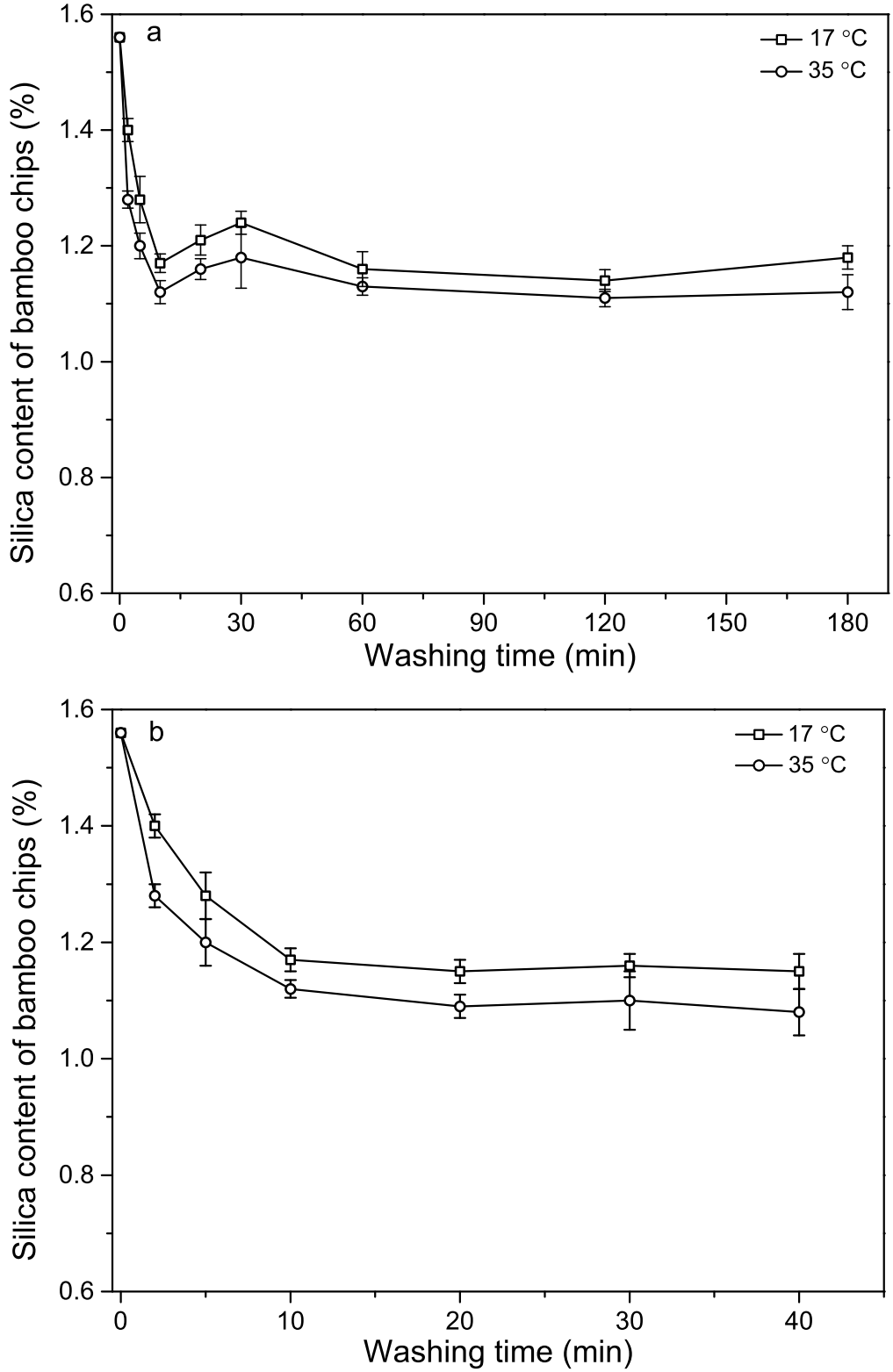

Figure A.2: Silica removal from bamboo chips by washing with water at two temperatures (a: continuous washing process, b: batch washing process). Note: batch process means wash water was replaced with fresh deionized water at 10 *min* intervals.

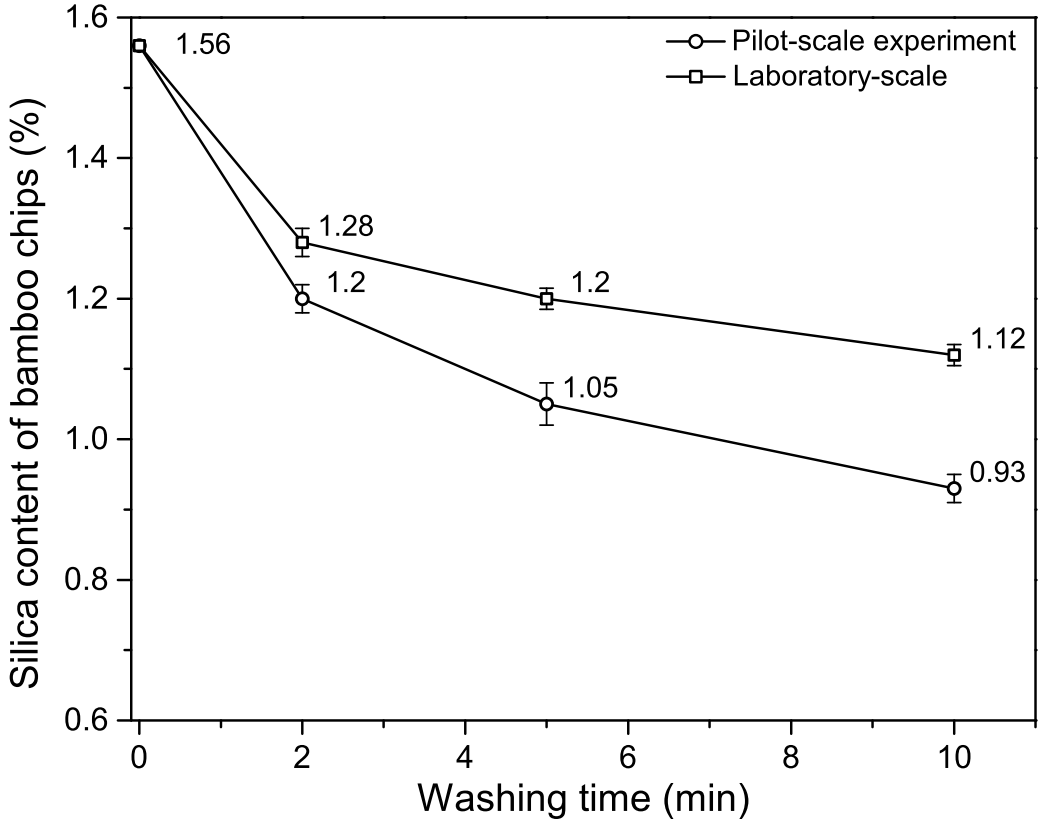

Figure A.3: Pilot-scale experiments on silica removal by washing with water.

wash water was changed every 10 *min*. This observation supports the idea that if the removed silica is still in the washing system, it might be regained by chips. This emphasizes the practical implications of wash water recycling in mill operations.

Based on the results obtained in the laboratory process, the washing technology was tested for silica removal from bamboo at pilot-scale during kraft pulping by the Lee & Man Paper Manufacturing, Ltd., China. In this mill, white water at about 35 ^oC, generated from a fourdrinier kraft bamboo pulp board machine, was used to wash the raw chips. Following the laboratory protocol, the mill changed the usual practice of a 2 *min* wash to a 10 *min* wash (Fig. A.3). The costs incurred by the prolonged washing time were negligible. Results of Fig. A.3 show that after a 10 min

wash the residual silica content of pilot-scale washed chips was about 0.93% (based on the dry weight of bamboo chips), which is lower than the value obtained in the lab (1.12%) (w/w). A likely reason for the higher effectiveness of the pilot-scale washing is the use of a screw press for dewatering which could make the chips abrade against each other and squeeze out liquid in chips. Therefore, it is possible that more silica-rich epidermal layers of the bamboo stem as well as some silica entrapped in the cell lumens were removed. Results of this set of experiments demonstrated that a 10 min wash at 35 ^oC was an economical and effective method for silica removal from bamboo chips.

A3 Mass Balance of the Pulping and Chemical Recovery Process

A3.1 Mass Balance of the Fibre Line

The calculation is based on 1 tonne of original bamboo chips, with the moisture content of 47%. Before carrying out the calculation, several definitions are made.

Q : Dry fibre content of the materials (kg)

D : Total weight of the material (kg)

C : Solids consistency of the material (%)

R : Reject ratio of each step (%)

S : Solution or water

K : Yield (based on the previous step)

Chip preparation process

1. Known:

   - $D_1 = 1000\ kg$
   - $C_1 = 1 - 47\% = 53\%$
   - $R_3 = 3.5\%$

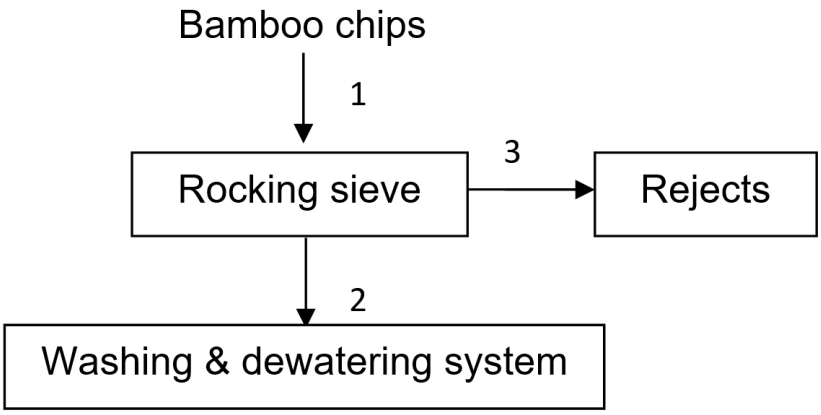

2. Calculation:

$$C_1 = C_2 = C_3 = 53\% \tag{5.1}$$

$$Q_1 = D_1 \times C_1 = 1000 \times 53\% = 530\ kg \tag{5.2}$$

$$Q_2 = Q_1 \times (1 - R_3) = 530 \times (1 - 3.5\%) = 511.45\ kg \tag{5.3}$$

$$D_2 = Q_2/C_2 = 511.45/53/Q_3 = Q_1 - Q_2 = 530 - 511.45 = 18.55\ kg \tag{5.4}$$

$$D_3 = Q_3/C_3 = 18.55/53\% = 35\ kg \tag{5.5}$$

Chip washing system

1. Known:

   - $Q_2 = 511.45\ kg$
   - $D_2 = 965\ kg$
   - $C_2 = 53\%$
   - $C_4 = 1 - 48\% = 52\%$ (moisture content of washed chips is 48%)
   - $S_5 = 2560\ L$ (liquid-to-solid ratio=5 L/kg, based on initial dry chips)

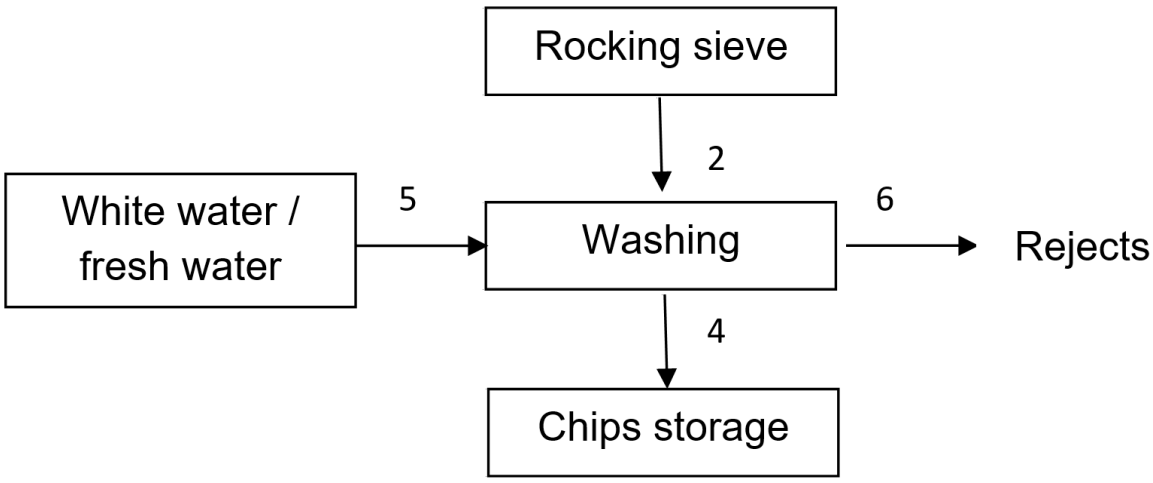

- $R_6 = 1.5\%$

2. Calculation:

$$Q_6 = Q_2 \times R_6 = 511.45 \times 1.5\% = 7.67\ kg \tag{5.6}$$

$$Q_4 = Q_2 - Q_6 = 511.45 - 7.67 = 503.78\ kg \tag{5.7}$$

$$D_4 = Q_4/C_4 = 503.78/52/D_6 = S_5 + D_2 - D_4 = 2650 + 965 - 968.81 = 2646.19\ kg \tag{5.8}$$

Silica and hemicellulose extraction process

1. Known:

- $Q_7 = Q_4 = 503.78\ kg$
- $C_7 = 52\%$
- $C_8 = 1 - 60\% = 40\%$ (moisture content of alkali treated chips is 60%)
- $D_7 = D_4 = 968.81\ kg$

- $S_9 = 8 \times Q_7 - (D_7 - Q_7) = 8 \times 503.78 - (968.81 - 503.78) = 3565.21\ L$ (L : $W = 8\ L/kg$)
- $K_8 = 85\%$ (based on previous step)
- $R_{11} = 1\%$
- $C_{11} = C_8 = 40\%$

2. Calculation:

$$Q_8 = Q_7 \times K_8 = 503.78 \times 85\% = 428.21\ kg \tag{5.9}$$

$$D_8 = Q_8/C_8 = 428.21/40\% = 1070.53\ kg \tag{5.10}$$

$$Q_{11} = Q_7 \times R_{11} = 503.78 \times 1\% = 5.04\ kg \tag{5.11}$$

$$D_{11} = Q_{11}/C_{11} = 5.04/40\% = 12.60\ kg \tag{5.12}$$

$$\begin{aligned} S_{10} &= S_9 + D_7 - D_8 - D_{11} = 3565.21 + 968.81 - 1070.53 - 12.6 \\ &= 3450.89\ kg \end{aligned} \tag{5.13}$$

$$Q_{10} = Q_7 - Q_8 - Q_{11} = 503.78 - 428.21 - 5.04 = 70.53\ kg \tag{5.14}$$

Kraft cooking process

1. Known:

- $Q_{12} = Q_8 = 428.21\ kg$
- $D_{12} = D_8 = 1070.53\ kg$
- $S_{12} = 1070.53 - 428.21 = 642.32\ L$
- $C_{12} = C_8 = 40\%$

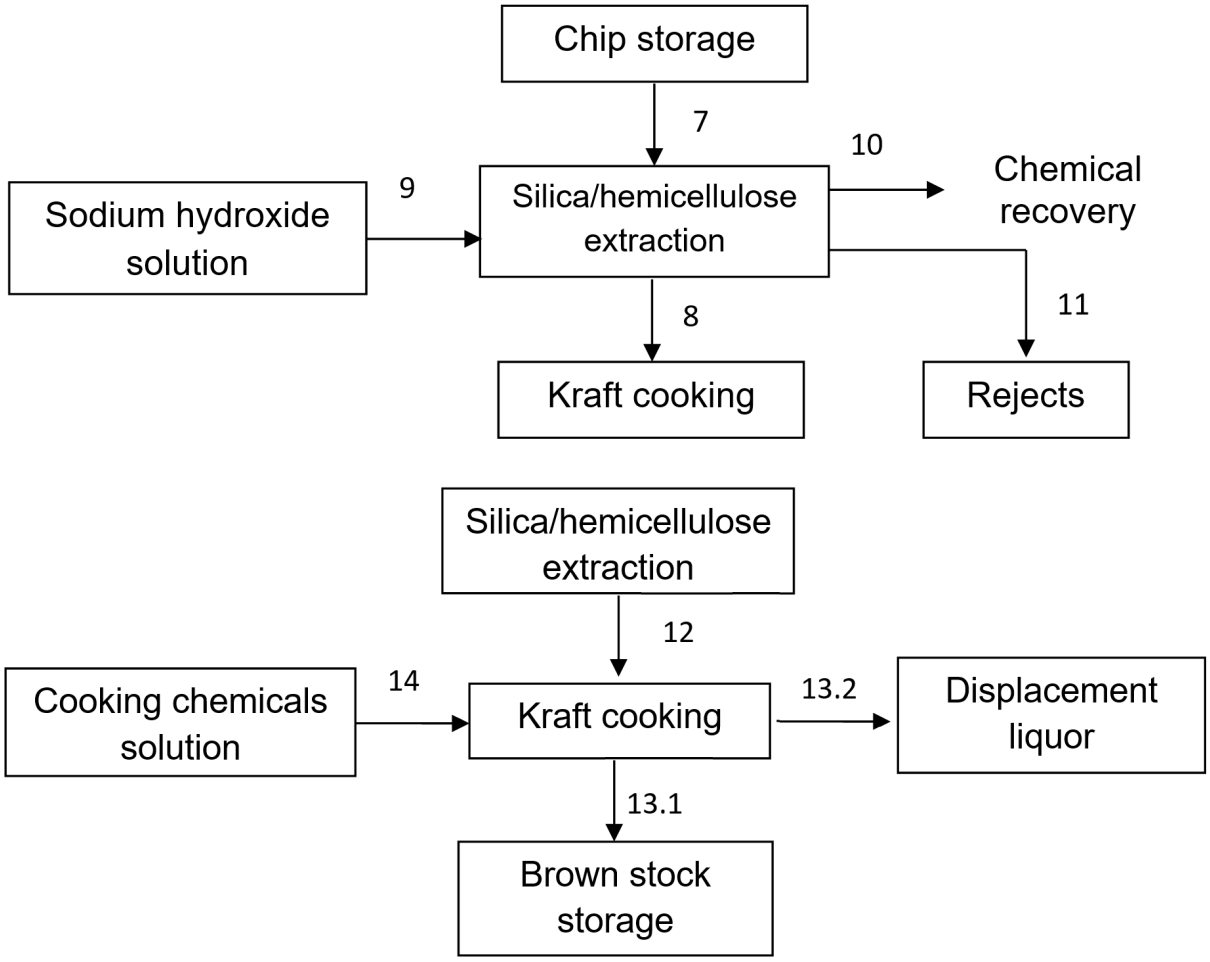

- $C_{13.1} = 17\%$
- $L : W = 4.4\ L/kg$
- $S_{14} = 428.21 \times 4.4 - 642.32 = 1241.8\ L$
- $K_{13.1} = 65\%$ (based on previous step)

2. Calculation:

$$Q_{13.1} = Q_{12} \times K_{13} = 428.21 \times 65\% = 278.34\ kg \tag{5.15}$$

$$D_{13.1} = Q_{13}/C_{13} = 278.34/17\% = 1637.29\ kg \tag{5.16}$$

$$S_{13.2} = S_{14} + D_{12} - D_{13.1} = 1241.8 + 1070.53 - 1637.29 = 675.04\ kg \tag{5.17}$$

Washing and screening before bleaching

1. Known:

   - $D_{15} = D_{13.1} = 1637.29\ kg$
   - $Q_{15} = Q_{13.1} = 278.34\ kg$
   - $C_{15} = 17\%$
   - $C_{16} = 10\%$
   - $S_{18} = 9.1\ m^3/t\ \ pulp$ (assumed the washing cleanliness with Kappa No.=8-9)
   - $R_{19} = 3\%$
   - $C_{19} = 20\%$ (water saturated)

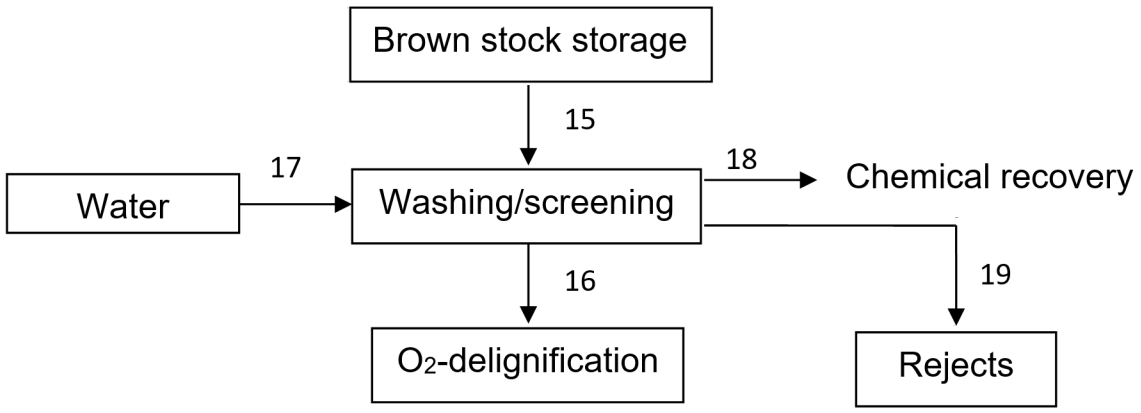

2. Calculation:

$$Q_{19} = Q_{15} \times R_{19} = 278.34 \times 3\% = 8.35\ kg \tag{5.18}$$

$$D_{19} = Q_{19}/C_{19} = 8.35/20\% = 41.75\ kg \tag{5.19}$$

$$S_{18} = 9.1 \times 278.34 = 2532.89\ kg \tag{5.20}$$

$$Q_{16} = Q_{15} - Q_{19} = 278.34 - 8.35 = 269.99\ kg \tag{5.21}$$

$$D_{16} = Q_{16}/C_{16} = 269.99/10\% = 2699.9\ kg \tag{5.22}$$

$$S_{17} = S_{18} + D_{19} + D_{16} - D_{15} = 2532.89 + 41.75 + 2699.9 - 1637.29 = 3637.25\ L \tag{5.23}$$

Two-stage O_2 delignification

1. Known:

   - $D_{20} = D_{16} = 2699.9\ kg$
   - $Q_{20} = Q_{16} = 269.99\ kg$
   - $C_{20} = 10\%$

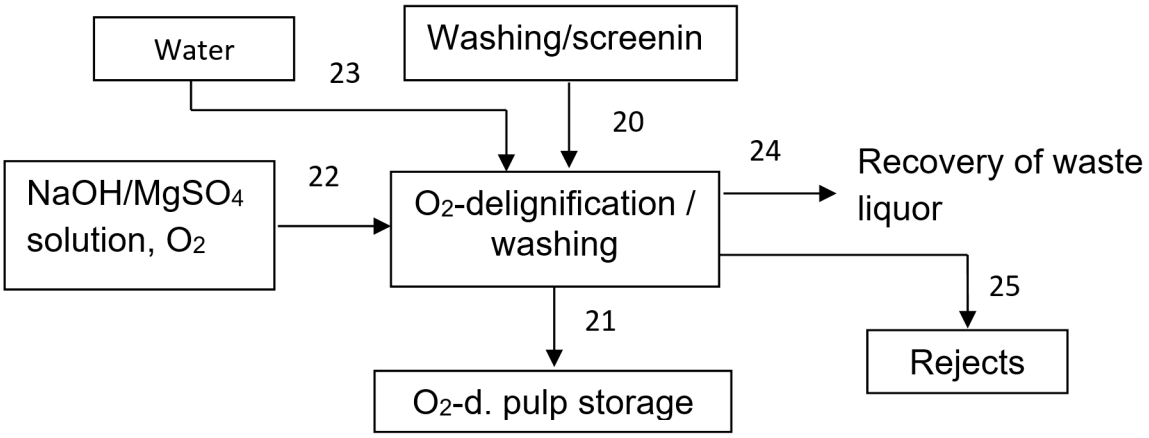

- $C_{21} = 10\%$
- $K_{21} = 90\%$ (based on previous step)
- S_{22} (determined by NaOH charge and conventration,

  which are 2.5% and 400 g/L, respectively)
- S_{23} (determined by pulp consistency in the washing machine, C=4%)
- $R_{25} = 1\%$
- $C_{25} = 20\%$ (water saturated)

2. Calculation:

$$Q_{21} = Q_{20} \times 90\% = 269.99 \times 90\% = 242.99\ kg \tag{5.24}$$

$$D_{21} = Q_{21}/C_{21} = 242.99/10\% = 2429.9\ kg \tag{5.25}$$

$$S_{22} = (Q_{20} \times 2.5\%)/0.4 = (269.99 \times 2.5\%)/0.4 = 16.87\ L \tag{5.26}$$

$$S_{23} = Q_{20}/4\% - S_{22} - D_{20} = 269.99/4\% - 16.87 - 2699.9 = 4032.98\ L \tag{5.27}$$

$$Teo - stagewashing : 2S_{23} = 2 \times 4032.98 = 8065.96\ L \tag{5.28}$$

$$Q_{25} = Q_{20} \times R_{25} = 269.99 \times 1\% = 2.7\ kg \tag{5.29}$$

$$D_{25} = Q_{25}/C_{25} = 13.5\ kg \tag{5.30}$$

$$\begin{aligned} S_{24} &= S_{22} + 2 \times S_{23} + D_{20} - D_{21} - D_{25} \\ &= 16.87 + 8065.96 + 2699.9 - 2429.9 - 13.5 = 8339.33\ kg \end{aligned} \tag{5.31}$$

D0 bleaching stage

1. Known:

   - $D_{26} = D_{21} = 2429.9\ kg$
   - $Q_{26} = Q_{21} = 242.99\ kg$
   - $S_{28} = 1.3\% \times Q_{26}$ (charge of ClO_2 is 1.3%, based on o.d. pulp)
   - S_{29} (determined by pulp consistency in the washing machine, C=4%)
   - $C_{27} = 10\%$
   - $K_{27} = 99\%$ (based on previous step)
   - $R_{31} = 0.5\%$
   - $C_{31} = 20\%$ (water saturated)

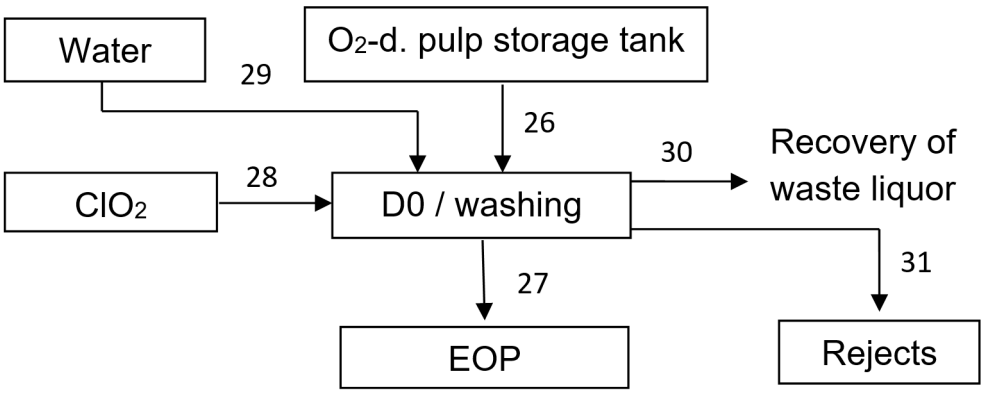

2. Calculation:

$$Q_{27} = Q_{26} \times K_{27} = 242.99 \times 99\% = 240.56\ kg \tag{5.32}$$

$$D_{27} = Q_{27}/C_{27} = 240.56/10\% = 2405.6\ kg \tag{5.33}$$

$$S_{28} = (Q_{26} \times 1.3\%) = (242.99 \times 1.3\% = 3.16\ kg \tag{5.34}$$

$$S_{29} = Q_{26}/4\% - D_{22} - S_{28} = 6074.75 - 2429.9 - 3.16 = 3641.69\ L \tag{5.35}$$

$$Q_{31} = Q_{26} \times R_{31} = 242.99 \times 0.5\% = 1.21\ kg \tag{5.36}$$

$$D_{31} = Q_{31}/C_{31} = 1.21/20\% = 6.07\ kg \tag{5.37}$$

$$\begin{aligned} S_{30} &= S_{28} + S_{29} + D_{26} - D_{27} - D_{31} \\ &= 3.16 + 3641.69 + 2429.9 - 2405.6 - 6.07 = 3663.08\ kg \end{aligned} \tag{5.38}$$

EOP bleaching stage

1. Known:

   - $D_{32} = D_{27} = 2405.6\ kg$
   - $Q_{32} = Q_{27} = 240.56\ kg$

- $S_{34} = (1.3\% \times Q_{32})/0.4 + 6 \times Q_{32}/1000$

  (charges of NaOH and

  H_2O_2 are 1.5% and 6 kg/t, respectively based on pulp)

- S_{35} (determined by pulp consistency in the washing machine, C=4%)

- $C_{33} = 10\%$

- $K_{33} = 98.8\%$ (based on previous step)

- $R_{37} = 0.5\%$

- $C_{37} = 20\%$ (water saturated)

2. Calculation:

$$Q_{33} = Q_{32} \times K_{33} = 240.56 \times 98.8\% = 237.67\ kg \tag{5.39}$$

$$D_{33} = Q_{33}/C_{33} = 237.67/10\% = 2376.7\ kg \tag{5.40}$$

$$\begin{aligned} S_{34} &= (Q_{32} \times 1.5\%)/0.4 + 6 \times Q_{32}/1000 \\ &= (240.56 \times 1.5\%)/0.4 + 6 \times 240.56/1000 = 10.46\ L \end{aligned} \tag{5.41}$$

$$S_{35} = Q_{32}/4\% - S_{34} - D_{32} = 240.56/4\% - 10.46 - 2405.6 = 3597.94\ L \tag{5.42}$$

$$Q_{37} = Q_{32} \times R_{37} = 227.47 \times 0.5\% = 1.2\ kg \tag{5.43}$$

$$D_{37} = Q_{37}/C_{37} = 1.2/20\% = 6.01\ kg \tag{5.44}$$

$$\begin{aligned} S_{36} &= S_{34} + S_{35} + D_{32} - D_{33} - D_{37} \\ &= 10.46 + 3597.94 + 2405.6 - 2376.7 - 6.01 = 3631.29\ L \end{aligned} \tag{5.45}$$

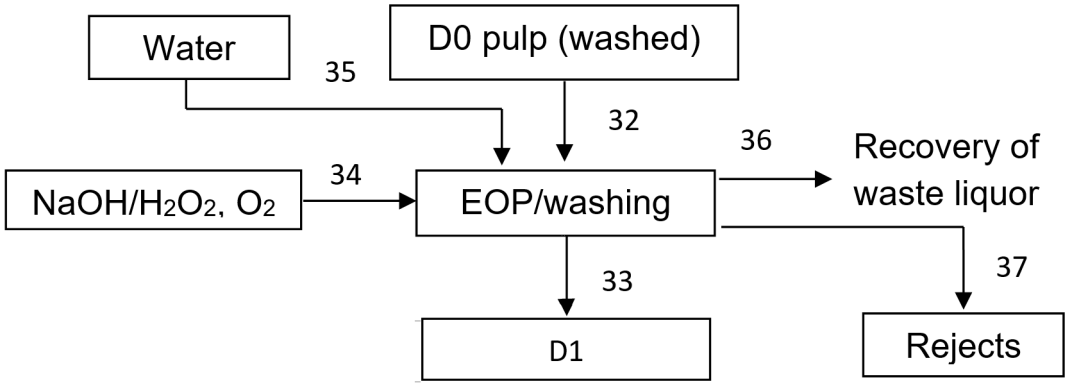

D1 bleaching stage

1. Known:

   - $D_{38} = D_{33} = 2376.7\ kg$
   - $Q_{38} = Q_{33} = 237.67\ kg$
   - $S_{40} = 0.05\% \times Q_{38}$ (charge of ClO_2 is 0.5%, based on o.d. pulp)
   - S_{41} (determined by pulp consistency in the washing machine, C=4%)
   - $C_{39} = 10\%$
   - $K_{39} = 99.5\%$ (based on previous step)
   - $R_{43} = 0.3\%$
   - $C_{43} = 20\%$ (water saturated)

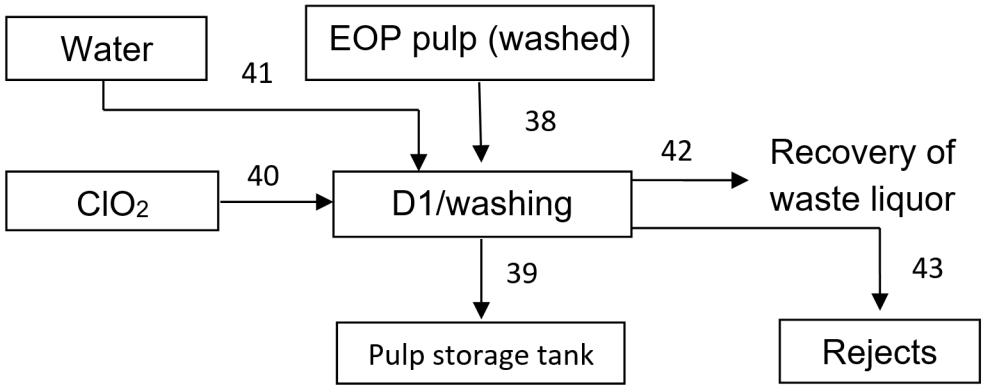

2. Calculation:

$$Q_{39} = Q_{38} \times K_{39} = 237.67 \times 99.5\% = 236.48\ kg \tag{5.46}$$

$$D_{39} = Q_{39}/C_{39} = 237.67/10\% = 2376.7\ kg \tag{5.47}$$

$$S_{40} = Q_{38} \times 0.5\% = 224.74 \times 0.5\% = 1.12\ kg \tag{5.48}$$

$$S_{41} = Q_{38}/4\% - D_{38} - S_{40} = 237.67/4\% - 2376.7 - 1.19 = 3563.86\ L \tag{5.49}$$

$$Q_{43} = Q_{39} \times R_{43} = 236.48 \times 0.3\% = 0.71\ kg \tag{5.50}$$

$$D_{43} = Q_{43}/C_{43} = 0.71/20\% = 3.55\ kg \tag{5.51}$$

$$\begin{aligned} S_{42} &= D_{38} + S_{40} + S_{41} - D_{39} - D_{43} \\ &= 2376.7 + 1.19 + 3563.86 - 2364.8 - 3.55 = 3573.4\ L \end{aligned} \tag{5.52}$$

A3.2 Mass Balance of the Chemical Recovery Process

According to the results in Chapters 3 and 4, 100% of silica in bamboo chips could be removed and 97% of the extracted silica could be recovered from the APEL with CO_2 treatment. The silica content of raw bamboo chips is 1.12% (based on the o.d. chips). Before carrying out the calculation, several definitions are made.

L : Liquor amount of each step (L)

D : Total weight of the material (kg)

M : Solids content of each step (kg)

E : Efficiency of each step (%)

W : Weight of silicon compounds in each step (kg)

H : Weight of hemicellulose in each step (kg)

Recovery of silica from the APEL

$$2\,NaOH + SiO_2 \longrightarrow Na_2SiO_3 + H_2O$$

$$Na_2SiO_3 + CO_2 + 2\,H_2O \rightleftharpoons H_2SiO_3\downarrow + NaHCO_3$$

1. Known:

   - $L_{44} = 3450.89\ L$

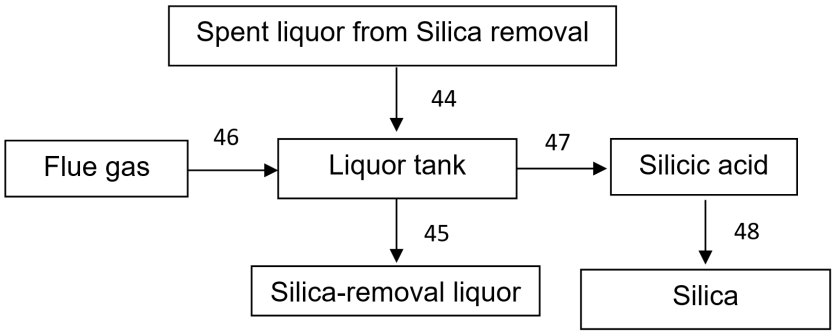

- $M_{44} = 503.78 \times 15\% = 75.57\ kg$ (dissolved lignin, hemicellulose, cellulose, sodium silicates etc.)
- $W_{44} = 503.78 \times 1.12\% \times 122/60 = 11.47\ kg$ (molecular weights of Na_2SiO_3 and SiO_2 are 122 and 60 g/mol, respectively)
- $C_{47} = 10\%$
- $E_{48} = 95\%$

2. Calculation:

$$W_{47} = W_{44} \times 97\% \times 78/122 = 11.47 \times 97\% \times 78/122 = 7.11\ kg$$

(molecular weight of Na_2SiO_3 and H_2SiO_3 are 122 and 78 g/mol, respectively)

(5.53)

$$D_{47} = W_{47}/C_{47} = 7.11/10\% = 71.1\ kg \tag{5.54}$$

$$W_{48} = W_{47} \times 60/78 \times E_{48} = 7.11 \times 60/78 \times 95\% = 5.19\ kg \tag{5.55}$$

$$L_{45} = L_{44} - D_{47} = 3450.89 - 71.1 = 3379.79\ L \tag{5.56}$$

$$M_{45} = M_{44} - W_{44} \times 97\% = 75.57 - 11.47 \times 97\% = 64.44\ kg \tag{5.57}$$

Residual alkali in the APEL was not included.

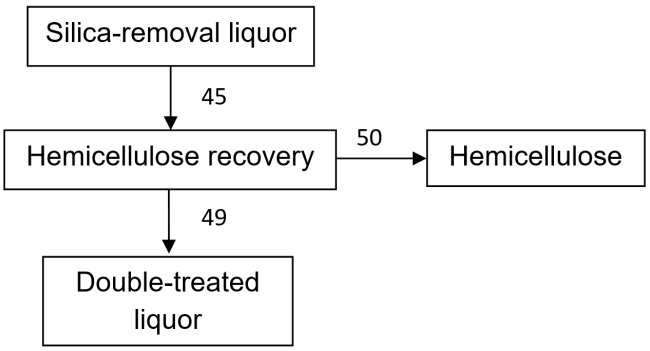

Recovery of hemicellulose from the silica removed APEL

1. Know:

   - $L_{45} = 3379.79\ L$
   - $M_{45} = 64.44\ kg$
   - $E_{50} = 95\%$
   - $H_{45} = M_{45} \times 55\%$
   - $C_{50} = 10\%$

2. Calculation:

$$H_{45} = M_{45} \times 55\% = 64.44 \times 55\% = 35.44\ kg \tag{5.58}$$

$$H_{50} = H_{45} \times E_{50} = 35.44 \times 95\% = 33.67\ kg \tag{5.59}$$

$$D_{50} = H_{50}/C_{50} = 33.67/10\% = 336.7\ kg \tag{5.60}$$

$$L_{49} = L_{45} - D_{50} = 3379.79 - 336.7 = 3043.09\ L \tag{5.61}$$

$$M_{49} = M_{45} - H_{50} = 64.44 - 35.44 = 29\ kg \tag{5.62}$$

Assuming no other components was removed except for hemicellulose.

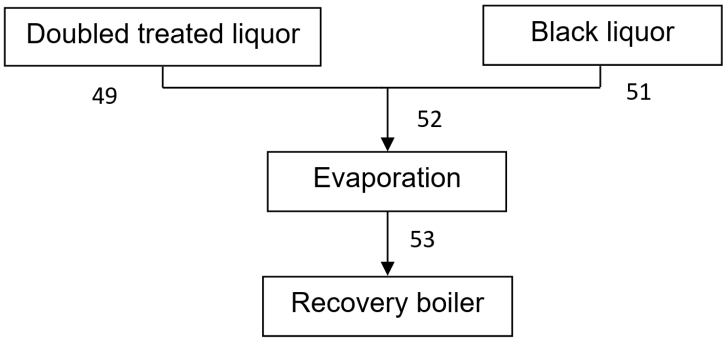

Evaporation system

1. Known:

   - $L_{52} = L_{49} + L_{51}$
   - $L_{49} = 3043.09\ L$
   - $L_{51} = 2532.89\ L$
   - $M_{49} = 29\ kg$
   - $M_{51} = 141.52\ kg$
   - $M_{53}/L_{53} = 60\%$

2. Calculation:

$$L_{52} = 3043.09 + 2532.89 = 5575.98\ L \tag{5.63}$$

$$M_{52} = M_{49} + M_{51} = 29 + 141.52 = 170.52\ kg \tag{5.64}$$

$$M_{53} = M_{52} = 170.52\ kg \tag{5.65}$$

$$L_{53} = 175.37/60\% = 284.2\ L \tag{5.66}$$

Recovery boiler, causticizing system and calcination

For the calculation of these three stages, accurate data are required for the specific pulping system. So, we did not do the mass balance of this part.